Optimized Aerosol Hood Design Performance and Clinical Efficacy to Protect Health Care Workers from Nosocomial Infection

A THESIS

SUBMITTED TO THE FACULTY OF THE GRADUATE SCHOOL

OF THE UNIVERSITY OF MINNESOTA

BY

Ewnet Gebrehiwot

IN PARTIAL FULFILLMENT OF THE REQUIREMENTS

FOR THE DEGREE OF

MASTER OF SCIENCE

Dr. Christopher J. Hogan Jr., Adviser

August 2021

Acknowledgements

I am deeply grateful for my adviser Professor Hogan for making my graduate school experience successful even though I was a new type of student. I came into the UMN with eagerness and drive to learn as a part-time master's student after 10 years with a full time R&D engineering job, two small children, new to aerosol technology and as a woman of color. After initial false starts inside and outside of Professor Hogan's Lab, together we found a new method that worked for both of us and it turned out to be a great experience for both of us! This would have not been possible had it not been for Professor Hogan's kind heart, his strong passion in mentoring students and willingness to listen and adjust to some difficult feedback.

I would like to thank Yuechen Qiao, Ian Marabella and Bernard Olson for their help in the lab and training me on various aerosol measurement equipment. I am also thankful for Khadar Abdi who worked with me closely in collecting measurements and assisting in data analysis by being more available in the lab.

I would like to extend my deep gratitude for Boston Scientific and my R&D Managers Jay Kokate and Ryan Hendrickson who support my goal of going back to school after 10 years. They were flexible and understanding when I attended some courses on campus during working hours.

I am grateful for my parents and sisters who prioritized my educational responsibilities and accepted my less availability in family gatherings. I would like to

thank my wonderful husband and my two daughters who have been patient with me for the number of weekday nights and weekends that were spent on schoolwork away from a wife and motherly duty.

At last but not the least, I would like to thank God who strengthens me to do all things in Christ and supports me solely as I become the person who He made me to be.

Dedication

This thesis is dedicated to my beautiful daughters Phoebe and Lydia for your inspiration to continuously learn in life.

"Always walk through life as if you have something new to learn, and you will."

- Vernon Howard

Preface

Health Care Workers (HCWs) are the most vulnerable group of professionals for SARS-CoV-2 virus infection via airborne or direct contact. The current main three protective methods are PPE, training, and the hospital's ventilations with negative pressure rooms. Negative pressure rooms are limited in availability in any hospital network. PPE and training also have the side effects of headache, skin injury and importantly, inconsistent donning and doffing procedures that affect the health and productivity of HCWs. Therefore, there is a clinical unmet need for additional modes of protection for HCWs against nosocomial infection.

An aerosol hood is a partially enclosed negative pressure chamber placed around the head of a patient to mitigate HCWs exposure during aerosol generating clinical procedures such as intubation. The optimized aerosol hood design is intended to be an engineering control to protect HCWs by combining a physical isolation hood with negative pressure system. The objective of this thesis is to1) model droplet trajectories and evaporation/settling rates and translate to the aerosol hood design performance; 2) to assess the optimized aerosol hood design performance; and 3) to evaluate the clinical efficacy of the aerosol hood during simulated intubation procedures.

Droplet trajectory modeling revealed that smaller droplets evaporate within 5 seconds in the aerosol hood and would get cleared by the negative pressure system, while larger droplets would follow an exhaled jet path impacting inside the aerosol hood. An aerosol hood design performance was assessed by measuring particle penetration, Air

Exchange Time, and Air Changes per Hour (ACH). At a half power blower setting, the particle penetration resulted in 10^{-4} with a corresponding protection efficiency of 99.99%. The aerosol hood has an average Air Exchange Time of 2.76 minutes for a 99.9% reduction using a half power blower setting and an average of 151.44 Air Changes per Hour (ACH). The clinical efficacy was studied in a simulated intubation procedure by measuring the aerosol exposure in the room and particle deposition on the participants' PPE. Bedside location to the SIM-man had a higher particle concentration exposure than a background location, however, when the negative pressure system aerosol hood is used, the bedside location has a lower particle concentration similar to the background exposure. Particle deposition decreased by 42% for the face shield and gowns: and 32% increase on the gloves when measuring the on participants' PPE substrate.

Overall, the optimized aerosol hood design has a high performance in clearance of human respiratory droplets and aerosols due to its design feature of a physical isolation and negative pressure system. The clinical study has shown the efficacy of the aerosol hood technology and promising in supplementing PPE and hospital's negative pressure rooms to protect HCWs against nosocomial infection.

Table of Contents

List of Tables

Table S6: Air changes/hour (ACH) and time required for airborne-contaminant removal by efficiency.

List of Figures

Figure 3: Droplet trajectories for variable size droplets and variable upward head tilt angle. A diameter of 50 um evaporates before reaching the ground. The rest of bigger diameter sizes fell off the jet trajectory and settled on the ground from a height of 2 meters.

Figure 4: Droplet trajectory of an upward (+ degrees) and downward (- degrees) head tilt. Upward head tilt represents the patient's head movement for the intubation procedure. Downward head tile represents the patient's head movement before or after intubation procedure.

Figure 5: Hypothetical overlay of Manikin in an aerosol hood and vertical distance of droplet trajectory. The distance between the patient's mouth opening to the filter is approximately 0.4 +/- .1 meters. Large droplets (greater than the critical diameter size of 60 – 70 um) start falling off the jet after 0.3 meters for 65 um to 1.2 meters for 200 um, which is beyond the distance of the filter location. Smaller droplets would evaporate shortly after exiting the patient's mouth and carried towards by the streamline of the aerosol hood negative pressure system. Note the droplet trajectory simulations are performed for angles closer to perpendicular to gravity than depicted.

Figure 6: Evaporation and Settling Curve at Relative Humidity (RH) 50%. The upward head tilt delayed the settling time by 30 seconds although it would travel a shorter distance than the centerline head position or downward head tilt. The upward head tilt had no effect on the evaporation rate of the particles.

Chapter 3

Figure 1: Aerosol hood design comparison between the previous design (left) and the optimized design (right) based on HCWs feedback. The optimized design has wider front

Contribution of the Author and Others

This thesis describes the research carried out by the Author with guidance and contribution from some collaborators. The Author worked closely with a graduate adviser, Dr. Christopher J. Hogan on the experiments plans, data analysis, and preparation of each chapter of this thesis and the manuscript(s) submitted (to be submitted) for publication. Contributions of other collaborators are mentioned below:

Chapter 1: This chapter serves as an introduction to the dissertation. The present Author prepared and edited the manuscript with the guidance of Professor Hogan.

Chapter 2: This chapter presents droplet trajectory model calculation and analysis. The present Author carried out the model calculation and data analysis with the guidance of Professor Hogan.

Chapter 3: This chapter presents aerosol hood design optimization and performance testing in a Research Lab and M Simulation Lab of the University of Minnesota. The present Author collaborated with Professor Hogan and lab members Ian Marabella, Bernard Olson, Khadar Abdi and Andrew Zarling to update the drawing design and manufacture in the UMN machine shop. Khadar Abdi and the Author conducted the aerosol hood performance in a Research Lab and M Simulation Lab. The present Author performed all the data analysis.

Chapter 4: This chapter presents clinical study results of aerosol exposure and particle deposition. The Protocol was submitted for IRB Approval in collaboration with Professor Hogan. Professor Hogan, Khadar Abdi and the Author conducted the clinical study with all participants. Khadar Abdi and the Author prepared the particle concentration measurements for aerosol exposure evaluation for the bedside and background locations. Khadar Abdi measured the fluorometry and prepared data for fluorescein deposition. The final data analysis on the aerosol exposure and fluorescein deposition was completed by the Author with guidance from Professor Hogan. The data for intubation time and participants' feedback were all prepared by Pankhuri Gupta. Final data analysis was conducted by the Author with guidance from Professor Hogan.

Appendix A: The Author obtained the copyright permission to reuse images from reference articles.

Appendix B: The Author obtained the equidistance flow rate measurements for the front of the aerosol opening. All other flow rate measurements were conducted by Khadar Abdi.

Appendix C: The intubation procedure steps were provided by Eugene Floersch from the M Simulation Lab Staff. The particle concentration graphs for aerosol deposition were prepared by Khadar Abdi. The exit interview was obtained by Lou Clark, M Simulation Lab Director. The participants' feedback was transcribed by Pankhuri Gupta.

Chapter 1: Introduction

1.1. Background

During the COVID-19 pandemic, the subject of infectious disease transmission via aerosols has become an increasingly important topic. After 2002-2003 SARS-CoV-1 outbreaks, a number of studies were conducted on the risk of transmission of respiratory infections, the impact of hospital ventilation, and identifying aerosol generating clinical procedures to minimize nosocomial infection to Healthcare Workers (HCWs) [1, 2]. However, a concern for SARS-CoV-2 virus transmission via aerosol routes has made clear that prior studies have not (1) fully clarified to what extent aerosol based disease transmission occurs for SARS-CoV-2 and (2) enabled the development of technologies to mitigate aerosols based infection.

Prevention controls for SARS-CoV-2 virus still heavily depend on Personal Protective Equipment (PPE) and HCW training [9, 10, 13, 14, 15]. However, inconsistent use of PPE and improper donning and doffing are common issues among HCWs that increases the likelihood of infection transmission. Evans et al. discusses a new role of 'dofficer' to ensure standard adherence to PPE procedure [9]. While that mitigates the concern of improper use of PPE, donning is laborious activity as shown in Figure 1 [32]. Moreover, recent studies showed a skin injury and headache associated with an increased PPE use in hospitals [32-35].

Figure 1: Donning Procedure for HCWs as a PPE before caring for COVID patients [32].

Although PPE and administrative controls are mandatory protection modes, the associated side effects and inconsistent use can impede HCWs' health and productivity. Thus, there is a need for a more effective disease control to alleviate the negative effects

of prolonged and frequent PPE use. According to the Center of Disease Control (CDC) Hierarchy of Controls (Figure 2), PPE and Training are the lowest level of disease control protection [11, 13, 14].

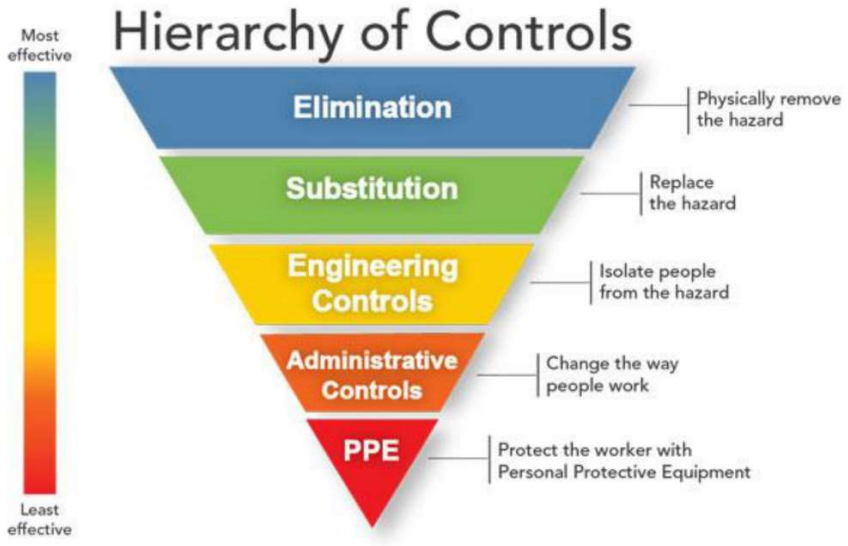

Figure 2: CDC's Hierarchy of Controls showing PPE and Administrative controls such as training, scheduling and in person monitoring being a lower level of controls [11].

There are not many engineering controls measures, which is the next level of control per CDC, designed and properly tested to protect HCWs from infectious disease transmission such as SARS-CoV-2 virus. Considering COVID-19 virus long term presence, a robust engineering control that can outlast the pandemic and bring relief to HCWs daily PPE requirement is a current unmet clinical need. The first step in tackling the unmet clinical need is to understand the relations between the aerosol principles of the respiratory droplets. The aerosol principles that are of interest in this study are droplet dispersion, evaporation and settling rates, residence time, critical diameter size, droplet and

fluid velocity for respiratory droplets generated during clinical procedures such as intubation. [3 - 8, 31].

Numerous articles have been published related to droplets dispersion and evaporation rate based on a jet model, physics-based numerical model, and Computer Fluid Dynamics (CFD) simulation [3, 7, 8]. Such studies facilitate the development of effective prevention controls for SARS-CoV-2 virus [7, 8], and technological developments based on aerosol engineering principles. Xie et al., used a non-isothermal jet model to recreate the Wells Evaporation and Falling curve that plots an evaporation and settling rates as a function of the diameter size [7]. Tang et al. discussed how the large droplets fall to the ground quickly and small droplets stay and follow the air flow current. In addition, it discussed the influence of hospital ventilation systems on the droplets path by containing or dispersing.

The hospital ventilation systems with a negative pressure rooms are the third prevention control for nosocomial infection [1, 2, 8]. Advanced mechanical ventilation systems with filtration reduce the risk of airborne transmission compared to conventional ventilation systems [2]. Current conventional ventilation systems will typically need at least a minimum of 15 minutes of air clearance time between surgical procedures [8] per CDC guidelines of 99.9% reduction of the particles produced during the procedure must be cleared via ventilation before preparation for a new procedure can commence. Walker et al. discusses how a negative pressure isolation in hospital rooms reduces aerosol transmission, which is one of the supportive studies towards the aerosol hood's negative pressure system [12, 14, 16]. Negative pressure rooms (Figure 3) are limited in availability

in many hospital networks, and furthermore, can be problematic to deploy for immunocompromised patients, where positive-pressure environments are desirable.

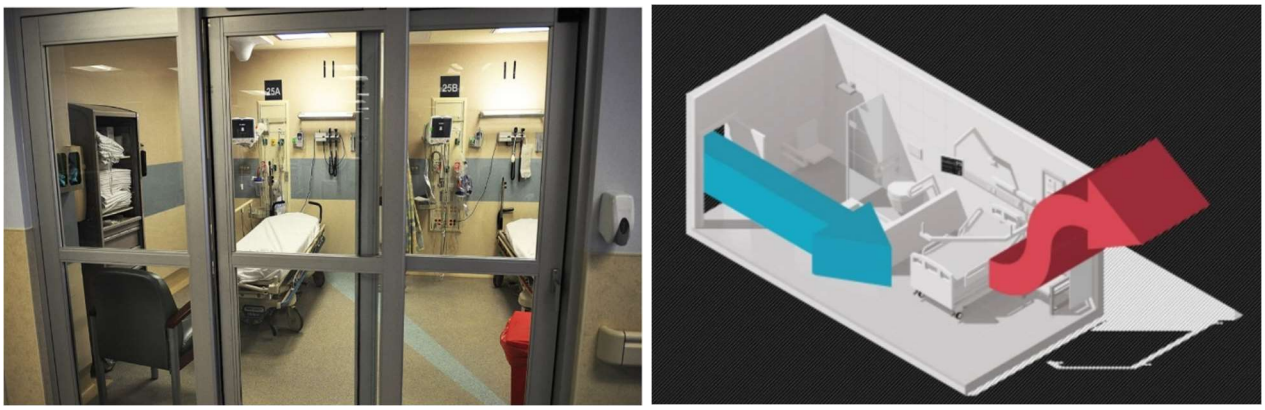

Figure 3: Negative pressure room in the hospital image and air flow schematic.
Figure Sources: 7e5003ccc151a4dd8889bebb467f35ce.png (1000×562) (pinimg.com) and Negative-pressure-rooms-save-lives.-Why-aren8217t-there-more-of.jpg (596×335) (webdesigntips.blog)

As an engineering control to both provide additional protection to HCWs and to reduce clearance time needed between procedures, an aerosol hood was recently designed [24]. An aerosol hood is a partially enclosed negative pressure chamber designed to mitigate health care worker aerosol exposure during potentially aerosol generating clinical procedures such as intubation. The aerosol hood (Figure 4) is composed of HEPA filter, clear polycarbonate isolation panels, iris ports with silicone rubber sheet coverings. The

aerosol hood has cord inlets and strap hook system to secure it with an inclined hospital bed position.

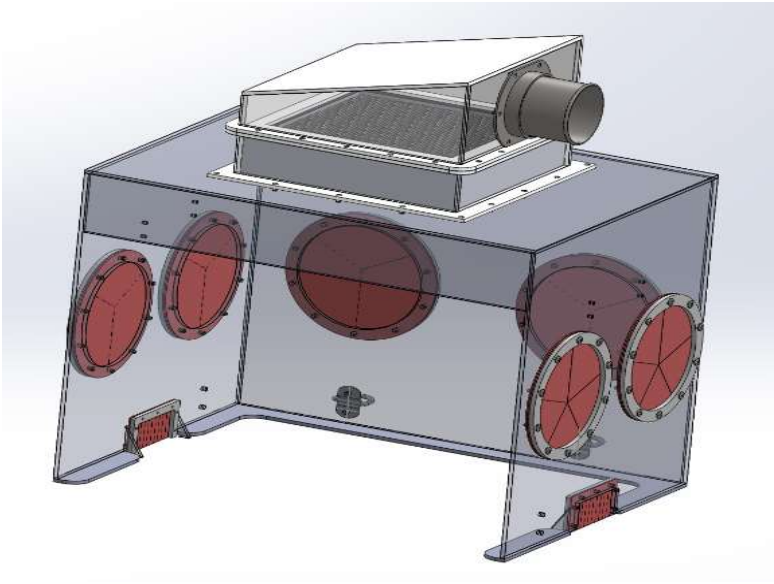

Figure 4: Optimized aerosol hood design.

The negative pressure system is created by connecting the HEPA filter with a blower using a duct tube as shown on Figure 5. When the blower is turned on the air flows into the aerosol hood and transport the patient's respiratory droplets through the HEPA filter then exhausted by the blower system that has a diffuser attached to it.

Figure 5: Aerosol hood connected with the blower to create the negative pressure system.

There are several aerosol hood designs with different naming conventions, such as the Aerosol Box, Containment Device, Safety Tent, and Aerosol Containment Device [15-23]. The common aspect of all designs have a physical isolation like a hood/box and it has an opening for HCWs to insert their hand for intubation procedures. Some designs have a suction system either using a vacuum/filter or temporary container [19, 25]. The main distinction of the aerosol hood design from others is the addition of High Efficiency Particulate Air (HEPA) filter and the silicone rubber sheet covered iris ports that prevent aerosols from escaping the aerosol hood. The aerosol hood was designed and patented in Chris Hogan's Lab as a portable negative pressure hood with HEPA filter [24]. This thesis

is a continuation of the initial design optimization based on Physicians and HCWs feedback and usability experience.

1.2. Overview of Dissertation

This thesis describes a combined laboratory and medical simulation clinical study of a negative pressure aerosol hood to mitigate aerosol-based disease transmission to healthcare workers. In this introductory chapter, the importance of developing engineering controls to prevent infection of health care workers via aerosols routes has been first discussed. The second chapter reviews the current state of knowledge on droplet and aerosol particle trajectories and residence time produced from human respiratory droplets. The remaining chapters focus on discussion of the studies performed, including design of the protective hood, laboratory testing, and medical simulation testing.

Chapter 2: Current State of Knowledge on Respiratory Droplets Trajectories and Residence Time

Chapter 3: Optimized Aerosol Hood Design and Efficacy as an Engineering Control to Protect HCWs

Chapter 4: Simulated Intubation Procedure in a Simulated Hospital Setting to Assess Exposure in a Room and Deposition on HCWs' PPE

Chapter 2: Current State of Knowledge on Respiratory Droplets Trajectories and Residence Time

2.1. Preface

Understanding respiratory droplet trajectories and residence times are critical in designing effective engineering controls for protection against aerosol-based disease transmission. The objective of this study was to utilize a model of respiratory droplet trajectory, including evaporation and settling rates to understand how an aerosol hood can be designed to mitigate dispersion of such droplets. Specifically, an isothermal jet model was used based on Xie et al. [7] that provided the fluid velocity and evaporation rate equations. The particle velocity was calculated based on the Verlet algorithm and, unique from Xie et al [7], a head tilt angle was incorporated in the model. The droplet trajectory model resulted in a critical diameter size near 65 μm traveling up to 0.3 meters before evaporation. Smaller particle diameter size, which evaporate to sub-micrometer particles, will be cleared by the half power blower setting with a 62-cfm flowrate of the aerosol hood. The evaporation and settling curves showed in a maximum of 30 seconds evaporation/settling rate for the critical diameter size of 65 μm. Smaller diameter size will be evaporating within 5 seconds and again will be cleared by the flowrate created in the aerosol hood. For large particles follow through a jet path leading to impaction inside the aerosol hood, if not entrained by flow. Overall, the isothermal jet model justifies the

effectiveness of the aerosol hood in capturing small and large particles either by the air flow streamlines or impaction to the aerosol hood.

2.2. Introduction

Droplets are generated from the respiratory tract and are introduced into the environment through normal breathing, talking, coughing, and sneezing [3, 4, 26]. The breathing rate, relative humidity and opening diameter of the respiratory jet determines the evaporation rate and droplet trajectory [7]; all these ultimately determine the size distribution of potentially infectious particles produced from human respiratory droplets. Higher velocity droplet generating events, such as sneezing, produce higher concentration and smaller droplets [4, 7]. Droplets generated by normal breathing are at lower concentrations [3, 4]. While this suggests sneezing would be of greater concern, it is important to note that breathing is continuous, while sneezing (and similarly coughing) is comparatively rare, hence the majority of droplets produced by an individual come from regular breathing activities (along with speaking).

The parameters governing droplet size and generation rate continue to be debated, as do the relevant droplet size ranges for which (1) rapidly settle to the ground, and (2) evaporate, yielding small particles with long airborne residence time. A recent article by Vuorinen et al. considered large droplets for sizes greater than 100 μm, small droplets between 5-100 μm sizes and droplet nuclei for sizes less than 5μm [7]. Droplet nuclei are small microparticles left after evaporation, with near indefinite residence time in the air.[7].

Meanwhile large droplet residence time are 2-20 seconds, while small droplet residence time are 20 sec – 1hr [7].

Beyond coarse size classifications, the physics of droplet migration and evaporation can be examined to understand droplet/particle residence time. This is in fact more important than size classifications, as the size of a droplet which evaporates to a droplet nuclei size is dependent on the environment (i.e. relative humidity). Historically, the Wells Evaporation-Falling curve is utilized to understand the relationship between droplet size, evaporation and settling rate. The original Wells curve was developed in 1934, and is shown in Figure 1 below. The x-axis is the droplet diameter, as expelled from an individual, and the y-axis is the time it takes to either evaporate or settle to the ground (the smaller of the two values). The first part of the curve (on the left side) shows (starting from 0 x-axis to 160 um) the time it takes for a droplet to evaporate. The second (from 160 – 200 um) and third (from 140 – 200 um) curves (on the lower right side) show the time it takes for a spherical droplet to reach on the ground from 2 meters height, leading to an inflection point before which droplets lead to particles with infinite residence time in an aerosol, and after which they have finite residence time determined by gravitational settling. Importantly, the Wells Evaporation-Falling curve also yields a critical droplet diameter (critical size), i.e. the droplet diameter where the settling time and evaporation time coincide, for the given input of relative humidity and temperature.

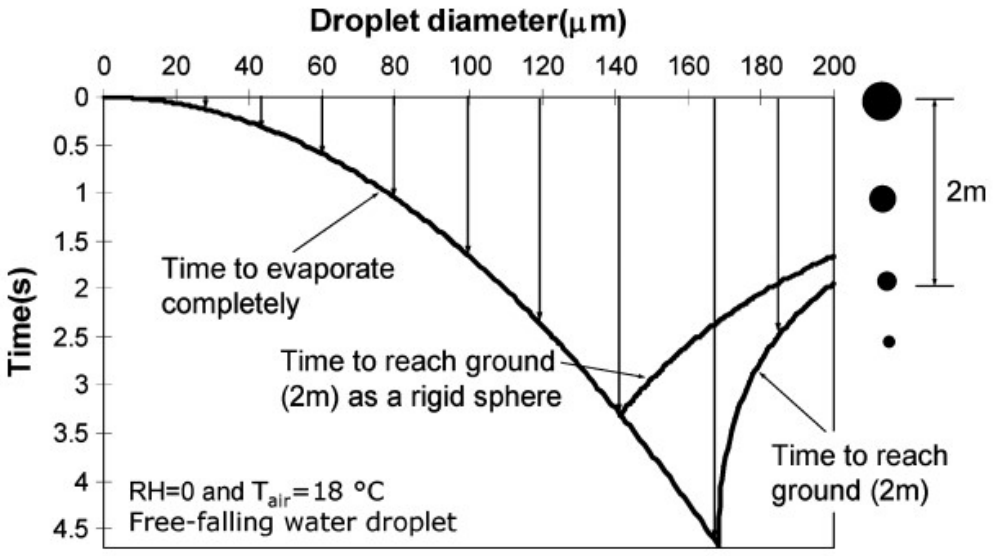

Figure 1: The Wells Evaporation-Falling curve developed in 1934. A curve that plots a relationship between evaporation rate, settling (falling) rate and particle diameter size. Reproduced with permission from [7]. Permission is included in the Appendix A, Figure S1.

However, the original Wells curve did not consider droplet trajectories, the surrounding air movement and the jet produced by respiratory droplets [7]. Therefore, following the work of Wells, Xie et al. refined evaporation and falling curves to not only determine droplet residence time but also model their trajectories either to deposition or until complete evaporation (where they are assumed to yield residual aerosol particles) [7]. This thesis uses the models laid out on Xie et al. to confirm the droplets generated by patient laying under the aerosol hood would have (1) trajectories leading beyond the hood if the hood was not present or (2) would yield aerosol particles which would be dispersed through the room in the absence of the hood. The development of this calculation procedure also results in a droplet trajectory spreadsheet, whose output tables are included as an Appendix A, Suppl. Figure S3 – S6 and with the spreadsheet itself available as

supporting information. The spreadsheet is formatted in a way to enable those unfamiliar with droplet trajectory calculations to utilize it to understand droplet trajectories and evaporation in a healthcare setting.

2.3. Calculation Methods

To construct an improved Wells Evaporation-Falling curve, Xie et al. presented both cases of non-isothermal and isothermal jet models for the droplet trajectory from the respiratory droplets [7]. In this thesis, the Xie et al model is largely followed, but an isothermal jet model is used assuming a minimal temperature difference between the respiratory tract and surrounding environment. The schematic below (Figure 2A) from Xie et al. shows the isothermal jet model that has a similar trajectory to a human sneeze jet shown on Figure 2B from Tang et al [7,8].

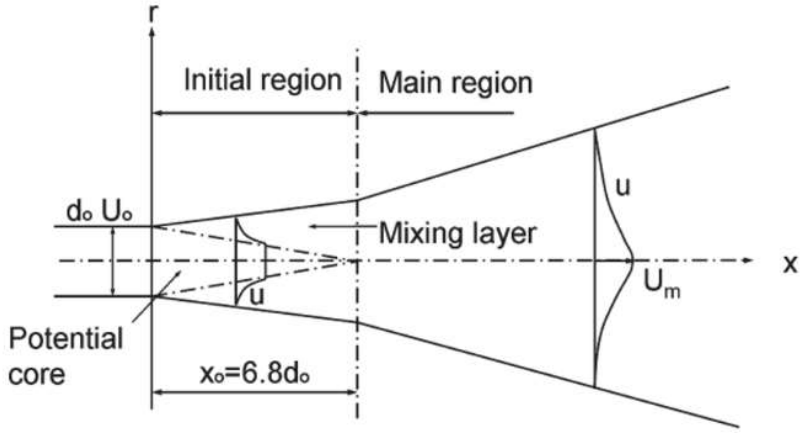

Figure 2A: Isothermal Jet Model from the Xie et al. reproduced with permission from [7]. Permission is included in the Appendix A, Figure S1.

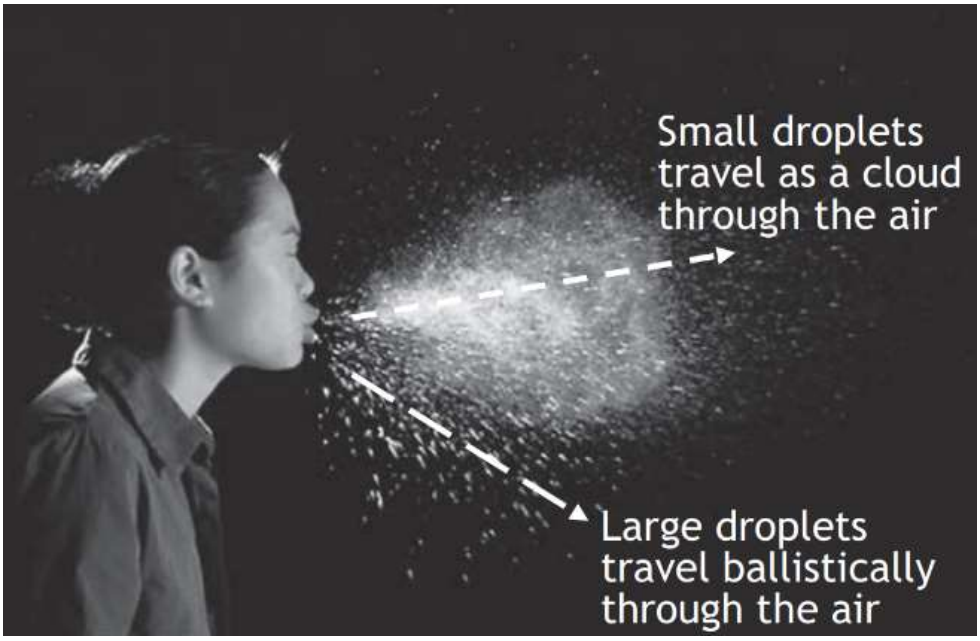

Figure 2B: A human sneeze jet model showing the trajectory of respiratory droplets. Reproduced with permission from [8]. Permission is included in the Appendix A, Figure S2.

Not only are the respiratory droplets visible in the jet but also one can see how the large droplets settle more quickly to the ground while the small droplets remain suspended as a cloud that would stay in the air and eventually evaporate, leaving aerosol particles. To quantify the critical size of the droplet diameter (i.e. the droplet size where it changes from evaporating to settling) and the droplet travel distance, two calculation steps were taken; each is adapted from the model of Xie et al [7]. The first step is to find droplet and fluid velocity and the second step was determining the evaporation rate of the droplets.

(1) *Particle and Fluid Velocity*: The two main forces that act upon a settling droplet are the gravity and drag force. The drag force (F_d), provided in equation (1) was calculated based

on the particle Reynolds Number (Re_p) and Drag Coefficient (C_d) that are shown in Equations (2) and (3).

$$F_D = C_d \left[\frac{1}{2}\rho_g(u - v)^2\right]\left(\frac{1}{2}\pi d_p^2\right) \quad (1)$$

$$Re_p = \frac{\rho_g d_p \sqrt{(v_x - u_x)^2 (v_y - u_y)^2}}{\mu} \quad (2)$$

$$C_d = \frac{24}{Re_p}\left(1 + \frac{1}{6}Re_p^{2/3}\right) \qquad Re_p \leq 1000 \quad (3)$$

The fluid velocity was calculated for both Streamline coordinates (s, r) and Cartesian coordinates (x,y) using Equations (4) – (9). Equation (8) and (9) incorporate angle in trajectories of the fluid velocity to simulate patient's head movement in the aerosol hood. θ is the head tilt angle from the centerline position of the patient. Positive degree is head tilted up representative of a patient head position during the intubation procedure. Negative degree refers to the head tilted down representing possible head movement by the patient before or after the intubation procedure.

$$U_m = 6.8U_0/\hat{s} \quad (4)$$

$$\bar{u}_s = U_m sech^2(\sigma\eta) \quad (5)$$

$$\bar{u}_r = U_m\left[\frac{a\eta(1+\eta^2-(1-b)(1+\eta^2)^{\frac{1}{2}})}{(1+\eta^2)(1-(1+b)(1+\eta^2)^{\frac{1}{2}})^2}\right] \quad (6)$$

$$\eta = \bar{r}/\bar{s} \text{ where } \bar{r} = r/d_0 \text{ and } \bar{s} = s/d_0 \quad (7)$$

$$u_{x\theta} = u_s \cos\theta + u_r \sin\theta \quad (8)$$

$$u_{y\theta} = u_r \cos\theta + u_s \sin\theta \quad (9)$$

Where U_m is centerline velocity decay, which is a function of the initial velocity (U_0) and normalized streamline axial distance ($\bar{s}$). The axial and radial fluid velocity used constants such as σ=10.4, a = 0.0046 and b=0.0075. η is also the ratio between the normalized streamline radial distance ($\bar{r}$) and the normalized streamline axial distance ($\bar{s}$). The Verlet algorithm equations (10) and (11) were used to calculate the droplet position using the droplet acceleration, droplet velocity and a time step (t)[39]. Mass (m_p), acceleration (a) and particle velocity (V_p) equations (12) – (14) were used for the Verlet Algorithm.

$$x(t + \Delta t) = x(t) + V_{px}(t)\Delta t + \frac{1}{2}a_x(t)\Delta t^2 \quad (10)$$

$$y(t + \Delta t) = y(t) + V_{py}(t)\Delta t + \frac{1}{2}a_y(t)\Delta t^2 \quad (11)$$

$$m_p = \frac{\pi {d_p}^3}{6\rho_p} \quad (12)$$

$$a_x = \frac{F_d}{m_p} \text{ and } a_y = \frac{F_d}{m_p} - 9.81 m/s \quad (13)$$

$$V_{px+} = \frac{x_{i+1} - x_i}{t} \text{ and } V_{py+1} = \frac{y_{i+1} - y_i}{t} \quad (14)$$

(2) *Evaporation rate of the droplet:* The above Equations (1) - (14) can be solved to model the trajectory (the *x* and *y* positions of droplets over time) of a fixed diameter particle ejected from a jet and subject to gravity, with the particle's inertia accounted for and the jet fluid velocity. For solid particles, this approach is highly accurate in predicting droplet motion in the absence of diffusion, i.e. larger super micrometer particles in flowing systems. However, droplets rapidly evaporate in most environments including indoor spaces. The evaporation rate of the droplet is a factor of air velocity relative to the droplet

velocity, diffusive mass transfer limitations, and temperature. These factors were incorporated into the Schmidt number (Sc) and Sherwood number (Sh) correlations shown in equations (15) and (16), and used to compute the evaporation rate. The Schmidt number is the ratio of momentum diffusion to mass diffusion. The Sherwood number is the ratio of convective mass transfer to diffusive mass transfer. The D in Equation (15) is the binary diffusion coefficient of vapor through air.

$$Sh = 1 + 0.3Rep^{\frac{1}{2}}Sc^{\frac{1}{3}} \tag{15}$$

The radius change rate $\left(\frac{dr_p}{dt}\right)$ can be calculated using Equation (17) and the diameter change $\left(d_{pi+1}\right)$ evaporation is calculated using Equation (18) below.

$$\frac{dr_p}{dt} = \left(\frac{CM_vD_\infty pS}{\rho_p r_p RT_\infty}\right) \ln\left(\frac{p-pva}{p-pv_\infty}\right) \tag{16}$$

$$d_{pi+1} = d_{pi} + 2\Delta t \frac{dr_p}{dt} \tag{17}$$

Where C is correction factor of temperature affecting the diffusion; M_v is the molecular weight of the vapor; R is the constant gas for water pressure; p is the total pressure and p_v is the vapor pressure. The important parameter from equation (16) is the $p_{v\infty}$, where the vapor pressure is multiplied with the Relative Humidity (RH) to represent the desired humidity level of the hospital room setting. In this thesis 50% RH in most calculations, unless it is stated.

2.4. Results and discussion:

2.4.1. Droplet Trajectories:

The droplet trajectories for diameter sizes of 50 μm, 100 μm, 150 μm and 200 μm were analyzed at four upward head tilt positions, 0 degrees, 15 degrees, 30 degrees and 45 degrees. The initial straight line shown Figures 3 and 4 refer to the droplet jet trajectory. When the jet changes direction, particles "fall out" of the jet and stop moving and either evaporate or settle on the ground once they exit the jet. Figure 3 shows as the droplet diameter size increases, the droplet travels longer distances. In the case of 50 μm diameter size, the droplet quickly evaporates before reaching the ground. For the rest of the diameter sizes, the settling distance increased approximately by 0.3 meter for every 15 degrees. The head tilt angle shown on Figure 3 are centerline (0 degrees) and upward tilt (+ degrees), where the higher the degree of tilt, the droplet horizontal settling distance is shorter and with a maximum difference of 0.1 meter from the centerline of 0 degrees.

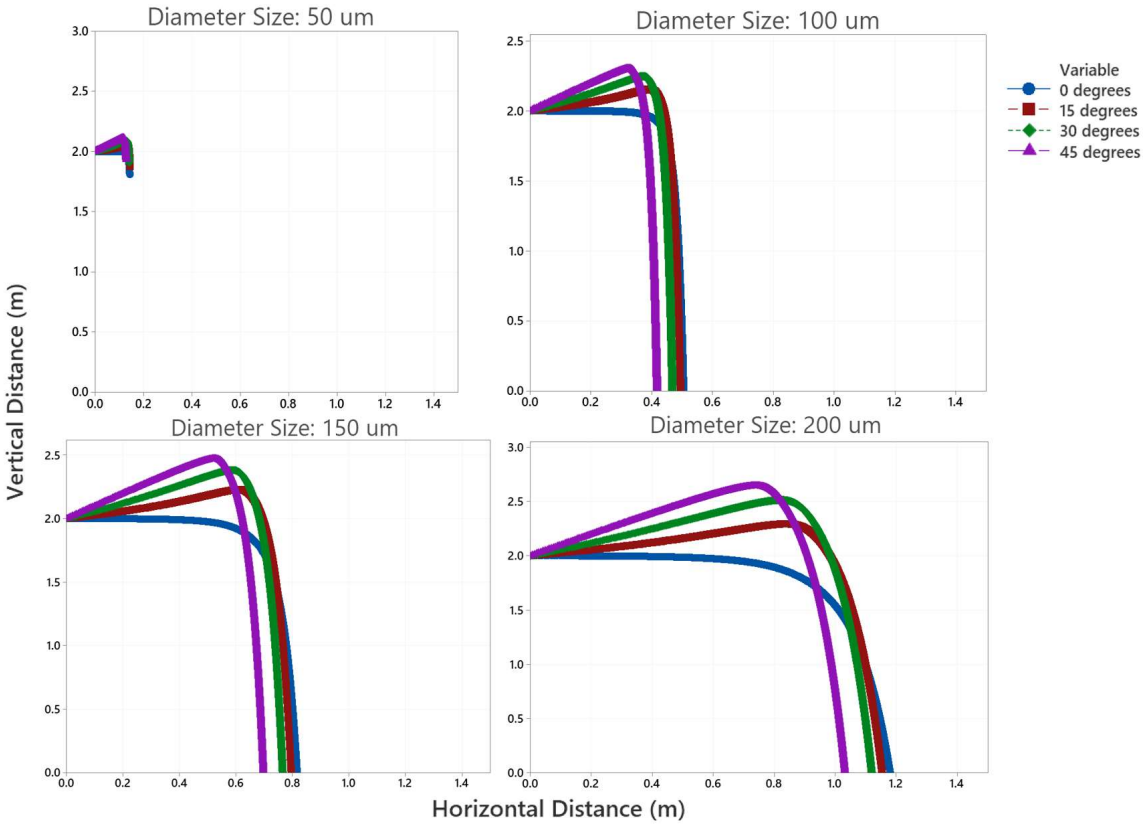

Figure 3: Droplet trajectories for variable size droplets and variable upward head tilt angle. A diameter of 50 um evaporates before reaching the ground. The rest of bigger diameter sizes fell off the jet trajectory and settled on the ground from a height of 2 meters.

The clinical relevance of an upward head tilt is the patient's head must be tilted to variable levels in hospital settings. Larger droplets with higher upward tilt angles should impact the hood because of travel distance. In the meantime, the downward head tilt is important to understand as the patient can look down occasionally. Figure 4 below shows the trajectories symmetry effect when the head tilt is upward or downward. It also shows the horizontal traveling distance remains the same with slight variation where the upward head tilt trajectory settles quickly, followed by the downward head tilt and the centerline travels the farthest.

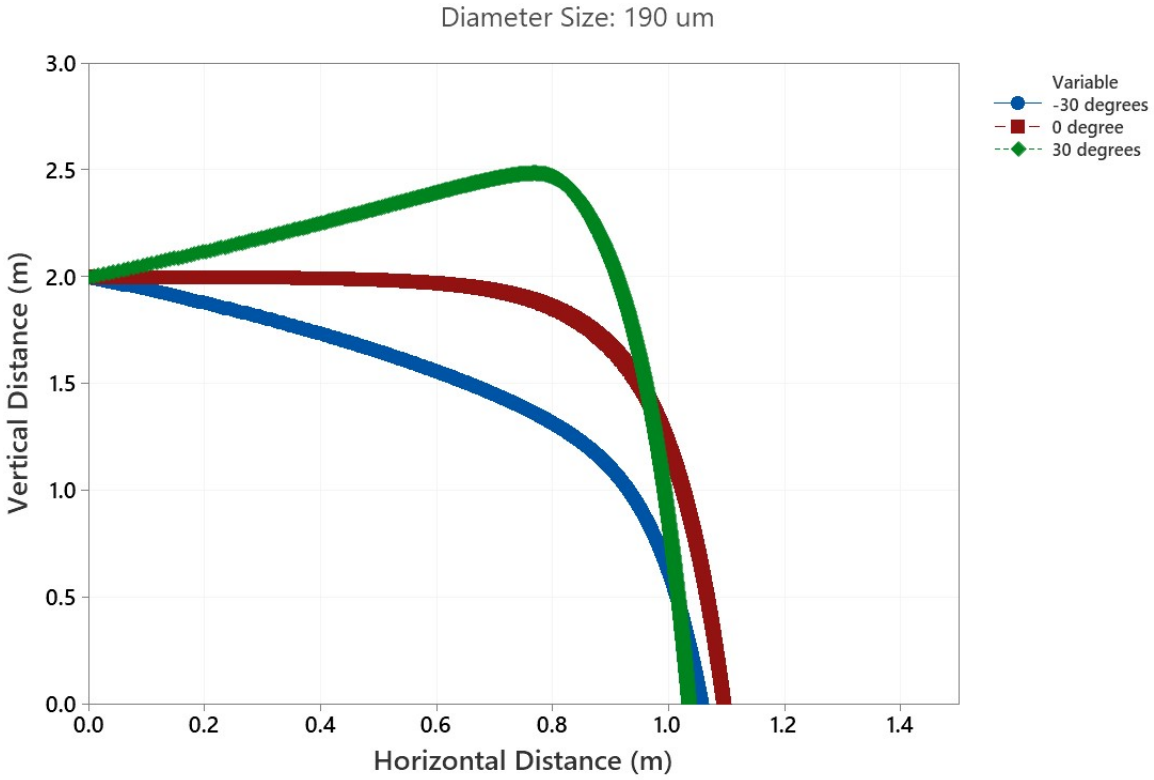

Figure 4: Droplet trajectory of an upward (+ degrees) and downward (- degrees) head tilt. Upward head tilt represents the patient's head movement for the intubation procedure. Downward head tile represents the patient's head movement before or after intubation procedure.

The droplet trajectories were used to estimate the Aerosol Hood capability in capturing the small and large droplet trajectories generated during intubation procedure. Figure 5 below shows an overlay of Manikin laying in the aerosol hood and droplet trajectory of Figure 4 rotated 90 degrees in CCW (diameter size: 190um, and head tilt -30 degrees, 30 degrees and 0 degree). The approximate distance between patient mouth opening and the aerosol hood filter is approximately 0.4 meters (15 inches). The droplet trajectory estimates large droplets are in the jet path and will be cleared within the filters.

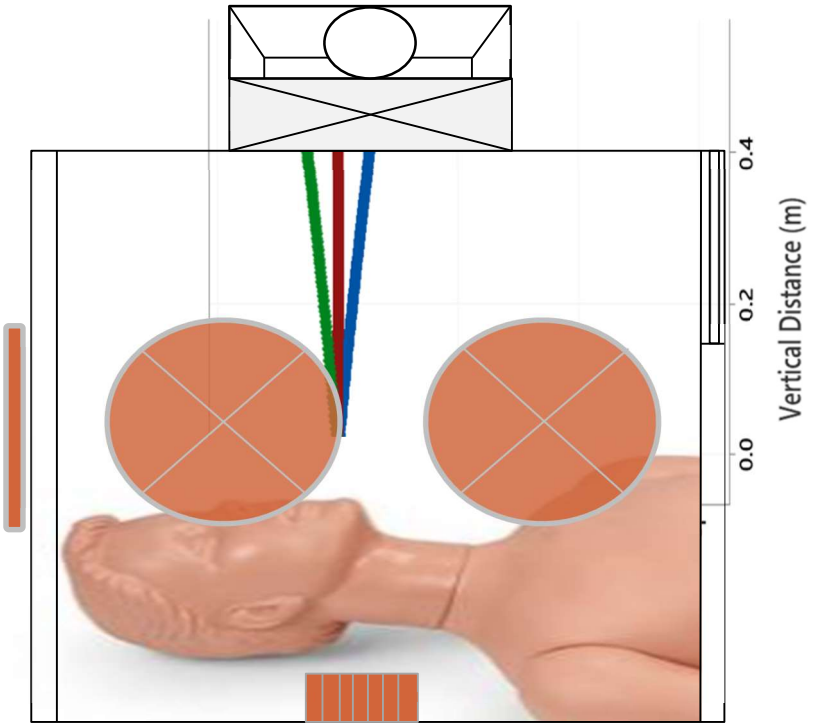

Figure 5: Hypothetical overlay of Manikin in an aerosol hood and vertical distance of droplet trajectory. The distance between the patient's mouth opening to the filter is approximately 0.4 +/- .1 meters. Large droplets (greater than the critical diameter size of 60 – 70 um) start falling off the jet after 0.3 meters for 65 um to 1.2 meters for 200 um, which is beyond the distance of the filter location. Smaller droplets would evaporate shortly after exiting the patient's mouth and carried towards by the streamline of the aerosol hood negative pressure system. Note the droplet trajectory simulations are performed for angles closer to perpendicular to gravity than depicted.

Droplet trajectory models for respiratory droplets, including those critically examining the 6ft rule distance during COVID pandemic in 2020-2021, depend strongly on the jet model [31, 37]. While not the focus of this work, these trajectories show that future work on better quantification of the jet expelled during human respiratory droplets would be necessary. To date, respiratory jets have been largely modeled using a "constant exhale" approach, which is of course not an accurate description of human breathing patterns. In the moment when droplets "fall out" of the jet strongly affects their ultimate

penetration distance into space, transient breathing models will be important to consider in the future.

2.4.2. Evaporation and Settling Curve:

The evaporation and settling curve connect the two phenomena of evaporation rate and settling rate in one graph plotted on a diameter size vs. time. The phase change between evaporation and settling time is the critical diameter size that differentiate between the small and large droplets for a given jet model and physical boundary conditions. The above Figure 6 shows the inflection point occurred at critical diameter size of 65 μm and 30 seconds at 50% Relative Humidity (RH) and 0 degrees (no head tilt). Based on our isothermal jet model, all other sizes evaporate or settle on the ground in less than 30 seconds. Diameter smaller than 65 μm evaporates within 0.3 meters of the beginning of the trajectory. Diameter larger than 65 μm settles to the ground up to 1.2 meters (in the case of 200 μm). Inside the aerosol hood, the distance between the patient's mouth and top panel where the filter is measured is approximately 0.4 meters. Given the flowrate of 64 cfm at a half power blower setting inside the aerosol hood small particles that would evaporate right away will be carried by the air flow streamlines. Larger particles will still be in the jet pathway beyond the HEPA filter. In the case of large droplets that fell off the jet path, it will be impacted inside the aerosol hood.

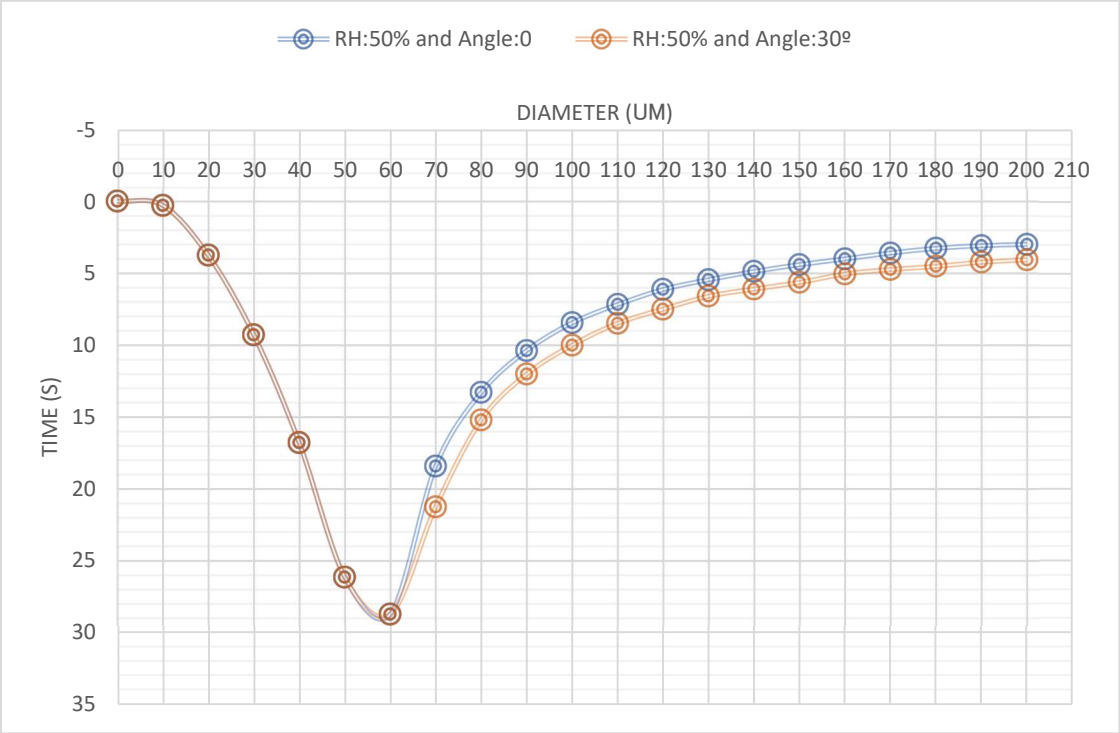

Figure 6: Evaporation and Settling Curve at Relative Humidity (RH) 50%. The upward head tilt delayed the settling time by 30 seconds although it would travel a shorter distance than the centerline head position or downward head tilt. The upward head tilt had no effect on the evaporation rate of the particles.

Figure 6 also shows a change in angle from 0 degree to 30 degrees and the settling time difference of an average of 1.4 seconds longer for the 30 degrees head tilt degree. However, the evaporation rate and the critical diameter of 65 μm did not change. The difference between the centerline and upward head tilt is statistically insignificant (p-value 0.7).

Besides the head tilt angle, the impact of relative humidity has been assessed on its effect on the evaporation and settling curve.

The typical SARS-CoV-2 virus is around 0.1 μm [38]. However, during droplet formation in a human respiratory tract, a wide range of droplets sizes are created [31]. The negative pressure system with a flowrate around 62 cfm will be able to maintain the jet stream of the respiratory droplets and pass both small and large droplets through the HEPA filter.

2.5. Conclusions

Droplet trajectories and residence time have been assessed based on current knowledge. Isothermal jet model was used to evaluate the effectiveness of the aerosol hood design to contain both small and large droplets. Following existing literature, droplet trajectory was calculated with a head tilt angle incorporated. The evaporation rate for the diameter change was also calculated that produced the evaporation and settling curve similar to Wells Evaporation and falling curve. The following conclusions were drawn:

1. The SARS-CoV-2 virus diameter size is around 0.1 μm [38], however, respiratory droplets can be as large droplets as 100 μm [31]. The 62-cfm flow rate of the half power blower setting will clear small droplets below the critical diameter size of 65 μm within seconds. While larger droplets would follow an exhaled jet path impacting inside the aerosol hood. Therefore, the aerosol hood will be able to contain both small and large droplets.

2. The evaporation and settling curve shows a critical diameter size of 65 μm at a time of 30 seconds. The head tilt angle has a non-significant impact on settling rate where a 30 degrees change resulted in an average of 1.4 seconds longer settling rates than a 0 degree.

2.6. Supplementary information

List of information available in Appendix A:

- Author's publication permission for Reference 7 and 8 in Figure S1 – Figure S2.
- Isothermal model inputs and calculation steps of the spreadsheet in Figure S3 – Figure S6.

Chapter 3: Optimized Aerosol Hood Design and Efficacy as an Engineering Control to Protect HCWs

3.1. Preface

A previous design of the aerosol hood was optimized to incorporate physician's feedback. The objective of this study is to assess the optimized aerosol hood design performance. The major design changes were the widening of the front panel opening and the use of a smaller HEPA filter (12 in. x 12 in.) than the previous HEPA filter (24 in. x 24 in.). Design features that were added to the optimized aerosol hood were iris ports, cord inlets, hospital bed straps. The air speed and noise level of the aerosol hood were measured and compared against known government guidelines. The flow rate profile showed a maximum of 0.8 mph (0.4 m/s) air flow rate in the aerosol hood which is equated to a calm wind based on Beaufort Number. The noise level for inside and outside of the hood for half power blower setting is under the NOISH recommended noise exposure limit of 85 dBA. The aerosol clearance time was used to calculate the air exchange time of the aerosol hood for a 99.9% reduction time. An average of 2.76 minutes air exchange time was observed, which is faster than the current 15 minutes air exchange time required for a 99.9% reduction time in many operating rooms. The particle penetration was calculated using a particle size distribution inside and outside of the aerosol hood with the aerosol and blower turned on.

A particle penetration of 10^{-4} with a corresponding protection efficiency of 99.99% was achieved for a half power blower setting.

Overall, the air flow and noise level inside the aerosol hood ensures in maintaining the patient's comfort inside the hood. The optimized aerosol hood design performance by a HEPA filter protection efficiency of 99.99% combined with an average air exchange time of 2.76 minutes (for 99.9% reduction corresponding to effective 151.44 air changes per hour, ACH), gives confidence in additional protection to HCWs from disease transmitting aerosols such as COVID-CoV-2 virus.

3.2. Introduction

The current infection protection modes (i.e. PPE, training, ventilation systems) in the hospital for HCWs are associated with side effects such as headache, skin injury and inconsistent application of the donning and doffing procedures. To address the unmet need, the aerosol hood was initially developed including a HEPA filter and blower [24]. After a limited use in hospitals, physician's feedback was collected for an improvement on the design. The previous design had a smaller front panel opening and one of the feedback was to widen the front opening to accommodate larger size patients more comfort [24]. Hence, the aerosol hood design was optimized from the previous design by widening the front panel opening, additional iris ports on the sides, minimizing the HEPA filter size, adding cord inlets and hospital bed straps. With the new design, the front opening is maximized to better fit a wide range of patient body size. The iris ports have been doubled on the optimized aerosol hood design to provide more accessibility and flexibility. The iris ports

of the back panel are intended for the primary HCW to reach the patient lying inside the hood. The iris ports on the side panels are intended for a support HCW to assist the primary HCW. The previous 24 in x24 in HEPA filter had a weight of aerosol hood up to 40 lbs, therefore, minimizing the HEPA filter footprint to 12 in x 12 in was essential to reduce the weight without compromising the protection efficiency. Adding cord inlets at the bottom center of the aerosol hood sides was intended to pass through any device cords needed for the patient while laying inside the aerosol hood. This also prevents HCWs using the iris ports as a cord inlet, which will not only wear out the iris ports, but also create a leak of aerosol particles out of the aerosol hood. The optimized aerosol hood has bed straps to secure the aerosol hood with the hospital bed using a hook system. In the event of inclining the hospital bed is desired, the straps will keep the aerosol hood secure on the inclined hospital bed.

The optimized aerosol hood performance was assessed in a standard laboratory environment where a BLAM Nebulizer was used to aerosolized droplet diameters sizes of 1-3 μm, which is in alignment with references for exhaled air particle sizes [4, 5]. The solution used to form aerosol was a 25ml of 20% Glycerol and DI water mix. The air speed and flow rate of the aerosol hood were characterized to determine the physical sense of the airflow on the patient during the Blower On setting that creates a negative pressure system. Furthermore, particle penetration and aerosol clearance time were evaluated to assess the efficacy of the aerosol hood design.

3.3. Experimental methods

Optimized Aerosol Hood Design: The aerosol hood was optimized from the previous design by widening the front panel opening, additional iris ports on the sides, reducing the HEPA filter size, adding cord inlets and hospital bed straps as shown on Figure 1 below. For the optimized design, the front panel opening width is 25.5 in. (65 cm) and the height is 15.1 in. (38 cm), which is 10 cm wider than the previous design.

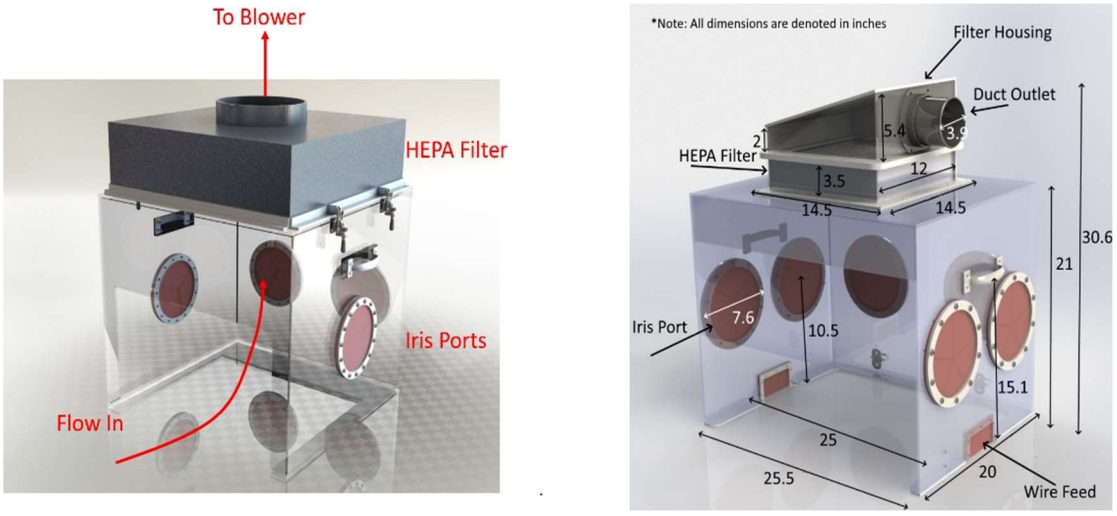

Figure 1: Aerosol hood design comparison between the previous design (left) and the optimized design (right) based on HCWs feedback. The optimized design has wider front panel opening, smaller HEPA filter footprint and more iris ports on the side panels. All dimensions are in inches.

Two 7 in. diameter 2-layer iris ports (with silicone rubber sheet) are placed on all sides of the hood to enable hand easily inside the hood. The HEPA filter unit has been reduced from a 24 in. x 24 in. to 12 in. x12 in to allow visibility from the top panel and minimize the weight of the hood without compromising filter efficiency. The optimized hood comes with a hook system that can be strapped to secure on an inclined hospital bed. Cord inlets have

been incorporated on both side panels bottom center to allow for device cord passage that is needed for the patient during clinical procedures.

Aerosol Hood Set Up: The aerosol hood set up consisted of a HEPA filter, a blower, and aerosolization method as shown in Figure 2 below. The HEPA filter was mounted on top of the aerosol hood inside a clear polycarbonate filter holder. A 4 in. diameter (0.25 in. wall thickness) and approximately 5 ft. long circular duct was used to connect the filter holder to the blower. An 8-speed setting blower (AC Infinity CLOUDLINE S8) with a diffuser was used to create the negative pressure system by withdrawing air from the aerosol hood.

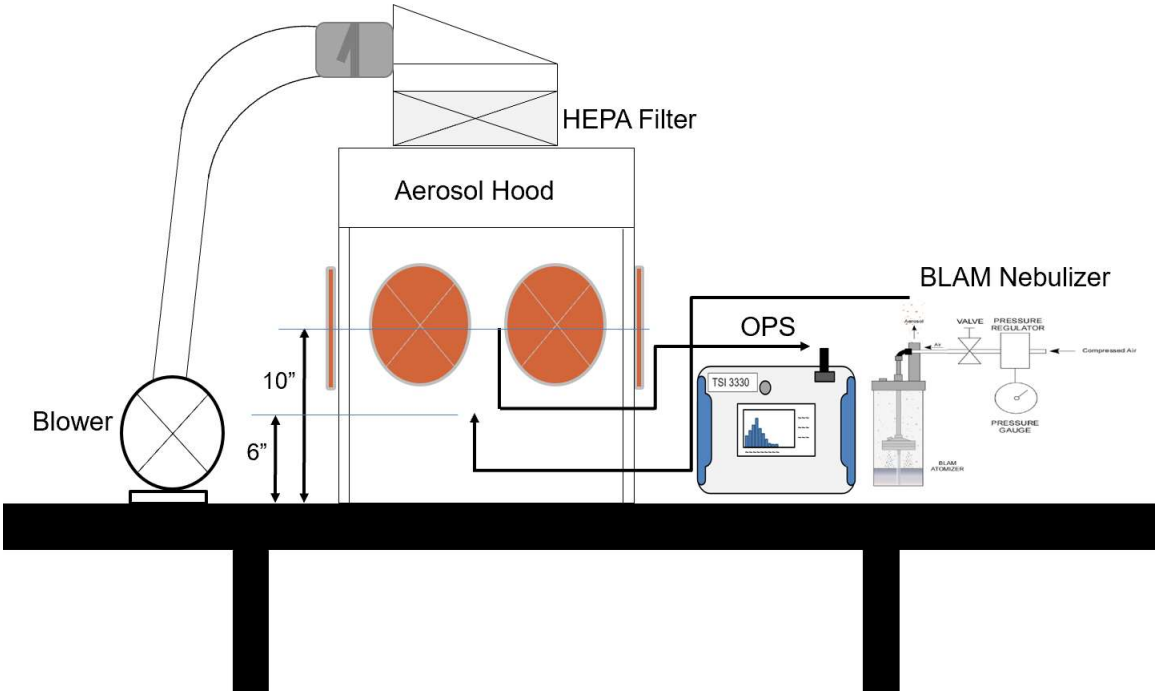

Figure 2: Schematic diagram of the aerosol hood set up to measure the protection efficiency of the blower-HEPA filter system**.** The aerosol hood connected with a blower that created the negative pressure system.

The aerosolization method used an 8-Jet BLAM Nebulizer with 20% glycerol and DI water in a 1:5 ratio. The nebulizer used compressed air to convert the liquid solution to an aerosol. Then the compressed air was regulated using a valve and a pressure gauge. The operating pressure of the nebulizer was correlated with the flow rate on a characterization data plot provided with the nebulizer. 30 psi operating gauge pressure was used that resulted in 15 L/min. flow rate of aerosol. The 8-Jet BLAM Nebulizer produced particles in the 0.5 – 3 μm size range. An outlet tube is fitted to the inlet of the nebulizer and placed at the center of the hood in an upward position in the case of a research lab. In the case of the M Simulation Lab of the University of Minnesota, the outlet tube was connected to the mannequin (SIM-man) esophagus to simulate a breathing pattern through the mouth.

Along with the aerosol hood set up, an air scrubber was used in the background to reduce the number of particles in the testing room. In the research lab, the use of an air scrubber reduced the particle number of the room by 95% after running the air scrubber for 10 minutes. In the M Simulation Lab of the University of Minnesota, the reduction in the particle number was 38% after 10 minutes, due to the clean room nature of the M Simulation Lab (i.e. the room was already low in particle concentration in comparison to the research lab.

Aerosol Hood Characterization: The flow rate measurement was conducted to assess the uniformity of incoming air (1) at the front opening of the hood, (2) directly under the filter of the top panel of the hood and (3) inside a 6 in. diameter duct using the Log Tchebycheff method. For the front opening of the hood (17 in. x 24 in) (see Figure 3 below) and directly under the filter (12 in. x12 in.), the flowrate and velocity were measured using VelociCalc at nine equidistant grid-type locations. Starting from the top left corner as a datum, 60 consecutive 1 second tests were collected.

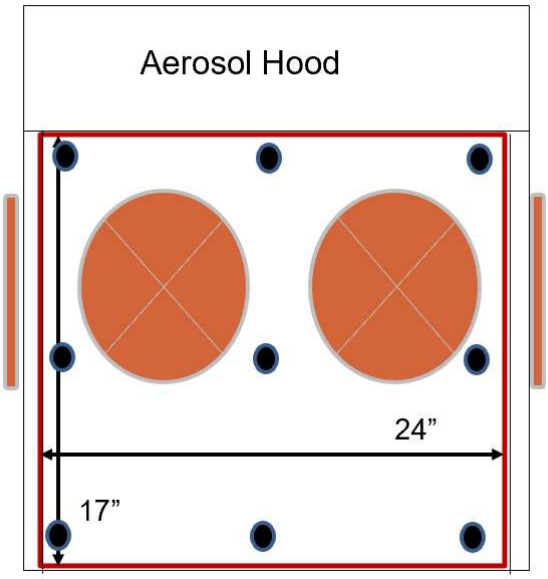

Figure 3: Nine equidistant locations of the front opening of the aerosol hood for flow rate measurement.

The average velocity of the aerosol hood was calculated from the flowrate and compared to the wind speed Beaufort number from weather.gov website [27] to determine the comfort level of the air speed for the patient that would be laying in the aerosol hood. In addition, the level of noise in the aerosol hood was measured using Digi-Sense Data Logging Sound Meter with NIST-Traceable Calibration. The previous aerosol hood design

was used to measure the noise level (because of availability), which is the worst case as it has a HEPA filter 24 in. x 24 in. 4 times bigger than the optimized aerosol hood design. The sound measure was taken at a single location at the center inside the hood and three locations at left, right, back outside the hood.

Aerosol Clearance Time: The particle concentration clearance time was tested in two environments: (1) in a Research Lab and (2) in a M Simulation Lab of the University of Minnesota. The Research lab testing showed the potential of clearance time without the interference of human factors; the transit time to the measurement instruments was minimized and data collection was automated. The M Simulation Lab was representative of clinical setting with the clearance time being impacted by human intervention to make the measurement and by tubing lengths to instruments, which would likely be the case for workers testing a product. In a research lab using a Laskin nozzle aerosol generator (ATI Model 4B, Owings Mills, MD) instead of the 8-Jet BLAM Nebulizer and Condensation Particle Counter (CPC, Model 3025A, TSI inc. Shoreview MN) instead of OPS. A sample was run for each blower settings (Half Power and Full Power) for 5 minutes continuously. In the M Simulation Lab, an 8-Jet BLAM Nebulizer was turned on for 5 seconds in the hood then turned off, which filled the hood with visible smoke. Then, the blower was turned on along with an Optical Particle Sizer (OPS, TSI Model 3330) to record the time it took for the blower to suction all the aerosol particles released for 5 seconds. A single sample consisted of 1 second data acquisition of 300 samples (5 minutes in total). Two blower settings, Setting 4 (Half Power) and Setting 8 (Full Power) were used to collect three samples for each setting.

Air Exchange Rate and Time: The air exchange time corresponds to the time required for 99.9% reduction in aerosol concentration following a "burst" of aerosol generation, coinciding with the CDC determined clearance time required for operating rooms [28]. To determine the air exchange time, the characteristic time for clearance (θ) is calculated using Equation (1) below. Second, the air exchange rate (units of inverse time) at which air is cycled through the hood is calculated using Equation (2). It is parameterized through a plot of particle concentration versus time for experiments where the aerosol is introduced prior to aerosol hood operation. The slope of the plot was inversely proportional to the negative value of τ, which is the time constant. Finally, the air exchange time is calculated by multiplying τ with the natural log of 0.001 (for a 99.9% reduction time greater than CDC requirements) using Equation (3).

$$\theta\ (Characteristic\ Time) = ln\left(\frac{Particle\ Concentration - Backgroun\ \ Concentration}{Maximum\ Concentration - Background\ Concentration}\right) \quad (1)$$

$$Slope\ =\ -1/\tau \quad (2)$$

$$Air\ Exchange\ Time\ =\ -ln\ (0.001) * \tau = 6.908 * \tau \quad (3)$$

Where the Particle Concentration is the number of particles per volume (#/cm^3) when the aerosol was turned on with the blower off. The Background Concentration is the number of particles per volume (#/cm^3) with no aerosol turned on but with the blower turned on and Maximum Concentration is the highest concentration value from the Particle Concentration used as a constant. Correspondingly the air changes per hour (ACH) is calculated as:

$$ACH = (1/\tau) * 3600 second/hour \quad (4)$$

Particle Penetration Calculation: The particle penetration (P) on Equation (5) is the ratio of the particles outside the hood to the inside of the hood while the aerosol is turned on. Where measurements consisted of a size distribution measurement of the outside of the hood with an aerosol generator turned on and a blower turned on (O_{on}) and inside the hood with an aerosol generator turned on and a blower turned on (I_{on}).

$$P = (O_{on})/(I_{on}) \quad (5)$$

An outside of the hood background air measurement (O_{off}) was also collected on the right, left and front sides, which were all overlapping [Suppl Figure 1]. Inside of the hood, the 6 locations were center (C), center 1 (C 1)(slightly to the right of the center), center 2 (slightly to the left of the center) (C 2), left (L), right (R) and front (F)as shown on Figure 4 below.

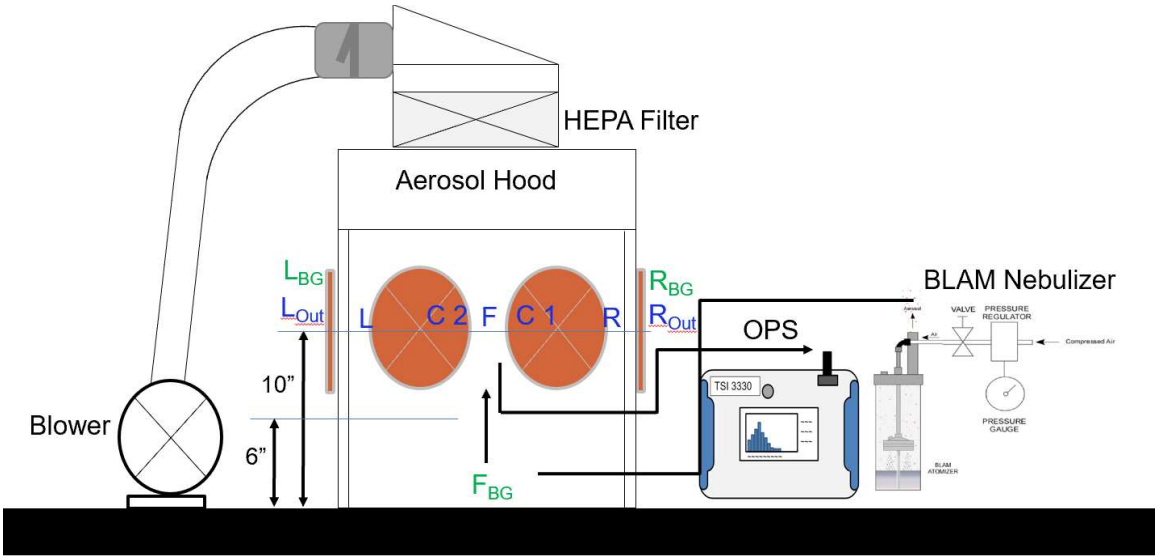

Figure 4: Location of particle penetration measurements on the aerosol hood set up.

All measurements were taken at a height of 10 in. from the bottom surface of the aerosol hood, which is the iris ports center as the worst-case condition where aerosol particles could escape. The aerosol generator outlet was 6 in. high at the center of the hood in both cases of the research lab set up and in the case of SIM-man. For the SIM-man, the aerosol was connected to the esophagus tract and through the mouth (i.e. approximately 6 in. in height).

3.4. Results and Discussion:

3.4.1. Level of Air Speed and Noise

The air speed and noise inside and outside of the hood are important for the patient and the HCW. The air speed ensures that the patient is not experiencing a high flow rate that causes discomfort during the procedure.

The flowrate of the aerosol hood front panel opening had an average of 133 cfm (cubic feet per minute, where 1 cfm = 1.7 m^3 hr^{-1}, used here as cfm is the most commonly used unit for ventilation rates in the United states) for a full power (Setting 8) and an average of 62 cfm for a half power (Setting 4) [Suppl Table 4]. Similar data was achieved for the flow rate directly under the HEPA filter that is provided on Supplemental Table 5. What is shown on Figure 5 is the flowrate profile contour plot for the average of both half and full lower power. The profile shows a range of flow rate from a minimum of 74 cfm at the bottom of the front panel opening to a maximum of 141 cfm at the top.

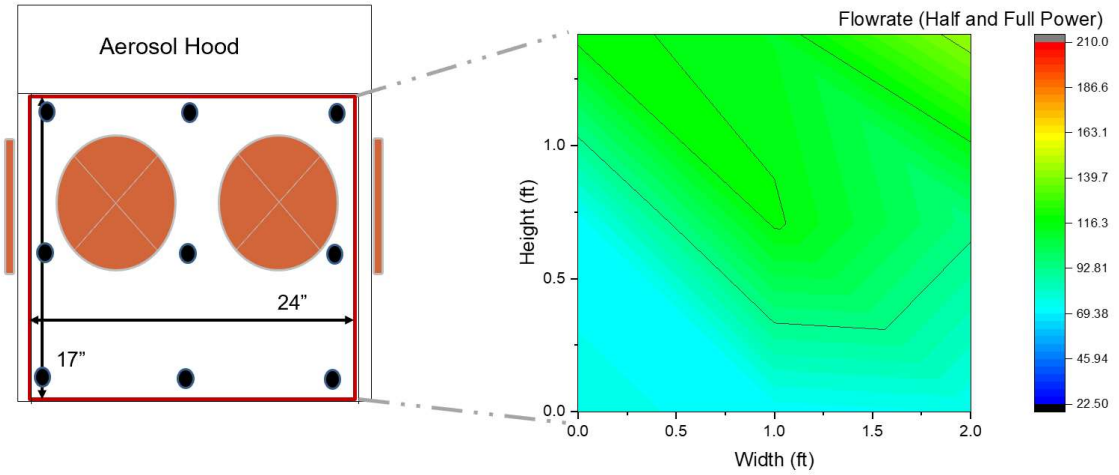

Figure 5: Flow Rate profile of half and full blower power average on the front opening of the aerosol hood.

The flowrate is higher on the top of the hood based on the opening proximity to the filter location. The flowrate result confirms that there is a uniform airflow into the hood that will direct the patient's respiratory droplets to the HEPA filter and suctioned by the blower. Therefore, the HCWs are protected from aerosol-based disease transmission due to the uniform flow rate of the negative pressure system of the aerosol hood.

The maximum velocity achieved from a full power blower setting resulted in 0.8 mph (0.4 m s^{-1}) velocity, which correlated with a Beaufort number of zero for an air speed less than 1 mph as shown in Figure 6 below. This indicates that the air speed is a calm wind where smoke rises vertically with little drift.

Estimating Wind Speeds with Visual Clues

Beaufort number	Description	Speed	Visual Clues and Damage Effects
0	Calm	Calm	Calm wind. Smoke rises vertically with little if any drift.
1	Light Air	1 to 3 mph	Direction of wind shown by smoke drift, not by wind vanes. Little if any movement with flags. Wind barely moves tree leaves.
2	Light Breeze	4 to 7 mph	Wind felt on face. Leaves rustle and small twigs move. Ordinary wind vanes move.
3	Gentle Breeze	8 to 12 mph	Leaves and small twigs in constant motion. Wind blows up dry leaves from the ground. Flags are extended out.

Figure 6: Beaufort number to estimate wind speed and its visual clues [27].

Similar analysis of the noise level was conducted as the air flow speed. The noise level inside the hood is also important for the patient to not be disrupted by the high level of noise. The noise level outside the hood impacts HCWs ability to communicate with the patient and with one another. For the outside the hood, the sound measurement indicated a maximum noise level of 64.3 dBA, which is a 2.7% increase from the blower off testing condition as a negative control for a half power blower setting (See Figure 7 below). A full power blower setting resulted in a maximum noise level of 81.5 dBA, which is 23.3% increase from the blower off testing condition. The minimum and average noise level data is found in the Appendix (Suppl. Table 2).

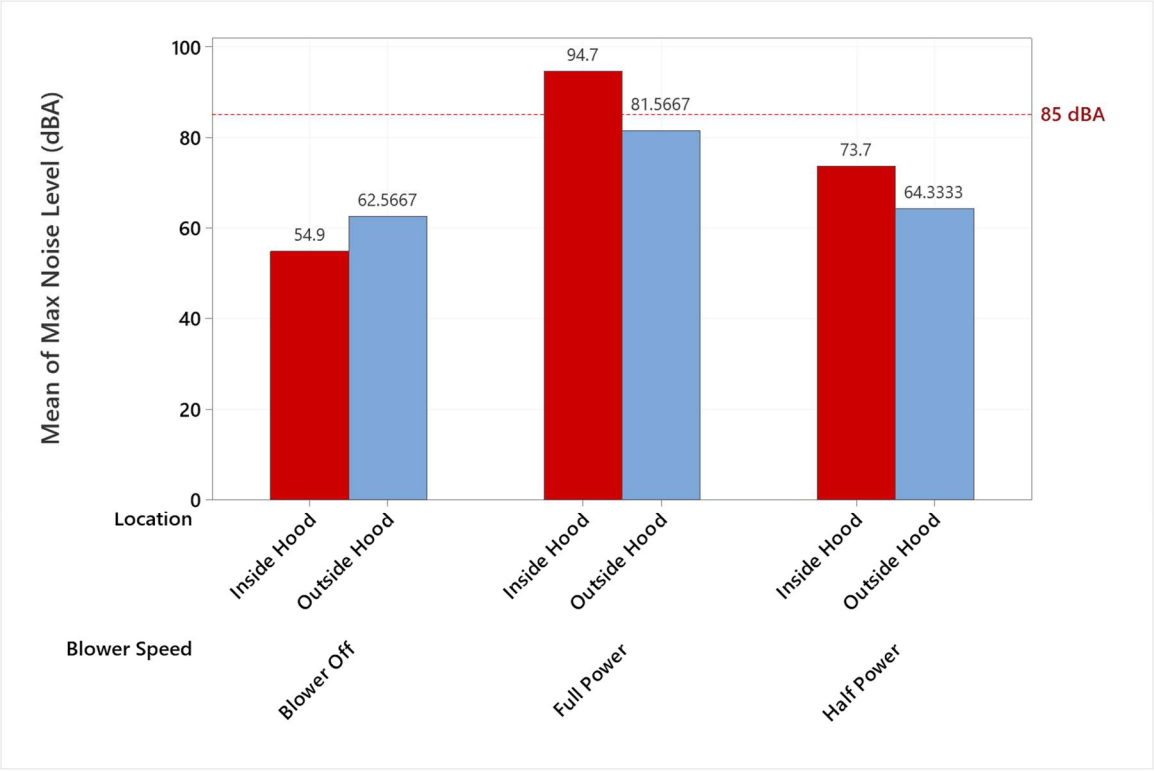

Figure 7: Maximum Noise level inside and outside of the aerosol hood using a sound measurement tool.

The results shown on Figure 7 above are in the range of safe sound levels except the full power inside the hood. According to the National Institute for Occupational Safety and Health (NIOSH), the recommended noise exposure limit is below 85 dBA as shown on Figure 8 below [36]. 60 dBA is a normal conversation and 70dBA is vacuum cleaner noise level [Suppl. Figure 3], which will be what a patient side the hood will experience with a half power blower speed. In the meantime, the outside of the hood noise level between blower off and half blower is less than 5%, which causes no barriers as HCWs communicate with one another or the patient. Although a full power blower setting has a

higher protection efficiency, we recommend a half power blower setting that has sufficient protection efficiency and allowable noise level.

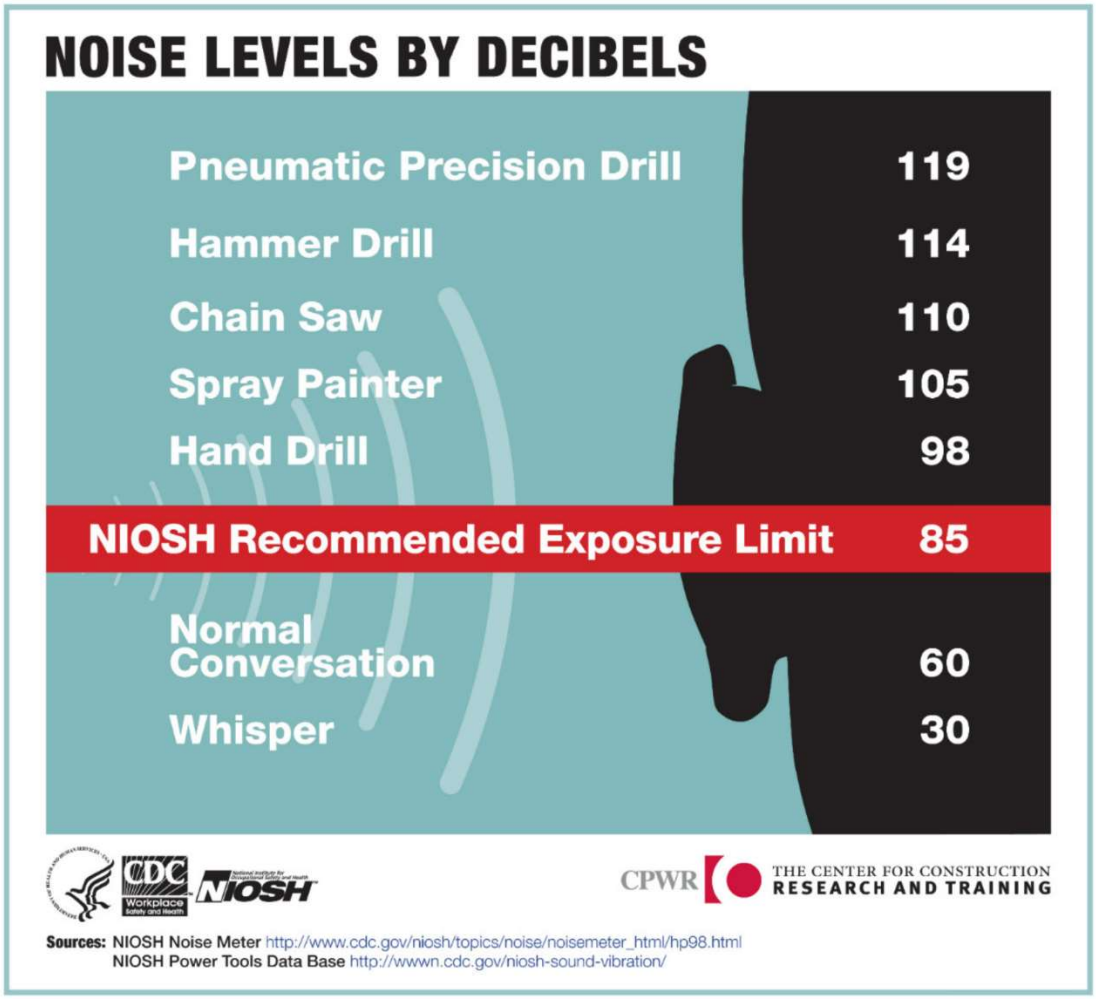

Figure 8: The recommended exposure limit of noise levels by NIOSH [36]. The half power blower setting is well under the exposure limit, while the full power blower setting nears the exposure limit.

Overall, the flow rate profile and sound measurement confirm that the aerosol hood design has a safe level air speed and noise level for both patients and HCWs.

3.4.2. Air Exchange Time

Figure 7 displays plots of raw data particle concentration versus time for both the research laboratory and M Simulation laboratory measurements. The Research Lab (Figure 7c) was characterized by a rapid drop of the particle concentration from a maximum of 60,000 cm^{-3} particle concentration. This is due to the research laboratory set up had an aerosol outlet tube directly in the hood that avoided delay in the time effects of the aerosol reaching the measurement system. Meanwhile in the M Simulation Lab (Figure 9a and 9b), the aerosol outlet tube was connected to the abdomen of the Sim-Man and had to travel through the esophagus and reach the mouth opening causing a delay, which is more representative what would be expected if the users of the hood choose to test its efficacy in a hospital setting, without the ability to automate the process as in an aerosol research laboratory. In addition, two different particle sizers (CPC and OPS) and two different aerosol generators (API and BLAM Nebulizer) were used for the Research Lab and M Simulation Lab.

The normalized particle concentration (θ) versus time was plotted for the M Simulation Lab as shown on Figure 10. The plot shows a gradual negative slope of the particle concentration reduction for approximately 60 seconds (1 minute). Unfortunately, similar type of graph could not be made for the Research Lab due to its rapid decrease, a single point measurement was performed to achieve the equivalent slop value (i.e. the condensation particle counter response time is not fast enough to accurately infer the concentration decay in the research lab setting). For the research lab the air changes time 2.25 seconds for half power and 0.53 seconds for full power.

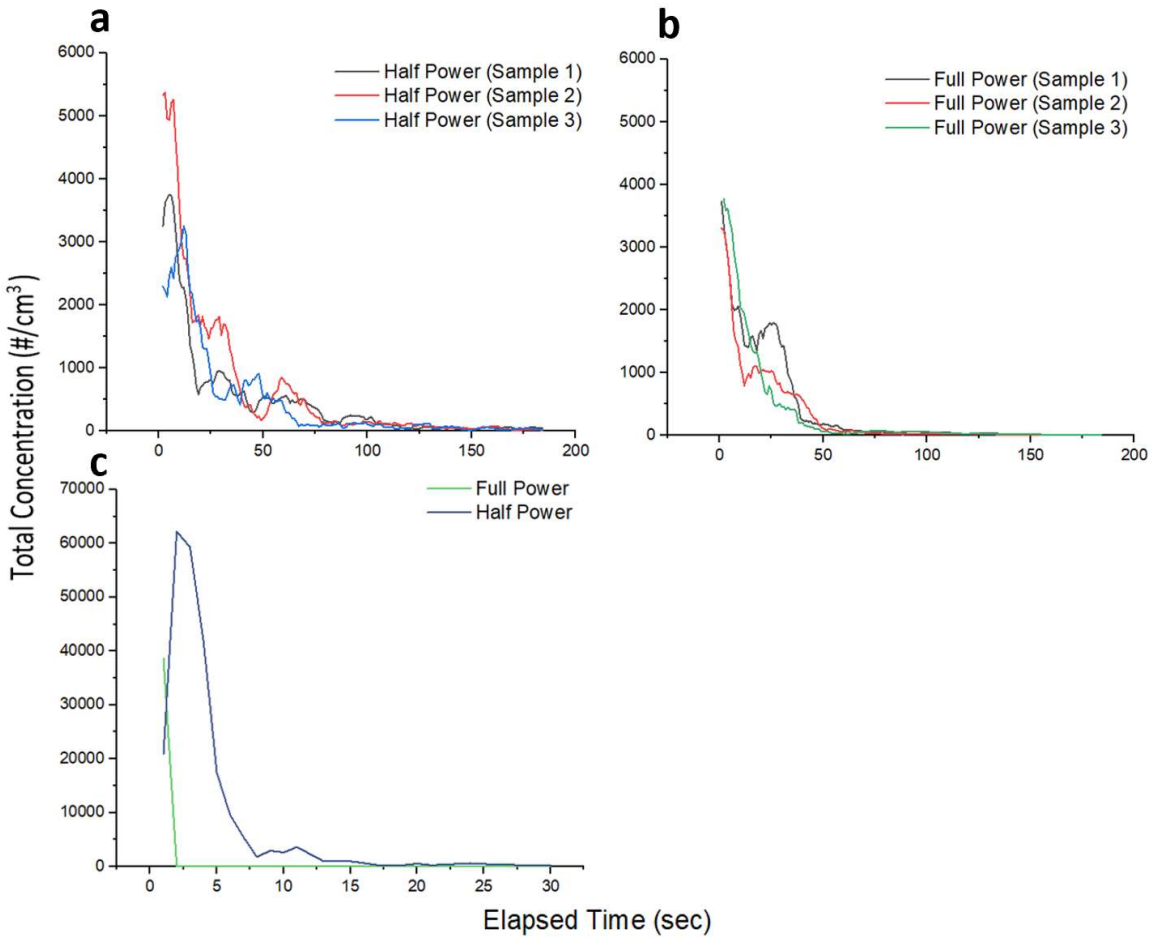

Figure 9: Raw data particle concentration clearance in the hood as a factor of time resulting in gradual negative slope for graph 9a and 9b, and rapid negative slope for graph 9c. (**a**) M Simulation lab set up half power, (**b**) M Simulation lab set up full power, and (**c**) Research lab set up half and full power.

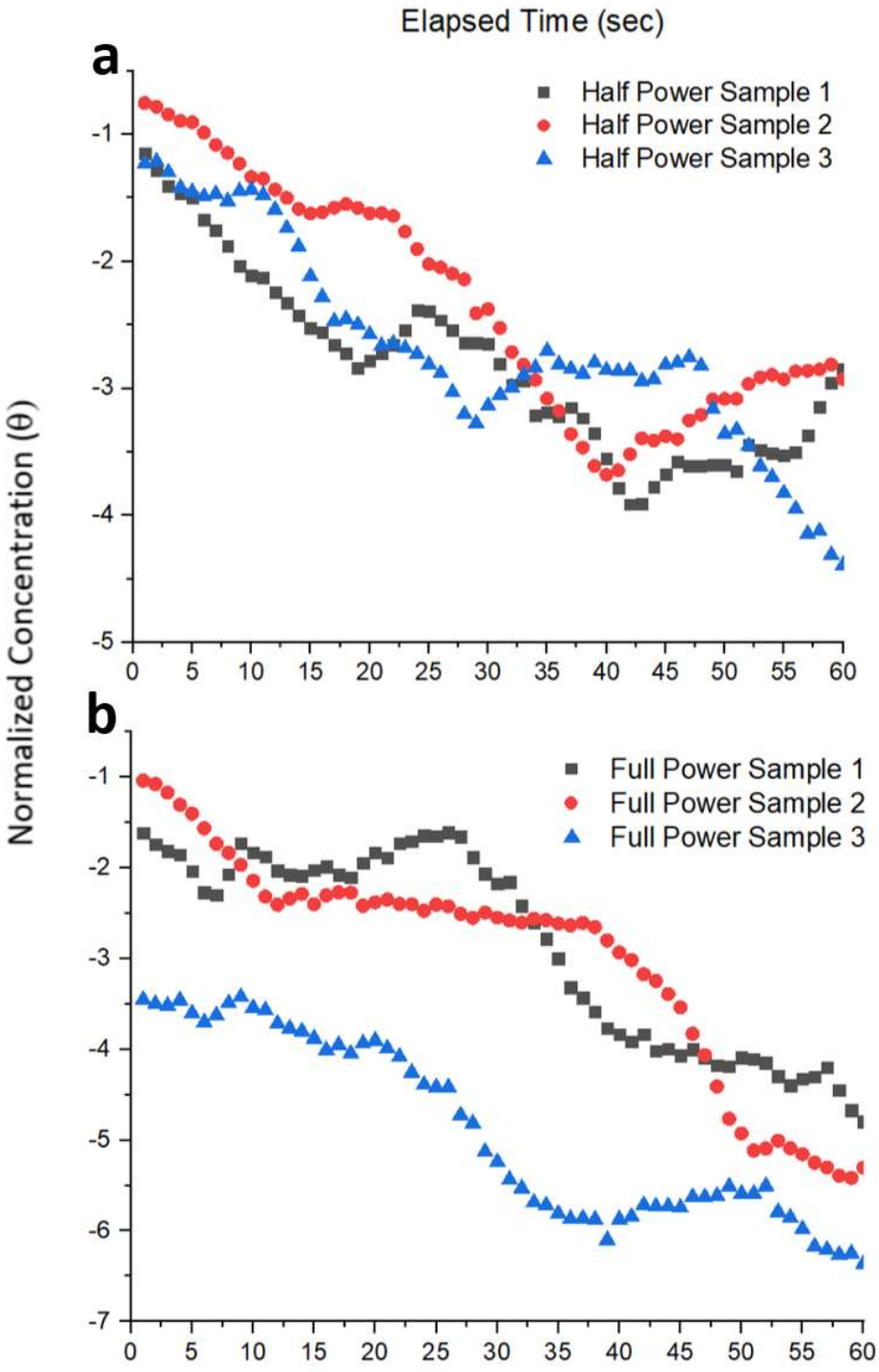

Figure 10: Normalized particle concentration (θ) with a negative slope for the first 60 seconds. (**a**) M Simulation lab set up half power, (**b**) M Simulation lab set up full power.

Table 1: Air change time and ACH for aerosol hood resulting higher than the recommended CDC guidelines.

Simulation Lab	Air Change Time (min)		ACH	
	Half Power	Full Power	Half Power	Full Power
Sample 1	3.18	2.07	129.96	199.8
Sample 2	2.44	1.71	169.56	242.28
Sample 3	2.67	2.17	154.8	190.44
Average	2.76	1.98	151.44	210.84

For the M Simulation lab, the negative slope was calculated from the graphs of Figure 10 above to calculated for the Air change time in minutes and ACH. Our results show the aerosol hood has an air exchange time of 2.76 minutes in average, even accounting for user error in measurement, with an average ACH of 151.44. The 2003 CDC guidelines for infection control tabulate airborne contamination removal times for an ACH (Air Change per Hour) is listed on Supplemental Table 6 in Appendix B. For 99.9% reductions, with ACH from 10 – 15, 28 – 41 minutes are required in a hospital setting and the results shown on Table 1 above for the aerosol hood exceeds the guideline requirement. Therefore, by confining aerosol release events to small volume and actively clearing such volume, we can greatly reduce the wait time between operating room procedures, as effectively no aerosol release event occurs in the first place. The aerosol hood hence not only reduces the risk of infection transmission per the flowrate profile results, but also increases hospitals capacity to provide more patient care.

3.4.3. Particle Penetration

High ACH and correspondingly reduced air change time are driven by the high flow rate to enclosed ratio of the aerosol hood. It is equally important to examine penetration of particles from inside to outside. Though certainly linked to the ACH, penetration, which is the ratio of outside particle concentration to inside particle concentration while the aerosol and blower are turned on, is also dependent on the quality of the filter used and the aerosol remaining leak tight aside intentional openings. Tables 1 and 2 below shows the raw data of particle concentration ($dN/dlogD_p$) for inside and outside of the hood while the aerosol and blower turned on (negative pressure system running). The full blower power (Table 2) has more difference between the inside and outside particle concentration resulting in higher penetration value. Depending on the flow streamlines, the center and right measurement locations had higher particle concentration compared to the left and front measurement locations. For comparison, Background (BG) measurements were taken outside of the hood with no aerosol generation, but the blower turned on. The measurement between BG outside the hood with aerosol off and with aerosol on were so close to one another slightly higher reading while the aerosol is turned off. This is due to the aerosol generated during aerosol turned on is negligible compared to the number of particles in a non-clean room, it is difficult to pick up clear difference whether the aerosol is turned on or off. This negligible level of aerosol production is representative of a patient respiratory activity compared to the particles in the hospital setting.

Table 2: Half blower power particle concentration by Diameter size. BG O(off) = Background Outside of the hood, aerosol turned off, blower on. O (on) = Outside of the hood with aerosol and blower turned on. I(on) = inside of the hood with aerosol and blower turned on.

Half Blower Power (Setting 4)			Aerosol Hood Locations I(on) (dN/dlogDp)				
MP Diameter Size (um)	BG O(off)	O(on)	Center 1	Center2	Right	Front	Left
0.337	1.51E+02	1.47E+02	4.68E+03	4.82E+03	9.95E+03	1.56E+02	4.90E+03
0.4195	4.50E+01	4.38E+01	3.92E+03	3.44E+03	7.17E+03	4.81E+01	3.65E+03
0.522	1.02E+01	9.79E+00	3.77E+03	2.69E+03	5.11E+03	1.21E+01	2.90E+03
0.65	2.00E+00	1.83E+00	1.66E+03	1.21E+03	2.13E+03	2.97E+00	1.25E+03
0.809	3.76E-01	3.41E-01	1.27E+03	8.00E+02	1.12E+03	6.87E-01	7.99E+02
1.007	2.35E-01	1.72E-01	4.69E+03	9.27E+02	9.66E+02	5.22E-01	1.65E+03
1.254	2.63E-02	2.63E-02	1.61E+03	2.63E+02	2.29E+02	8.12E-02	5.25E+02
1.5615	1.41E-02	1.41E-02	1.29E+03	2.21E+02	2.02E+02	9.70E-02	4.28E+02
1.944	4.25E-03	4.25E-03	7.51E+02	1.24E+02	1.11E+02	4.40E-02	2.47E+02
2.4205	2.27E-03	0.00E+00	1.22E+02	1.70E+01	1.33E+01	3.41E-03	3.80E+01
3.014	1.83E-03	9.13E-04	9.18E+00	1.44E+00	1.46E+00	9.13E-04	3.02E+00
3.7525	1.47E-03	0.00E+00	4.99E-01	1.50E-01	1.91E-01	0.00E+00	2.10E-01
4.672	0.00E+00	0.00E+00	2.56E-02	6.40E-03	7.66E-03	5.89E-04	1.01E-02
5.8165	0.00E+00	0.00E+00	0.00E+00	0.00E+00	6.55E-04	0.00E+00	1.64E-04
7.2415	0.00E+00	0.00E+00	7.36E-04	4.24E-04	0.00E+00	3.80E-04	3.85E-04
9.016	0.00E+00	0.00E+00	5.57E-04	0.00E+00	0.00E+00	0.00E+00	1.39E-04

Table 3: Full blower power particle concentration by Diameter size. BG O(off) = Background Outside of the hood, aerosol turned off, blower on. O (on) = Outside of the hood with aerosol and blower turned on. I(on) = inside of the hood with aerosol and blower turned on.

Full Blower Power (Setting 8)			Aerosol Hood Locations I(on) (dN/dlogDp)				
MP Diameter Size (um)	BG O(off)	O(on)	Center 1	Center2	Right	Front	Left
0.337	8.44E+01	8.41E+01	4.78E+03	1.42E+03	1.29E+04	9.63E+03	6.36E+03
0.4195	2.80E+01	2.83E+01	5.34E+03	1.17E+03	1.19E+04	9.01E+03	6.13E+03
0.522	6.79E+00	6.91E+00	6.60E+03	1.00E+03	1.37E+04	1.04E+04	7.09E+03
0.65	1.29E+00	1.52E+00	3.85E+03	5.34E+02	8.02E+03	6.07E+03	4.13E+03
0.809	3.36E-01	3.55E-01	3.65E+03	3.78E+02	7.57E+03	5.72E+03	3.87E+03
1.007	3.09E-01	1.83E-01	1.56E+04	4.63E+02	9.40E+03	8.95E+03	8.49E+03
1.254	5.04E-02	3.78E-02	6.71E+03	1.51E+02	3.34E+03	3.37E+03	3.40E+03
1.5615	6.31E-03	3.15E-02	6.79E+03	1.62E+02	3.51E+03	3.50E+03	3.48E+03
1.944	1.89E-02	1.89E-02	4.76E+03	9.95E+01	2.31E+03	2.35E+03	2.39E+03
2.4205	6.30E-03	0.00E+00	8.55E+02	1.15E+01	3.16E+02	3.55E+02	3.94E+02
3.014	1.26E-02	6.31E-03	6.25E+01	8.54E-01	2.25E+01	2.55E+01	2.86E+01
3.7525	6.31E-03	6.31E-03	2.75E+00	8.09E-02	1.44E+00	1.43E+00	1.43E+00
4.672	0.00E+00	6.31E-03	5.89E-02	0.00E+00	3.81E-02	3.52E-02	3.23E-02
5.8165	0.00E+00	0.00E+00	0.00E+00	0.00E+00	0.00E+00	0.00E+00	0.00E+00
7.2415	6.31E-03	0.00E+00	0.00E+00	0.00E+00	1.37E-02	9.11E-03	4.55E-03
9.016	0.00E+00	0.00E+00	0.00E+00	0.00E+00	0.00E+00	0.00E+00	0.00E+00

Using the above O (on) and I(on) data, the particle penetration results were 10^{-4} to 10^{-5} for a half power and 10^{-5} for the full power for particle size between 0.5 – 3.0 μm (Figure 8). The 10^{-4} (half power) and 10^{-5} (full power) particle penetration resulted in 99.99% and 99.999% protection efficiency (protection efficiency = 1- particle penetration) of the HEPA filter, respectively. The previous aerosol hood design resulted in particle penetration around 10^{-3} to 10^{-4} for particle size of 0.1 – 0.5 um [24]. Although the particle sizes were different between the two studies, this indicates that the protection efficiency has not been compromised even if the HEPA filter size was reduced by half size.

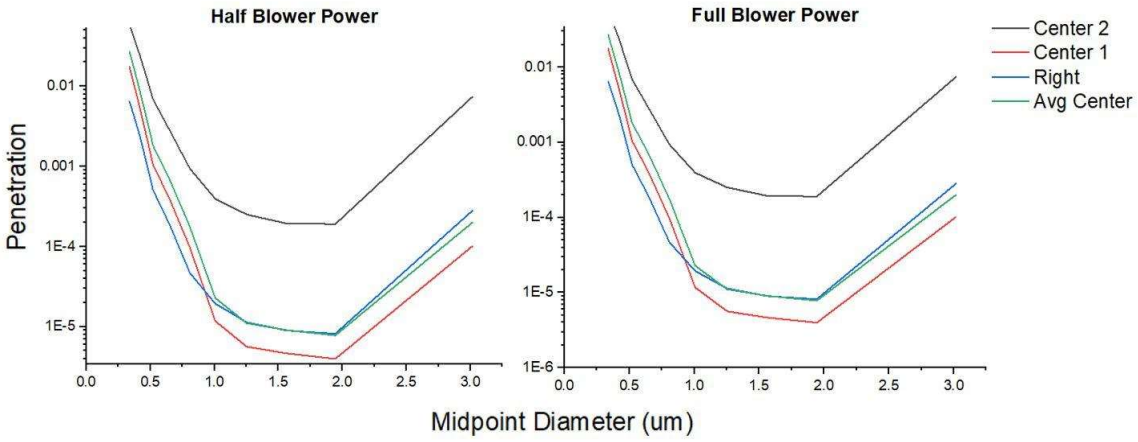

Figure 11: Particle penetration results of half and full blower power setting.

Since the full blower power has higher noise that is safe but too loud for normal noise level, we recommend using half blower power with a 99.99% protection efficiency, which is still higher than the standard 99.9% aerosol reduction guideline from CDC [28].

3.5. Conclusions

The aerosol hood design has been optimized based on physicians and HCWs feedback. The optimized aerosol hood design performance was assessed by measuring the characteristics of the flow rate profile, sound measurement, air exchange time and particle penetration. The two testing conditions were half power (Setting 4) and full power (Setting 8) of the blower. The flow rate was measured using a grid type equidistance velocity measurement. The air exchange time was calculated from the slope of particle concentration vs. elapsed time plot to achieve the 99.9% aerosol reduction. The particle penetration was taken as a ratio between the particle concentration inside and outside of

the hood when the aerosol generation and blower were both turned on. The following conclusions were drawn:

1. The maximum flow rate with the full power blower setting was 0.8 mph (0.4 m/s), which is at the level of Beaufort Number 0 for calm air speed. The maximum sound measurement for half power blower speed inside the hood is 73.7 dBA, which is near a vacuum cleaner noise level and under the NOISH recommended noise exposure limit of 85 dBA. Outside of the hood, the noise level is 64.3 dBA, which is near the conversation speech level of 60dBA. The optimized aerosol hood design provides a uniform air speed and safe noise level inside the hood with a half power blower setting.
2. The aerosol hood has an average of air exchange time of 2.76 minutes and an ACH that is 151.44 on average for 99.9% reduction in M Simulation Lab. The true air exchange rate, however, is much faster than this, but difficult to quantify due to the slow time response of aerosol measurement instruments in comparison to the air exchange time. The aerosol hood effectively contains the aerosol generated within the hood and results in higher air change rates. Therefore, this result shows the potential of eliminating wait time between procedures for the 99.9% reduction time and increase hospital's capacity to provide for more patient care. The aerosol hood not only reduces the risk of infection transmission towards HCWs but can enable improved care through increasing the number of procedures per day in a hospital network.
3. The recommended half power blower setting has a particle penetration of 10^{-4} for a particle size range of 0.5 – 3.0 μm. This particle penetration results in a protection efficiency of 99.99%. The optimized aerosol hood design performance by HEPA filter

protection efficiency of 99.99% combined with an average air exchange time of 2.76 minutes, gives confidence in protecting HCWs from disease transmitting aerosols such as COVID-CoV-2 virus.

3.6. Supplementary information

List of information available in Appendix B:

- Sound measurement of the hood and level of noise exposures in Table S1 and Figure S1
- Flow rate measurement using equidistance locations and Log Tchebycheff fraction of duct inner diameter from Table S2 to Table S5
- Air changes/hour (ACH) and time required for airborne-contaminant removal by efficiency in Table S6
- Background particle concentration with the blower on and aerosol generation off in Figure S2

Chapter 4: Simulated Intubation Procedure in a Simulated Hospital Setting to Assess Exposure in a Room and Deposition on HCWs' PPE

4.1. Preface

PPE, training, and hospital ventilation systems (including high air change rates and negative pressure rooms) are the common controls for protecting Health Care Workers (HCWs) from disease transmitting aerosols such as the SARS-CoV-2 virus. The objective of this study is to assess the aerosol hood technology efficacy as an additional engineering control for both hospital room ventilation and HCWs PPE. A simulated intubation procedure was conducted in a simulated hospital setting with 4 participants (currently registering 6 more participants). Participants performed the simulated intubation on a SIM-man who is connected to aerosolization mixture of fluorescien dye with glycerol and DI water. The aerosol exposure was evaluated by taking particle concentration measurements in two locations in the room: next to the SIM-man by the bedside and in the corner of the room as a background. The particle deposition was evaluated by using fluorescein dye in the generated aerosol and collected on tape substrates that were placed on participants PPE (face shield, gloves, and gowns). In both cases evaluations testing conditions were Baseline, Blower On and Blower Off for each participant.

Because of aerosol continuously released from the mouth of the Sim-Man, the aerosol exposure by the bedside had a 5 times higher particle concentration than the background location in the absence of hood. With the Blower On testing condition, the particle concentration by the bedside reduced by 78% for all participants compared to Blower Off and Baseline testing conditions. Particle deposition on a face shield and gowns had a 42% decrease for all participants in compared to the Baseline testing. However, the gloves had 32% higher particle deposition when compared to Baseline testing. The intubation and overall procedure time were tracked manually and using video footage. There was no statistical difference (p-value 0.685) among the testing conditions except a 30 second increase for the use of aerosol hood when compared to the Baseline testing. Physicians were interviewed on their feedback regarding the aerosol hood technology use and their feedback are 1) the potential for the aerosol hood negative pressure in being used in clinical use and physicians adjusting to it 2) a continuous improvement need on the aerosol hood design in making it ergonomically friendly to give more hand flexibility and account for challenging intubation procedures.

Overall, the localized negative pressure system of the aerosol hood has a potential in reducing the wait time for 99.9% aerosol reduction in a hospital room. The physical isolation property of the aerosol hood would protect HCWs PPE from experiencing high deposition. The amount of particle deposition varies from participant to participant based on their intubation procedure practice, therefore, PPE, especially gloves are still critical disease control measures. Given the benefit of an additional protection from infectious

viruses such as SARS-CoV-2, outweighs the concerns of the minimal increase in procedure time and adaptation of a new technology.

4.2. Introduction

HCWs use three protection methods to control risk of disease transmitting aerosol exposure that are PPE, training, and the hospital ventilation system, including negative pressure rooms, and the high air change rates in operating rooms. According to CDC Hierarchy of Controls, PPE and training are the least effective forms of controls [11]. The introduction of the aerosol hood as an engineering control is one level higher than PPE and Training. Although the presence of an aerosol hood does not eliminate the need for proper PPE use and training, it provides a physical isolation and a negative pressure system as an additional control to relief from PPE side effects such as skin injury and headache [33-35].

The aerosol hood not only enhances the current use of PPE and Training, but also improves the hospital ventilation system. The current hospital ventilation system Air Change per Hour (ACH) can often take 15 minutes or more to achieve 99.9% aerosol reduction. In Chapter 3, a localized negative pressure system of the aerosol hood can achieve the same percentage of aerosol reduction in less than 4 minutes, which has the potential to significantly decrease the wait time in between aerosol generating clinical procedures.

To quantify the aerosol exposure control measures, a simulated intubation procedure clinical study was conducted with 4 HCW participants (registering 6 more participants to complete the study) in a simulated hospital setting (see Figure 1). The

particle concentration of the simulated hospital setting was analyzed by elapsed time and categorized by the three study conditions (i.e. Baseline, Aerosol Hood with Blower Off and Aerosol Hood with Blower On). A piece of tape was placed on participants' PPE such as the face shield, gloves, and surgical gown to quantify the aerosol deposition using a fluorescein dye marker. Duration of the intubation time and overall procedure time were also tracked to compare time difference with and without the aerosol hood. The last step of the clinical trial was an interview with the participants on their use experience and feedback for future design improvement. Based on such practical user experience, a continuous improvement can be made to achieve an effective ergonomic design that facilitates the adaption of the aerosol hood technology.

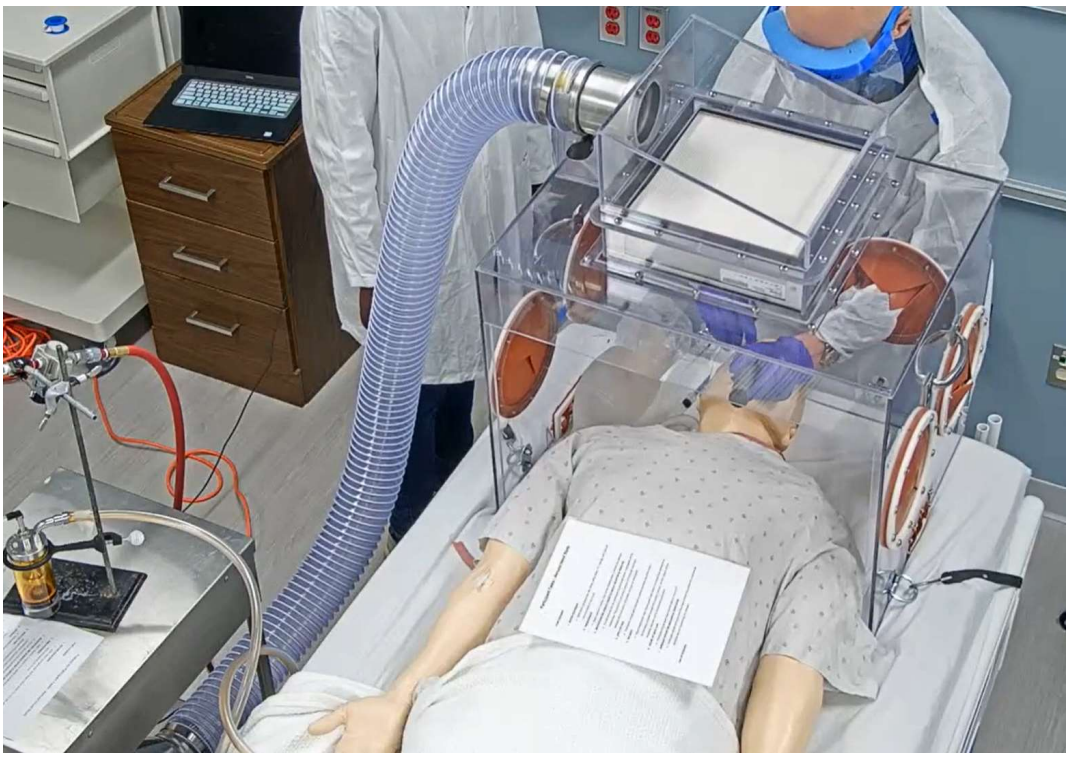

Figure 1: Clinical trial of simulated intubation procedure being conducted in a simulated hospital setting in the UMN M Simulation Lab.

The clinical trial enabled a collaboration between engineers and physicians for a common cause of improving the development of aerosol hood technology and promoting early adaptors for more use of the aerosol hood in hospitals. Such collaboration of the primary user at the early stage of technology prototype and development facilitates the translation of clinical research to a practical product. According to the NASA Technology Readiness Level [30], there are nine levels of technology; where level 1 – 3 are early research, level 4 – 6 are technology development and level 7 – 9 technology ready for use as products (see Figure 2). In our case, early research (Level 1-3 is) is understanding aerosol science and conducting experiments to prove feasibility of the scientific findings. Most of academia work is at the level of technology in understanding through research and establishing science and early engineering principles. Technology development (Level 4-6) is when the well-research knowledge with promising prototypes/feasibility data is translated into an iterative developmental phase to understand the engineering principles relation to performance of the technology. The last developmental phase of technology ready to launch (Level 7-9) is a manufacturing step in scaling up production of the technology without compromising the performance of the technology. The aerosol hood is at a level of 4 – 6 where the basic science and engineering principles have been proven and now it is at a level of understanding its performance and usability to ensure a high efficacy technology solution.

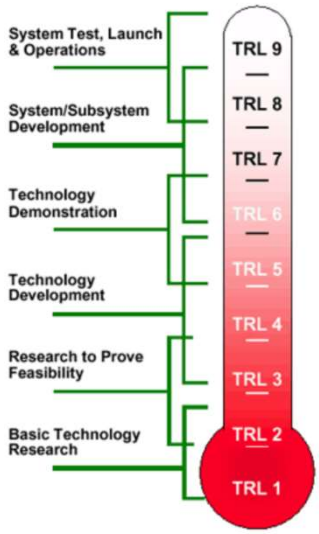

Figure 2: Leveraging NASA's technology readiness level to assess the development phase of the aerosol hood technology [30].

The benefit of the aerosol hood by providing an isolation and filtration of infectious aerosols and increased throughput of clinical procedure, outweighs the risk of adopting new technology, time added to incorporate to standard use.

4.3. Experimental Methods

HCW Participants: After IRB protocol (#STUDY00012371) approval for medical study clinical trial, recruitment emails were sent to the respiratory therapy, pulmonary, and critical care divisions to recruit 10 volunteers in participating in the clinical study. At the time of writing this thesis, only 4 participants completed the study and in the process of registering 6 more participants to complete the clinical study. The inclusion criteria were HCWs who performed intubation as part of their regular work activities (and are licensed to do so). There were no exclusion criteria. A written consent was obtained from the

participants before starting the study and participants were able to watch a training video prior to the study. At the end of the study, participants had an interview with a health science professional on their use of aerosol hood and feedback for future improvements.

Simulated Hospital Setting Set Up: Participants went through a PPE donning procedure of wearing a surgical gown, face shield and gloves prior to the study testing. A substrate (masking tape with $1in^2$) was placed on their PPE and inside of the aerosol hood, as shown in Figure 3 below. A 50 g/L Uranine powder was mixed with DI water to achieve 5% Uranine concentration by weight to form the fluorescein dye. A solution of 5% fluorescein dye mixed with 20% Glycerol and DI water was used to generate aerosol using a BLAM Nebulizer. One side of the Nebulizer was connected to that non-humidified compressed air at a pressure of 30 psi resulting in 15 L/min flow rate of aerosolization. And the other side of the Nebulizer was connected to the SIM-Man (Manikin) through the esophagus as it is illustrated on Figure 3 below.

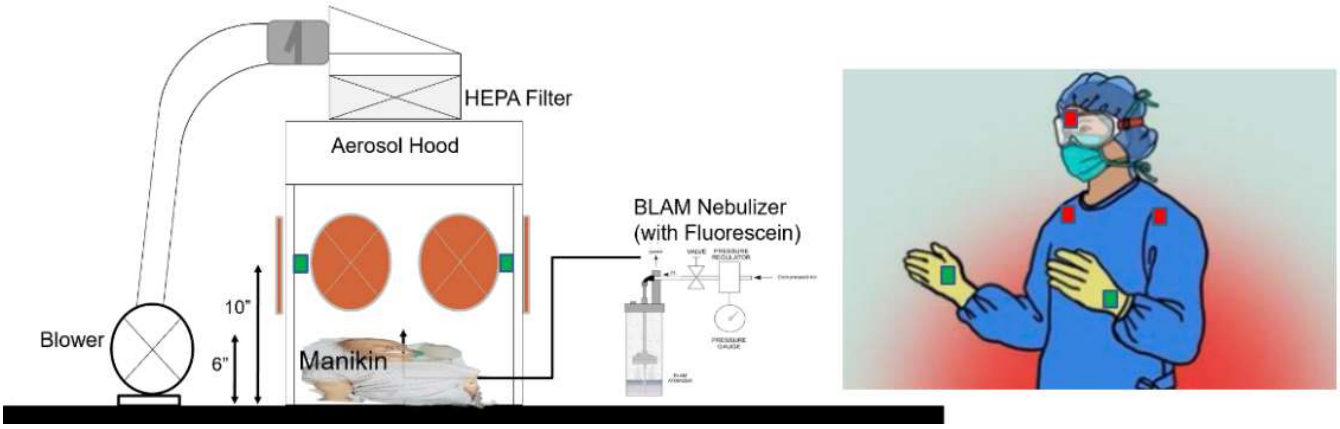

Figure 3: Substrate of a masking tape placement location on the outside and inside the aerosol hood.

Simultaneously, the particle concentration in the simulated hospital setting was measured using two OPS machines: one next to the bedside and the other at the corner of

the simulated hospital setting as a background (See Figure 4 below). The bedside particle counter represented HCWs usual standing place as they took care of the patient. The background particle counter was as a sample on how far the particles would be spreading around the room during testing.

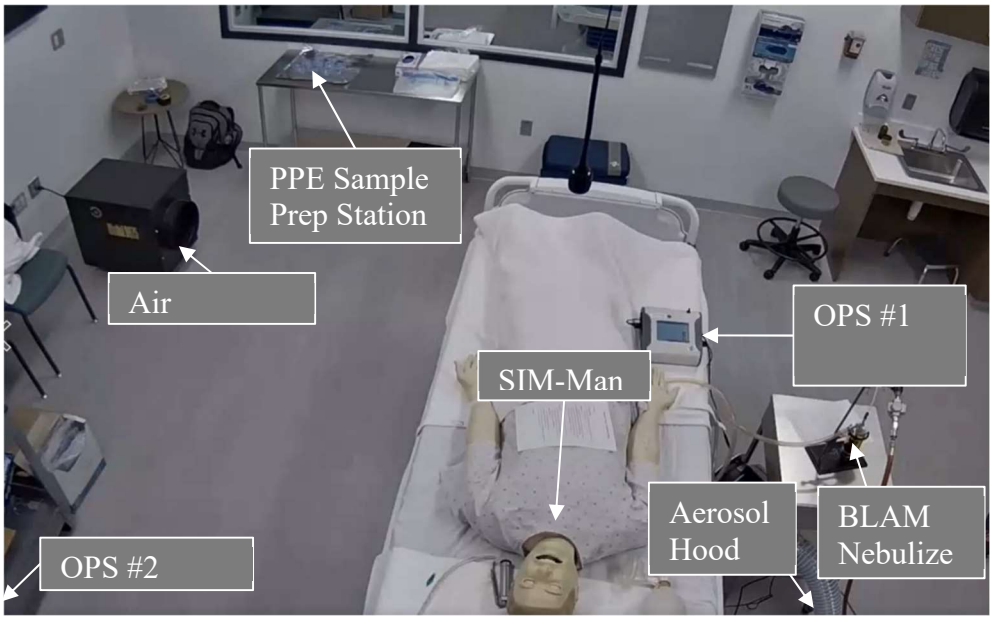

Figure 4: Simulated hospital setting for the clinical study in the UMN M Simulation Lab. (BG = Background, OPS = Optical Particle Sizer)

The simulated hospital room was 20.3 ft x 15 ft x 10 ft (3050 ft^3, or 86.4 m^3) had an air scrubber (Electrocorp Air Rhino Jr 9975 Carbon/HEPA Air Scrubber) with a maximum of 735 cfm running the whole time of the test conditions to minimize the room particle count. The ACH in the room is 2.5 from the ventilation system, but the total ACH combining the recirculating scrubber was 2.5 + 735 cfm x 60 min/hr /3050 ft^3 = 17, beyond the 10-15 observed in many hospital settings. It is important to note not all hospital settings can have the same level of clean room and the aerosol hood data performance might be

skewed in a high particle number concentration room. However, that was not the case in this study because of the additional portable ventilation utilized.

Testing Conditions: There were three testing conditions with each participant and each testing had three replicates. The first testing was a baseline intubation procedure without the use of the aerosol hood. The second testing was a simulated intubation procedure using the aerosol hood but without using the blower (Blower Off), therefore, the aerosol hood is acting merely as a physical isolation. The third testing was a simulated intubation procedure using the aerosol hood with the blower (Blower On) that created the negative pressure system. The two OPS machines were measuring particle concentration for replicates of each testing condition (3x3 samplers per participant). After each testing conditions, the tape substrates were collected and participants replaced their gloves for the next testing, while keeping the same gown and face shield.

Participants followed a protocol of a 7-step intubation procedure (see Supp. Figure 1) to standardize practices and reduce variations. The intubation procedure is one of the highest aerosol-generating clinical procedures and risky to HCW as they need to get in close contact with the patient and place a tube inside an airway through the throat [1].

Substrate preparation for fluorescence measurement: The participants' tape substrates were removed from the PPE and placed into a petri dish after every test condition. A solution of 3ml Sodium Hydroxide (NaOH) was added to the sample tapes in the petri dish to dilute the fluorescein dye particles with Sodium Hydroxide. The diluted solution was then transferred to a glass vial for fluorescein concentration measurement using Sequoia-Turner Model 450 Fluorometer. For fluorescein measurement, the shoulder (Sample 1) and

face shield (Sample 2) substrates were measured separately but pulled together for analysis as an 'Outside the Hood Exposure' and the inside of the hood (Sample 3) and gloves (Sample 4) substrates were measured separately but pulled together for analysis as an 'Inside the Hood Exposure'.

fluorescein measurement: SC515/NB490 wavelength fluorescein reader was inserted into the Sequoia-Turner Model 450 Fluorometer. The fluorometer is calibrated before measurement by first setting the desired 'gain' value. Then, using a known zero concentration sample vial to zero out the reading followed by setting the 'span' value to 1200 using a known fluorescent concentration. Then the vial samples are tested and the value from the Fluorometer is divided by the gain value for correction. Then the data is normalized by dividing the corrected value by the total area of the tape used per sample (a single tape had an area of $1in^2$ ($6.45cm^2$).

4.4. Results and Discussion

4.4.1. Aerosol exposure in a simulated hospital setting

The aerosol exposure in a simulated hospital setting was assessed by measuring the particle concentration during participants conducting a simulated intubation procedure. The particle concentration measurements were taken in two locations: by the bedside and at a corner of the room as a background. For all participants, the bedside location particle concentration (~ 7000 $\#/cm^3$) was 5 times higher than the background location (~1450 $\#/cm^3$). In Figure 5, the total concentration of particles measured during the Baseline,

Blower On and Blower Off testing conditions near to the patient by the bedside. The Blower On testing, where the aerosol hood was on the SIM-man and the negative pressure system was running, the total concentration remained less than 1000 particles/cm^3 compared to the Baseline and Blower Off testing. The Blower Off testing, where the aerosol hood was on the SIM-man without the negative pressure system running, the physical isolation of the aerosol hood has been able to delay the maximum particle concentration approximately 10-15 sec from the Baseline. In the case of participant 4, the Blower Off maximum particle concentration was delayed by over one minute. This is because during the 1-minute preoxygenation step of the intubation, the participant was squeezing on an air bag for one minute (the other participants were not) that might have disrupted the airflow direction. The Baseline testing represented the current standard of intubation with direct contact with the patient without the isolation of the aerosol hood or the addition of the negative pressure system the participle concentration reached up to 7000 particles/cm^3.

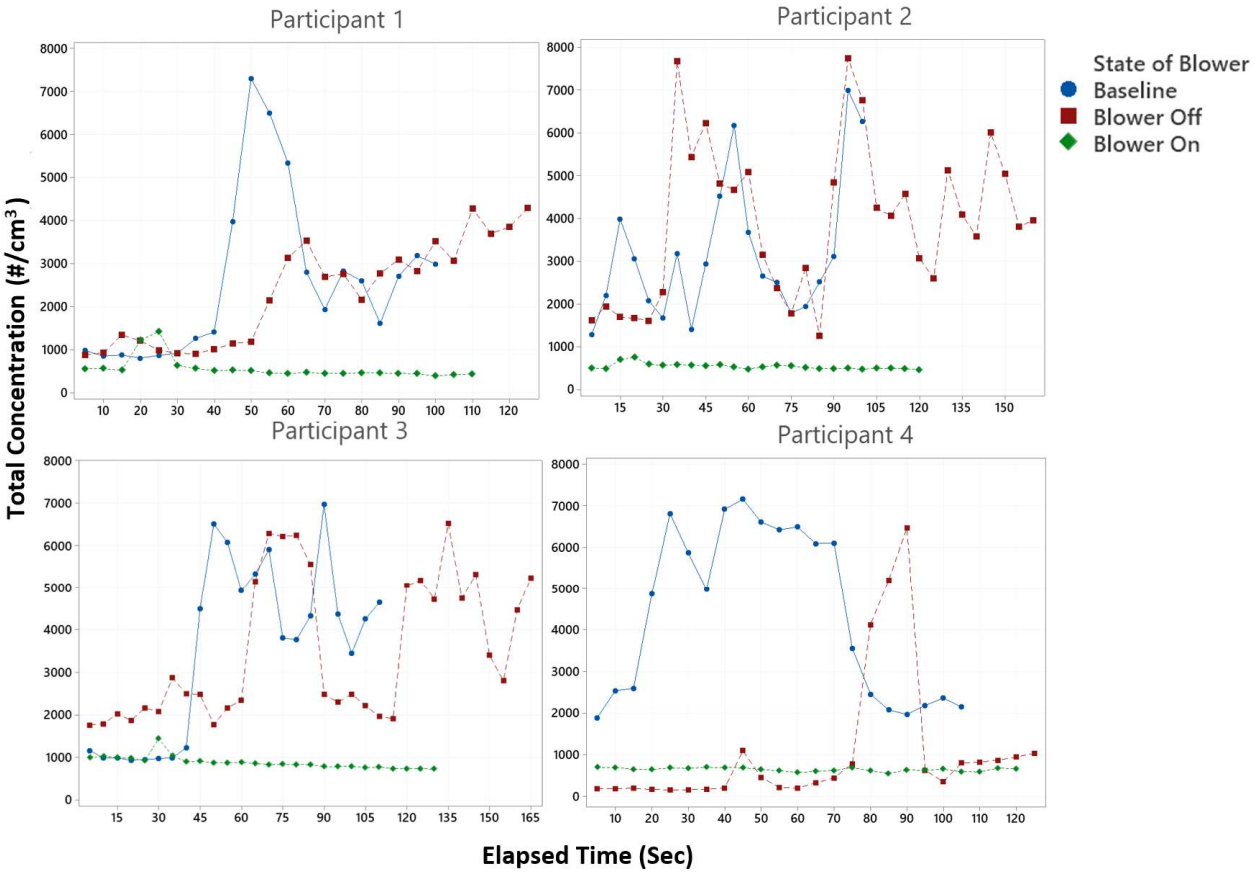

Figure 5: Bedside particle concentration measurement to assess the aerosol exposure during the Baseline, Blower On and Blower Off testing of a simulated intubation procedure. The Blower On testing resulted in much lower particle concentration than the Baseline and Blower Off testing. The Blower Off testing resulted in the delay of the maximum particle concentration than the Baseline testing.

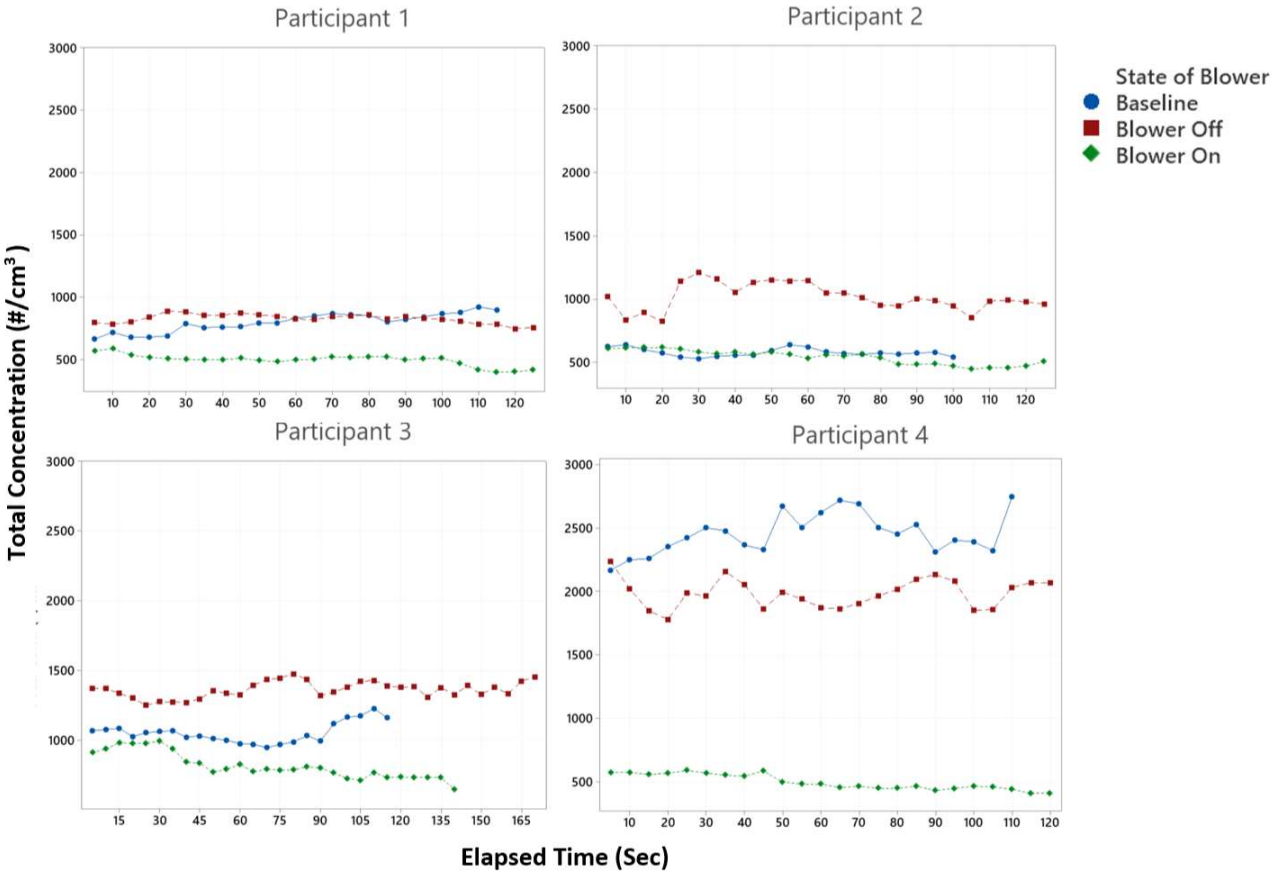

Figure 6: Background particle concentration measurement to assess the aerosol exposure during the Baseline, Blower On and Blower Off testing of a simulated intubation procedure. All testing resulted in much lower particle concentration than the Bedside measurement. Similar to Figure 5, the Blower On testing resulted in being lower than the other two testing conditions (Blower Off and Baseline).

While Figure 5 showed the bedside particle concentration during intubation procedure time, Figure 6 shows the background particle concentration during the same procedure time. At a far distance from the SIM-man, all participants testing conditions resulted in a much lower count of the particle an average of 1000 #/cm^3 than the Bedside particle concentration of an average nearly 5000 #/cm^3. For the bedside measurement, the Blower setting was a significant factor in resulting 78% particle concentration reduction

when Blower On as shown in Figure 7 below. This result confirms the effectiveness of the aerosol hood negative pressure system ability to reduce risk of aerosol exposure in the immediate surrounding of the patient bedside.

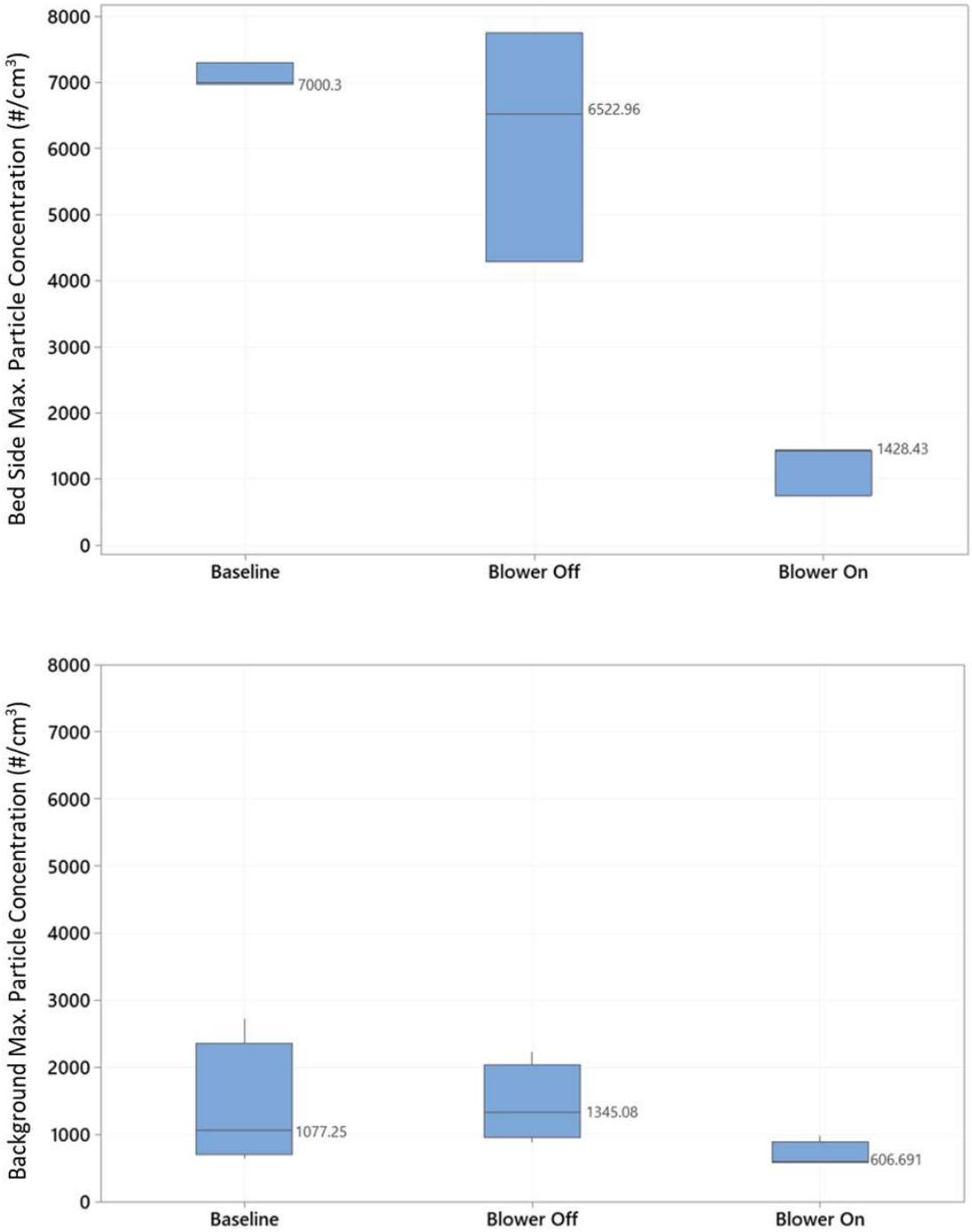

Figure 7: Comparison of Bedside and Background maximum particle concentration in a Simulated Hospital Setting of all participants. The Blower On for Bedside comparable to the Background particle concentration showing the effectiveness of the aerosol hood negative pressure system.

In addition, due to the localized aerosol containment and filtration of the aerosol hood, the existing hospital ventilation system can be enhanced in achieving the 99.9% aerosol reduction time faster than the current 15 minutes, nominal average in many hospital settings. Therefore, with the introduction of aerosol hood technology for aerosol generating procedures, a typical surgery room wait time can be reduced and more procedures can be done.

4.4.2. Particle Deposition on HCW's PPE

Other than the simulated hospital setting, the clinical study also tested the particle deposition on HCW's PPE. PPE is the primary form of protection for HCWs for aerosol related transmission disease control [9, 10, 13, 14, 15], consequently, understanding how the aerosol hood technology affects the PPE use is important. The three PPE used in this study were face shield, gloves, and surgical gowns. The face shield and surgical gowns were considered outside of the hood deposition measurements. The gloves were considered inside of the hood. Figure 8 shows the fluorescein deposition for Blower Off inside the hood was the highest with an average of 2.87 ug/cm^2 and the Blower On outside of the hood was the lowest with an average of 0.94 ug/cm^2 for all participants. For participle deposition, the physical isolation of the aerosol hood has a larger role than the Blower setting as shown in Figure 9.

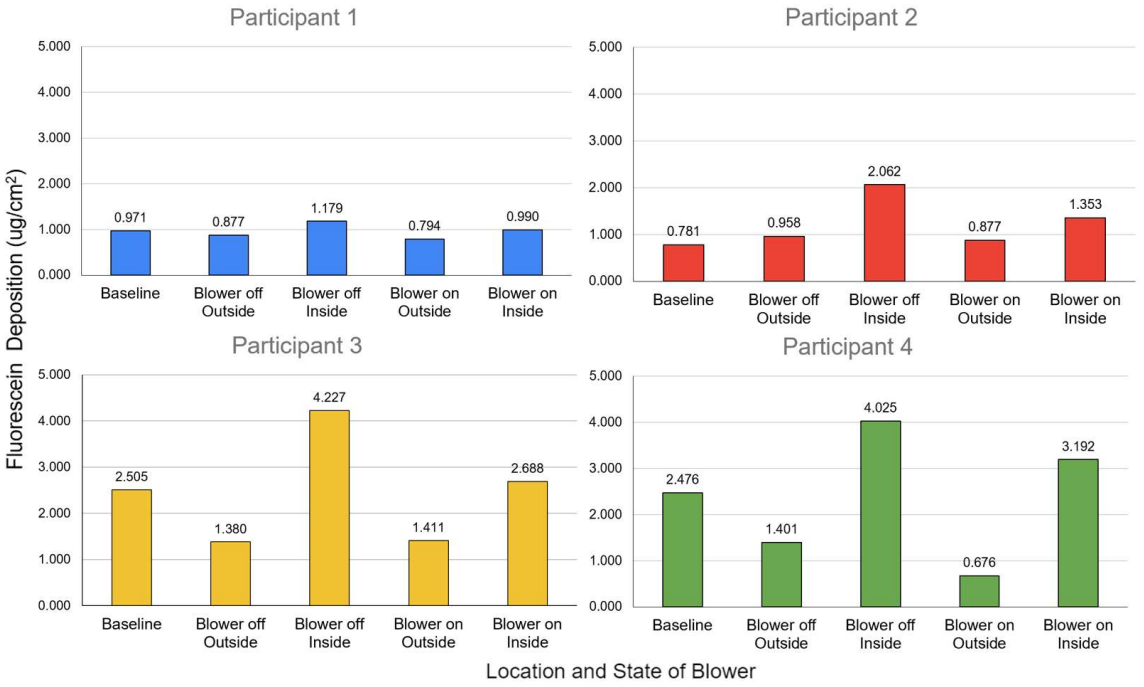

Figure 8: Each participant's fluorescein deposition inside and outside of the aerosol hood for the testing of Baseline, Blower On and Blower Off. Blower Off inside the hood has the highest deposition and Blower On outside of the hood has the lowest deposition.

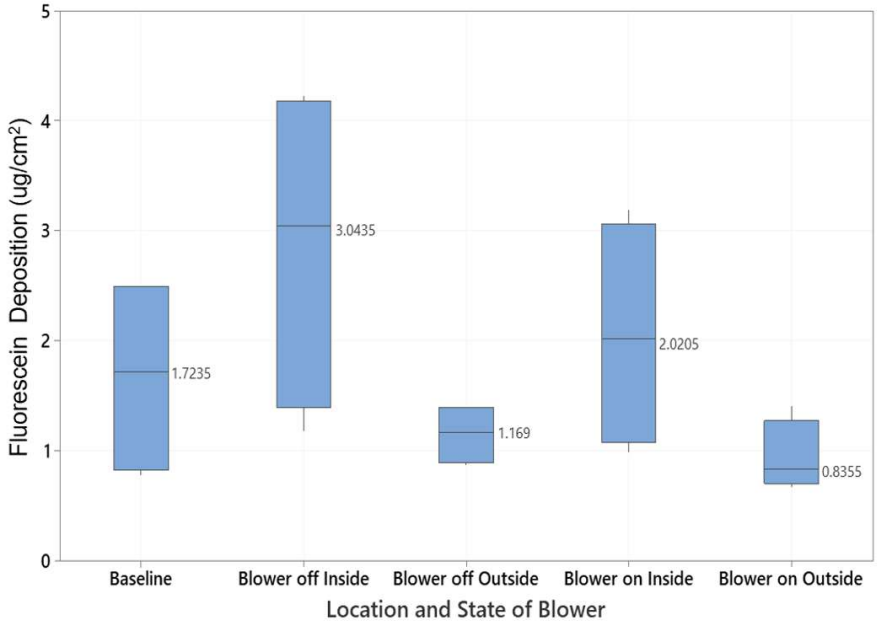

Figure 9: All participant's fluorescein deposition inside and outside of the aerosol hood for the testing of Baseline, Blower On and Blower Off. Inside the hood has the highest deposition than the Baseline testing. Outside of the hood has the lowest deposition than the Baseline testing.

Outside of the hood whether it is Blower On or Off, the deposition results were lower by 42% from the Baseline testing, which is another strong indication of the physical isolation property of the aerosol hood protects the HCW's from being exposed to aerosols on their gowns and face shields.

Inside of the hood for Blower On and Off testing conditions, the deposition results were higher by 32% from the Baseline testing, indicating the importance of PPE, especially gloves. The particle deposition is a product of fluid velocity, number of particles, area of substrate and procedure time. With the physician isolation of the aerosol hood, the velocity and number of particles are going to increase resulting in a high deposition amount. Therefore, the use of an aerosol hood does not negate the need for proper PPE, especially the use of gloves.

4.4.3. HCW Performance and Feedback

The intubation and overall procedure time were tracked to assess any differences due to the use of aerosol hood. Figure 10 shows that the average and median simulated intubation time was 20 seconds and the average and median overall intubation procedure time was 2 minutes across all testing with and without the aerosol hood. The results are promising that this is not a significant addition of time for using the aerosol hood. Participant 4 'Baseline replicate 1 testing' took an extra time to select the right tools during the initial intubation procedure, therefore, it yielded a higher deposition amount.

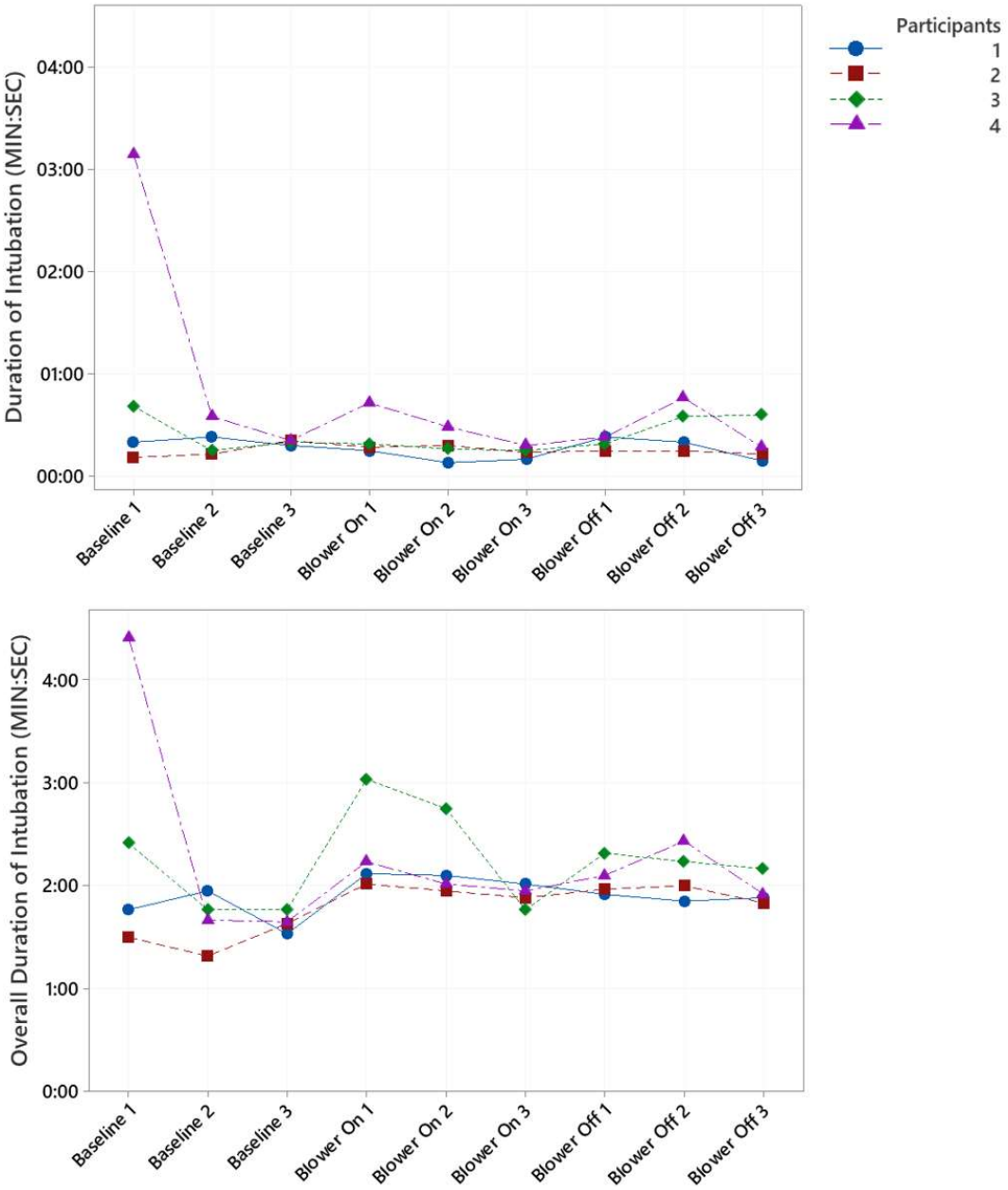

Figure 10: Time record of the simulated intubation and overall procedure time of all participants for each testing of Baseline, Blower On and Blower Off. Overall no significant statistical or practical time difference between Baseline and Aerosol Hood (Blower On and Off) testing.

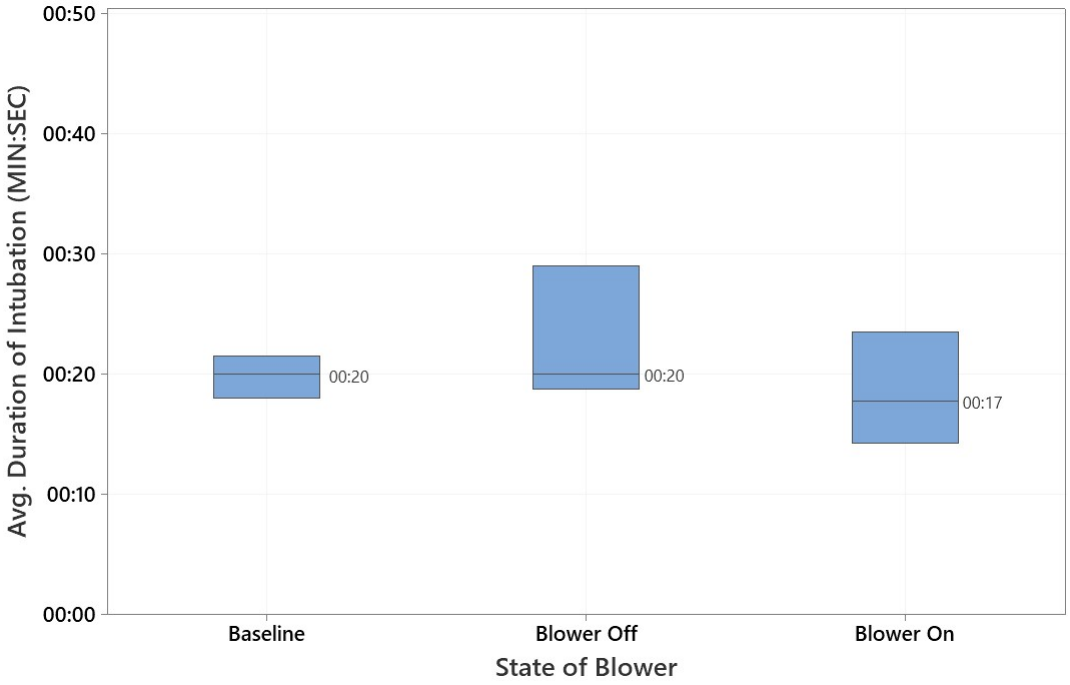

Figure 11A. All participants time of intubation that is the time it took to access airway using intubation tools was around 20 seconds.

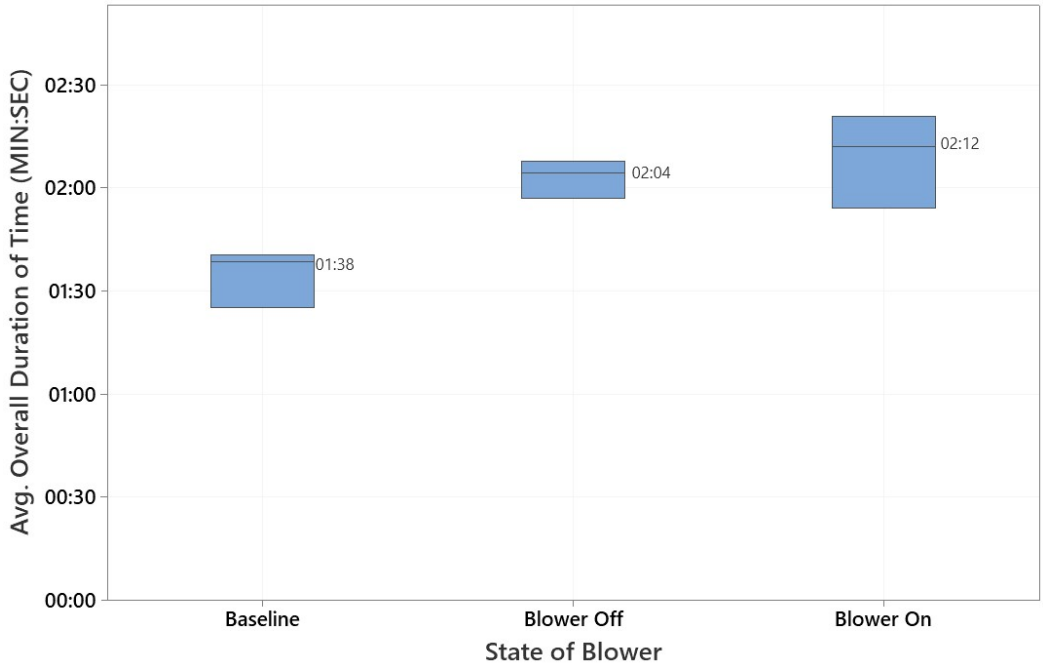

Figure 11B. All participants overall intubation that includes the oxygenation, intubation and the use of aerosol hood was around 2 minutes in average and 30 seconds higher for the aerosol hood compared to the baseline.

Without including the Participant's 4, Baseline 1 into the Boxplot of Figure 11A and 11B above, the overall duration of the procedure time, the Blower On testing has a maximum of 34 seconds faster than the Baseline testing and statistically insignificant with a p-value of 0.689 with a 2 sample t-test. Furthermore, considering the benefit of lowering the risk of disease transmitting aerosols by using the aerosol hood as an engineering control along with PPE, a 30-second procedure time increase should be tolerable.

The intubation time can also be correlated with the particle deposition on the PPE, where we can hypothesize that the longer the intubation time it takes, the higher the fluorescein deposition on the PPE. Figure 12 below shows the correlation between the intubation time to fluorescein deposition for outside of the hood PPEs such as face shield and shoulders. The results show an overall trend of higher deposition for higher procedure time. On the contrary, the Blower On testing for the duration of intubation time shows lower deposition for all testing conditions especially when compared with Baseline. This result indicates that the aerosol hood technology decreases particle deposition on HCW's PPE.

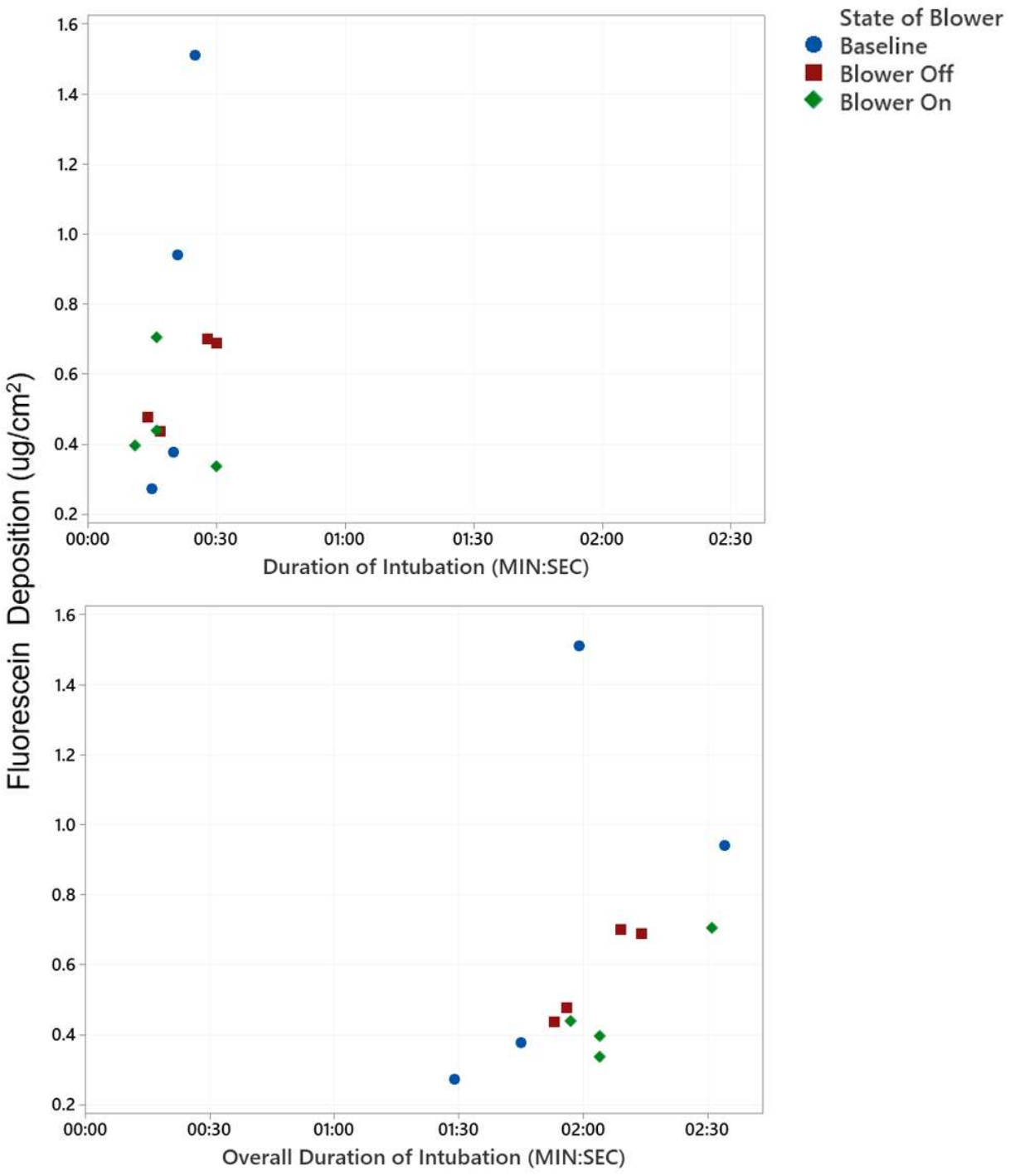

Figure 12: Correlation between the intubation procedure time and fluorescein deposition outside of the aerosol hood of all participants. A general trend of longer procedure time with higher deposition of fluorescein is observed.

The above study results show the effectiveness of the aerosol hood in minimizing aerosol exposure in a simulated hospital setting, HCW's PPE outside of the hood and similar duration of procedure time between aerosol hood and Baseline testing. The final step was to get physicians feedback on their use of the aerosol hood and suggestions for future improvement. In Figure 13, at least 3 out of 4 participants gave feedback on the potential of the aerosol hood in being able to be adjusted and strategized and it is practical for clinical use. They also commented that the hood/box felt constraining and being challenging for difficult airways.

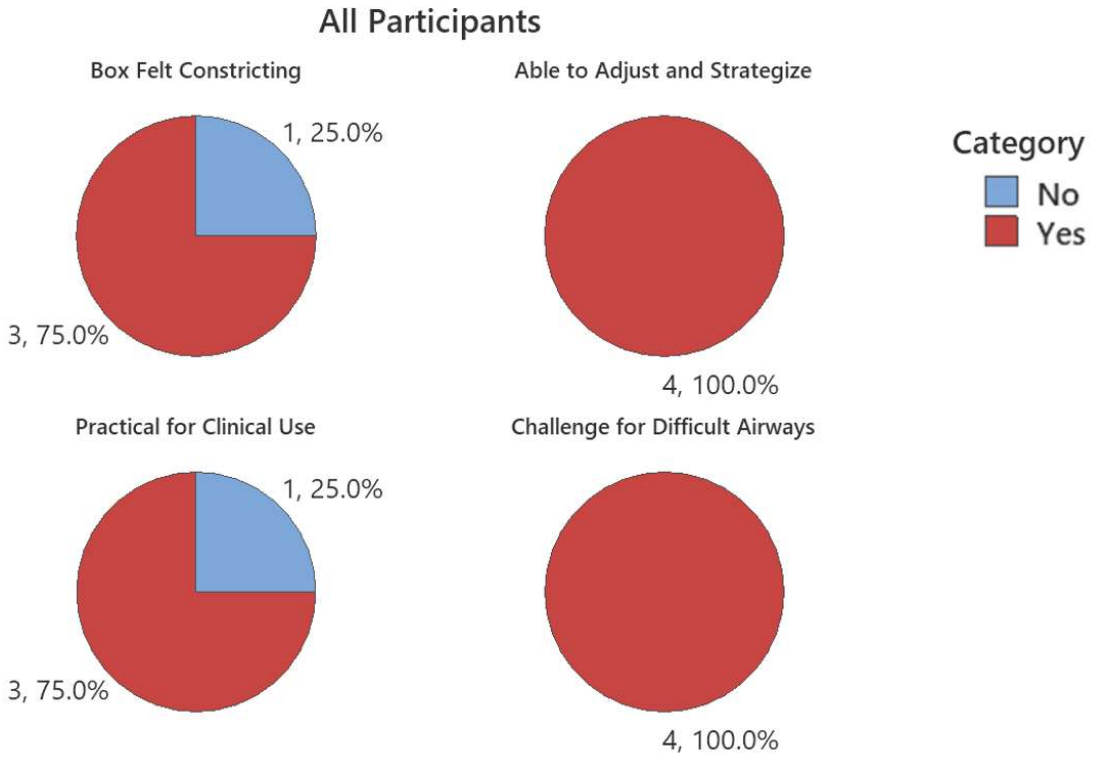

Figure 13: Total of 4 Participants' feedback on the aerosol hood during exit interview as part of the clinical study.

The participants' feedback is a confirmation of the aerosol hood at the level of 4-6 technology readiness. The results show a continuous improvement of the aerosol design box is needed to make it more ergonomically compatible. In the meantime, the performance of the HEPA filter and negative pressure system's ability to capture respiratory droplets is appreciated as an engineering control to protect HCWs.

4.5. Conclusions

In a simulated hospital setting, a simulated intubation procedure was conducted to study the impact of aerosol hood technology on hospital ventilation system, HCW PPE and physician's performance. To assess aerosol exposure in the hospital setting room, maximum particle concentration was measured by the SIM-Man bedside location and at a corner of the room as a background location. The particle deposition was analyzed by placing tape substrate on participant's PPE and using fluorescein dye in the solution for aerosolization. The intubation and procedure time were tracked manually and by video footage and participant's feedback were analyzed after the intubation procedure was completed in an exit interview session. The following conclusions were drawn:

1. The localized aerosol hood technology over the patient's respiratory droplets has the potential to enhance the standard hospital ventilation system because of the negative pressure system. The results show a Blower On setting by the bedside location is 78-80% lower particle concentration than the Blower Off and Baseline testing. In addition, the background location for all testing has an average of 1000 #/cm^3 particle concentration, which is 5 times lower than a bedside location. The current hospital

ACH wait time of 15 minutes to achieve 99.9% aerosol reduction time can be greatly reduced using aerosol technology that effectively localize aerosol dispersion due to the negative pressure system.

2. The physical isolation aspect of the aerosol hood technology reduced the particle deposition on PPEs such as face shields and gowns by 42% from the Baseline testing. The containment of the aerosol inside the hood indicates its efficacy in protecting HCWs exposure to disease transmitting aerosols. However, PPE such as gloves are still primary protection from particle deposition as the data inside the hood shows an increased deposition by 32% from the Baseline testing. The aerosol hood technology does not eliminate the use of PPE and Training as a control, but it is an additional engineering control in containing respiratory droplets from patients.
3. There was no statistical or significant difference between baseline and aerosol hood use for overall intubation procedure time with p-value of 0.689 with a 2-sample t-test. This data indicates the use of this new technology is not going to add a significant amount of procedure time. Given the benefit of additional protection to HCWs, adapting the aerosol hood technology is highly recommended.
4. Participants' feedback highlights the positive side of the aerosol hood in its potential in providing a negative pressure system in capturing respiratory droplets. Also, an opportunity for design improvement of the aerosol hood design in making it ergonomically friendly to give more operating flexibility and account for challenging intubation procedures.

3.7. Supplementary information

List of information available in Appendix C:

- Standardized intubation procedure for the clinical study in Figure S1
- Bedside and background exposure replicate data of total particle concentration for each participant from Figure S2 to Figure S9
- Participants' feedback on the aerosol hood from Figure S10 to Figure S13

Chapter 5: Conclusions and Future Directions

SARS-Cov-2 virus appears to be a long-term occurrence that will require a more efficient way of protecting HCWs now and in the future. The current method of PPE, training and hospital's ventilation system will not be long term sustainable protection considering the side effects such as headache, skin injury and inconsistent donning and doffing procedures. There is a clinical unmet need for an engineering control such as aerosol hood that will alleviate a dependence on current controls. Literature shows that the current aerosol boxes and containment devices are not as advanced in development as the aerosol hood presented in this thesis. To continue improving the aerosol hood, understanding the droplet trajectory, and getting HCWs feedback has been instrumental.

Chapter 2 dealt with modelling isothermal jet model to understand the respiratory droplets trajectories with a head tilt angle and residence time of droplets as a function of evaporation and settling rates. These aerosol principles are critical inputs in redesigning the aerosol hood and assessing the performance of the design. Some of the important results obtained from this study are:

1. The 62-cfm flow rate of the half power blower setting of the aerosol hood, would be able to clear small droplets below the critical diameter size of 65 μm in the air flow streamline. Large droplets will be cleared in two ways; a) staying in the jet path and impacting on aerosol hood. b) evaporation to small sizes which are easily transported to the HEPA filter of the device.

2. The evaporation and settling curve shows a critical diameter size of 65 μm at a time of 30 seconds. For smaller diameters the evaporation rate is within few seconds, which will be cleared again by the 62-cfm half power blower setting of the aerosol hood.

Based on the research described in Chapter 2, the following issues may be investigated in the future:

1. Modeling that simulated the breathing pattern and accounting for the thermal plume in droplet transport modeling.
2. Considering the aerosol hood itself in flow modeling.
3. As more is learned about rates of droplet and particle production by human respiratory activities and about the concentrations of viable viruses in such particles, more detailed exposure models can be developed using trajectory modeling.

Chapter 3 dealt with the optimized aerosol hood design performance by evaluating the flow rate profile, level of noise, air exchange time and particle penetration. The negative pressure system at the half power blower setting resulted in high performance and potential in the aerosol hood as an engineering control by achieving aerosol reduction of 99.9%. Some of the important results obtained from this study are:

1. The maximum flow rate with the full power blower setting was 0.8 mph (0.4 m/s), which is at the level of Beaufort Number 0 for calm air speed. The maximum sound measurement for half power blower speed inside the hood is 73.7 dBA, which is near a vacuum cleaner noise level and under the NOISH recommended noise exposure limit

of 85 dBA. The optimized aerosol hood design provides a uniform air speed and safe noise level inside the hood with a half power blower setting.

2. The aerosol hood has an air exchange time of average of 2.76 minutes for an ACH that is 151.44 on average for aerosol reduction of 99.9%. The aerosol hood not only reduces the risk of infection transmission towards HCWs, but also increases the hospital's capacity to provide more patient care.
3. This particle penetration resulted in 10^{-4} with a corresponding protection efficiency of 99.99%. The optimized aerosol hood design performance by HEPA filter protection efficiency of 99.99% combined with high air exchange time of 2.76 minutes, gives confidence in protecting HCWs from nosocomial infection.

Based on the research described in Chapter 3, the following issues may be investigated in the future:

1. Further design refinement to improve device ergonomics, reduce weight, and ideally, incorporate directly into hospital's ventilation systems or beds.
2. Development of a battery-operated model for use in emergency settings.
3. Development of a "foldable" model for ease of storage.

Chapter 4 dealt with the IRB approved clinical trial results in aerosol exposure during a simulated intubation in a simulated hospital setting and particle deposition on HCWs' PPE. In addition, assessed the impact of the aerosol hood on the participants intubation time and user experience compared to baseline intubation as a control. The clinical study results indicated a significant improvement with the blower turned on and

the potential of the aerosol hood for practical clinical use. Some of the important results obtained from this study are:

1. The localized aerosol hood technology over the patient's respiratory droplets enhances the standard hospital ventilation system because of the negative pressure system. The results show a Blower On setting by the bedside location is 78-80% lower particle concentration than the Blower Off and Baseline testing. In addition, the background location for all testing has an average of 1000 #/cm^3 particle concentration, which is 5 times lower than a bedside location. The current hospital ACH wait time of 15 minutes to achieve 99.9% aerosol reduction time can be greatly reduced using aerosol technology that effectively minimizes aerosol exposure due to the negative pressure system.
2. The physical isolation aspect of the aerosol hood technology reduced the particle deposition on PPEs such as face shields and gowns by 42% from the Baseline testing. The containment of the aerosol inside the hood indicates its efficacy in protecting HCWs exposure to disease transmitting aerosols. However, PPE such as gloves are still primary protection from particle deposition as the data inside the hood shows an increased deposition by 32% from the Baseline testing. The aerosol hood technology does not eliminate the use of PPE and Training as a control, but it adds protection as an engineering control.
3. There was no statistical or significant difference between baseline and aerosol hood use for intubation time and overall procedure time with a p-value of 0.689 for 2-sample t-test. This data indicates that the use of this new technology is not going to add a

significant amount of procedure time. Given the benefit of additional protection to HCWs, adapting the aerosol hood technology is highly recommended.

4. Participants' feedback highlighted the positive side of the aerosol hood in its potential future clinical use and in providing a negative pressure system in clearing respiratory droplets. Also, an opportunity for design improvement for ergonomically friendly aerosol hood to give more hand flexibility and account for challenging intubation procedures.

Based on the research described in Chapter 4, the following issues may be investigated in the future:

1. With EUA approval for the aerosol hood recently issued. Physicians could now use the device for intubation on patients and lead an actual human trial with it. This would be highly similar in design to the simulation study, but rather than examine tracer particles, sampling for infectious particles during an actual procedure would be required. This study would be a much larger undertaking than a simulation study, requiring coordination with a hospital system, multiple HCWs, and patient consent.

References

1. Tran, K., Cimon, K., Severn, M., Pessoa-Silva, C. L., & Conly, J. (2012). Aerosol Generating Procedures and Risk of Transmission of Acute Respiratory Infections to Healthcare Workers: A Systematic Review. *PLoS ONE*, *7*(4), e35797.
2. Stockwell, R., Ballard, E., O'Rourke, P., Knibbs, L., Morawska, L., & Bell, S. (2019). Indoor hospital air and the impact of ventilation on bioaerosols: a systematic review. *Journal of Hospital Infection*, *103*(2), 175–184.
3. Vuorinen, V., Aarnio, M., Alava, M., Alopaeus, V., Atanasova, N., Auvinen, M., Balasubramanian, N., Bordbar, H., Erästö, P., Grande, R., Hayward, N., Hellsten, A., Hostikka, S., Hokkanen, J., Kaario, O., Karvinen, A., Kivistö, I., Korhonen, M., Kosonen, R., . . . Österberg, M. (2020). Modelling aerosol transport and virus exposure with numerical simulations in relation to SARS-CoV-2 transmission by inhalation indoors. *Safety Science*, *130*, 104866.
4. Gaeckle, N. T., Lee, J., Park, Y., Kreykes, G., Evans, M. D., & Hogan, C. J. (2020). Aerosol Generation from the Respiratory Tract with Various Modes of Oxygen Delivery. *American Journal of Respiratory and Critical Care Medicine*, *202*(8), 1115–1124. https://doi.org/10.1164/rccm.202006-2309oc
5. Fennelly, K. P. (2020). Particle sizes of infectious aerosols: implications for infection control. *The Lancet Respiratory Medicine*, *8*(9), 914–924.
6. Gupta, J. K., Lin, C. H., & Chen, Q. (2010). Characterizing exhaled airflow from breathing and talking. *Indoor Air*, *20*(1), 31–39.
7. Xie, X., Li, Y., Chwang, A. T. Y., Ho, P. L., & Seto, W. H. (2007). How far droplets can move in indoor environments ? revisiting the Wells evaporation?falling curve. *Indoor Air*, *17*(3), 211–225.
8. Tang, J., Li, Y., Eames, I., Chan, P., & Ridgway, G. (2006). Factors involved in the aerosol transmission of infection and control of ventilation in healthcare premises. *Journal of Hospital Infection*, *64*(2), 100–114. https://doi.org/10.1016/j.jhin.2006.05.022
9. Evans, H. L., Thomas, C. S., Bell, L. H., Hink, A. B., O'Driscoll, S., Tobin, C. D., & Salgado, C. D. (2020). Development of a Sterile Personal Protective Equipment Donning and Doffing Procedure to Protect Surgical Teams from SARS-CoV-2 Exposure during the COVID-19 Pandemic. *Surgical Infections*, *21*(8), 671–676.
10. Beam, E. L., Gibbs, S. G., Boulter, K. C., Beckerdite, M. E., & Smith, P. W. (2011). A method for evaluating health care workers' personal protective equipment technique. *American Journal of Infection Control*, *39*(5), 415–420.
11. *Hierarchy of Controls | NIOSH | CDC*. (2015). Centers for Disease Control and Prevention. https://www.cdc.gov/niosh/topics/hierarchy/default.html

12. Walker, J., Hoffman, P., Bennett, A., Vos, M., Thomas, M., & Tomlinson, N. (2007). Hospital and community acquired infection and the built environment – design and testing of infection control rooms. *Journal of Hospital Infection*, *65*, 43–49.
13. Hossain, M. A., Rashid, M. U. B., Khan, M. A. S., Sayeed, S., Kader, M. A., & Hawlader, M. D. H. (2021). Healthcare Workers' Knowledge, Attitude, and Practice Regarding Personal Protective Equipment for the Prevention of COVID-19. *Journal of Multidisciplinary Healthcare*, *Volume 14*, 229–238.
14. KORKUSUZ, R., ŞENOĞLU, S., POLAT, Z., & KART YAŞAR, K. (2021). The Importance of Healthcare Workers to Comply with Infection Prevention and Control Instructions During COVID-19 Outbreak-A Survey Study. *Bezmialem Science*, *9*(1), 329.
15. Mousavi, E. S., & Grosskopf, K. R. (2015). Ventilation Rates and Airflow Pathways in Patient Rooms: A Case Study of Bioaerosol Containment and Removal. *Annals of Occupational Hygiene*, *59*(9), 1190–1199.
16. Turer, D. M., Good, C. H., Schilling, B. K., Turer, R. W., Karlowsky, N. R., Dvoracek, L. A., Ban, H., Chang, J. S., & Rubin, J. P. (2021). Improved Testing and Design of Intubation Boxes During the COVID-19 Pandemic. *Annals of Emergency Medicine*, *77*(1), 1–10. https://doi.org/10.1016/j.annemergmed.2020.08.033
17. Sorbello, M., Rosenblatt, W., Hofmeyr, R., Greif, R., & Urdaneta, F. (2020). Aerosol boxes and barrier enclosures for airway management in COVID-19 patients: a scoping review and narrative synthesis. *British Journal of Anaesthesia*, *125*(6), 880–894.
18. Saito, T., & Asai, T. (2020). Aerosol containment device for airway management of patients with COVID-19: a narrative review. *Journal of Anesthesia*.
19. Gupta, V., Sahani, A., Mohan, B., & Wander, G. (2020). Negative pressure aerosol containment box: An innovation to reduce COVID-19 infection risk in healthcare workers. *Journal of Anaesthesiology Clinical Pharmacology*, *36*(5), 144.
20. Goneppanavar, U., Bidkar, P., Kaur, J., & Ramamoorthy, S. (2020). Safety tent for enhanced personal protection from aerosol-generating procedures while handling the COVID-19 patient airway. *Journal of Anaesthesiology Clinical Pharmacology*, *36*(5), 157.
21. Dehghani, F., Omidi, F., Yousefinejad, S., & Taheri, E. (2020). The hierarchy of preventive measures to protect workers against the COVID-19 pandemic: A review. *Work*, 1–7.

22. Bianco, F., Incollingo, P., Grossi, U., & Gallo, G. (2020). Preventing transmission among operating room staff during COVID-19 pandemic: the role of the Aerosol Box and other personal protective equipment. *Updates in Surgery*, *72*(3), 907–910.
23. Begley, J. L., Lavery, K. E., Nickson, C. P., & Brewster, D. J. (2020). The aerosol box for intubation in coronavirus disease 2019 patients: an in-situ simulation crossover study. *Anaesthesia*, *75*(8), 1014–1021.
24. Phu, H. T., Park, Y., Andrews, A. J., Marabella, I., Abraham, A., Mimmack, R., Olson, B. A., Chaika, J., Floersch, E., Remskar, M., Hume, J. R., Fischer, G. A., Belani, K., & Hogan, C. J. (2020). Design and evaluation of a portable negative pressure hood with HEPA filtration to protect health care workers treating patients with transmissible respiratory infections. *American Journal of Infection Control*, *48*(10), 1237–1243.
25. Kumar, N., Kumar, A., Kumar, A., & Sinha, C. (2020). Modified Negative Airflow Aerosol Prevention Box for COVID-19 Patients. *Indian Journal of Critical Care Medicine*, *24*(10), 981–982. https://doi.org/10.5005/jp-journals-10071-23633
26. Tang, J. W., Nicolle, A. D., Klettner, C. A., Pantelic, J., Wang, L., Suhaimi, A. B., Tan, A. Y. L., Ong, G. W. X., Su, R., Sekhar, C., Cheong, D. D. W., & Tham, K. W. (2013). Airflow Dynamics of Human Jets: Sneezing and Breathing - Potential Sources of Infectious Aerosols. *PLoS ONE*, *8*(4), e59970.
27. National Weather Service. (2020). *Estimating Wind*. https://www.weather.gov/pqr/wind
28. *Air | Appendix | Environmental Guidelines | Guidelines Library | Infection Control | CDC*. (2003). Centers for Disease Control and Prevention: Infection Control. https://www.cdc.gov/infectioncontrol/guidelines/environmental/appendix/air.html
29. Wilson, N. M., Norton, A., Young, F. P., & Collins, D. W. (2020). Airborne transmission of severe acute respiratory syndrome coronavirus-2 to healthcare workers: a narrative review. *Anaesthesia*, *75*(8), 1086–1095. https://doi.org/10.1111/anae.15093
30. Wikipedia contributors. (2021, May 11). *Technology readiness level*. Wikipedia. https://en.wikipedia.org/wiki/Technology_readiness_level
31. Stadnytskyi, V., Anfinrud, P., & Bax, A. (2021). Breathing, speaking, coughing or sneezing: What drives transmission of SARS-CoV-2? *Journal of Internal Medicine*. Published. https://doi.org/10.1111/joim.13326
32. Nelson, S. (2020, November 23). *Isolation Gowns - Combatting PPE Shortages*. Vintex Inc. - Custom Engineered Coated Textile Solutions. https://www.vintex.com/isolation-gowns-combatting-ppe-shortages/
33. *Shibboleth Authentication Request*. (2021, February 3). Best-Practices for Preventing Skin Injury beneath Personal Protective Equipment during the COVID-19 Pandemic: A Position Paper from the National Pressure Injury Advisory Panel. https://login.ezp1.lib.umn.edu/login?qurl=https://onlinelibrary.wiley.com%2fdoi%2f10.1111%2fjocn.15682

34. Ong, J. J. Y., Chan, A. C. Y., Bharatendu, C., Teoh, H. L., Chan, Y. C., & Sharma, V. K. (2021). Headache Related to PPE Use during the COVID-19 Pandemic. *Current Pain and Headache Reports*, *25*(8). https://doi.org/10.1007/s11916-021-00968-x
35. Orzeł, B., & Wolniak, R. (2021). Clusters of Elements for Quality Assurance of Health Worker Protection Measures in Times of COVID-19 Pandemic. *Administrative Sciences*, *11*(2), 46. https://doi.org/10.3390/admsci11020046
36. S. (2015, December 29). *The Sound of Safety*. SafeStart. https://safestart.com/news/sound-safety/
37. Yang, X., Yang, H., Ou, C., Luo, Z., & Hang, J. (2021). Airborne transmission of pathogen-laden expiratory droplets in open outdoor space. *Science of The Total Environment*, *773*, 145537. https://doi.org/10.1016/j.scitotenv.2021.145537
38. Jazie, A. A., Albaaji, A. J., & Abed, S. A. (2021). A review on recent trends of antiviral nanoparticles and airborne filters: special insight on COVID-19 virus. *Air Quality, Atmosphere & Health*. Published. https://doi.org/10.1007/s11869-021-01055-1
39. Hairer, E., Lubich, C., & Wanner, G. (2003). Geometric numerical integration illustrated by the Störmer–Verlet method. *Acta Numerica*, *12*, 399–450. https://doi.org/10.1017/s0962492902000144

Appendix A: (Supplementary material for Chapter 2)

JOHN WILEY AND SONS LICENSE
TERMS AND CONDITIONS

Jun 14, 2021

This Agreement between University of Minnesota -- Ewnet Gebrehiwot ("You") and John Wiley and Sons ("John Wiley and Sons") consists of your license details and the terms and conditions provided by John Wiley and Sons and Copyright Clearance Center.

License Number	5087480778646
License date	Jun 14, 2021
Licensed Content Publisher	John Wiley and Sons
Licensed Content Publication	Indoor Air
Licensed Content Title	How far droplets can move in indoor environments – revisiting the Wells evaporation–falling curve
Licensed Content Author	W. H. Seto, P. L. Ho, A. T. Y. Chwang, et al

Figure S1: Author permission for Reference 7 for Figure 1 and 2A.

ELSEVIER LICENSE
TERMS AND CONDITIONS

Jul 07, 2021

This Agreement between University of Minnesota -- Ewnet Gebrehiwot ("You") and Elsevier ("Elsevier") consists of your license details and the terms and conditions provided by Elsevier and Copyright Clearance Center.

License Number	5103600525426
License date	Jul 07, 2021
Licensed Content Publisher	Elsevier
Licensed Content Publication	Journal of Hospital Infection
Licensed Content Title	Factors involved in the aerosol transmission of infection and control of ventilation in healthcare premises
Licensed Content Author	J.W. Tang,Y. Li,I. Eames,P.K.S. Chan,G.L. Ridgway
Licensed Content Date	Oct 1, 2006
Licensed Content Volume	64

Figure S2: Author permission for Reference 8 for Figure 2B.

Isothermal Jet Model to predict the droplet movement from the respiratory tract to the aerosol hood.		
INITIAL Droplet dian	65	micrometers
Calculating Fluid Velocity		
U_m	Centerline velocity decay	$6.8U_0/\hat{s}$
$\bar{u}_s$	mean axial velocity component	$U_m \sec h^2(\sigma\eta)$
$\bar{u}_r$	mean radial velocity component	$U_m\,[a\eta(1+\eta^2 - (1+b)(1+\eta^2)^{1/2}) / (1+\eta^2)(1-(1+b)(1+\eta^2)^{1/2})^2]$
$\hat{s}$	Normalized Streamline Distance	s/d_0
$\check{r}$	Normalized Radial Distance	r/d_0
η	Ratio of radial/streamline	$\check{r}/\hat{s}$
σ	Constants	10.4
a	Constants	0.0046
b	Constants	0.0075
dp_0	initial Droplet diameter (m)	0.0001
d_0	jet diameter	0.04
U_0	Initial Velocity	10
A_0	opening area	0.001256637
Time Step and Angle		
T_0	Initial Temperature	310
Tr	outside air temp	298
Ar_0	Archimedes Number	0.000143136
ρ_g	gas density	1.2
Time step	1.00E-03	Second
pp	Particle Density	1000
Theta (degrees)	0	Degrees
Theta (radians)	0	Radians
Evaporation Rate and Diameter Change		
C	Correction factor	1.011969258
	Lamda	1.6-2
M_v	molecular weight of the vapor -	0.018
D_{inf}	binary diffusion cofficient far	1.75E-05
pv_{inf}	vapor pressure of gas far away	1755.75
pv_a	vapor pressure of gas at the	6148
p	Total pressure	101325
	Ln (p-pva/p-pvinf)	-0.045115066
pp	particle density	1000
μ	viscocity	1.82E-05
D	Binary diffusion cofficient of	1.87581E-05
ρ_g	gas density	1.2
T_∞	Env. Temperature	293.15
T_p	Droplet Temperature	306.15
Sc	Schmidt #	8.09E-01
Sh	Sherwood #	$Sh = 1 + 0.3Re_p^{\frac{1}{2}}Sc^{\frac{1}{3}}$
R	Gas Constant for water vapor	461.5
dr_p/dt	$\frac{dr_p}{dt} = \left(\frac{CM_v D_\infty pSh}{\rho_p r_p RT_\infty}\right)\ln\left(\frac{p - pva}{p - pv_\infty}\right)$	rp - diameter at the same level
D_i+1 =	$D_{i+1} = Di + 2\Delta t\frac{dr_p}{dt}$	delta t is the time step

Figure S3: All inputs used for Isothermal Jet Model.

	1. Calculating Fluid Velocity in (s,r) and (x,y) with angle incorporated based on the given parameters and constants of isothermal jet model									
time (s)	s (m)	ŝ	Um (m/s)	r	r̂	η	$\bar{u}_s$	$\bar{u}_r$	u_x (Angled)	u_y (Angled)
0.00	0.27	6.8	10	0.00	0.00E+00	0.00E+00	1.00E+01	0.00E+00	1.00E+01	0.00E+00
0.00	0.28	7.05	9.645390071	0.00	1.23E-04	1.74E-05	9.65E+00	-1.03E-04	9.65E+00	-1.03E-04
0.00	0.30	7.55	9.006622517	0.00	3.63E-04	4.81E-05	9.01E+00	-2.66E-04	9.01E+00	-2.66E-04
0.00	0.33	8.2995846	8.193181104	0.00	7.26E-04	8.75E-05	8.19E+00	-4.39E-04	8.19E+00	-4.39E-04
0.01	0.37	9.2974187	7.313857985	0.00	1.21E-03	1.30E-04	7.31E+00	-5.84E-04	7.31E+00	-5.84E-04
0.01	0.42	10.540805	6.451120338	0.00	1.82E-03	1.73E-04	6.45E+00	-6.83E-04	6.45E+00	-6.83E-04
0.01	0.48	12.025441	5.654678504	0.00	2.55E-03	2.12E-04	5.65E+00	-7.35E-04	5.65E+00	-7.35E-04
0.01	0.55	13.745419	4.947102842	0.00	3.40E-03	2.47E-04	4.95E+00	-7.50E-04	4.95E+00	-7.50E-04
0.01	0.63	15.693423	4.333025398	0.00	4.37E-03	2.79E-04	4.33E+00	-7.41E-04	4.33E+00	-7.41E-04
0.01	0.71	17.861034	3.807170419	0.00	5.47E-03	3.06E-04	3.81E+00	-7.15E-04	3.81E+00	-7.15E-04

Figure S4: First step of calculating fluid velocity using Xie et al. [7] equations with an incorporated head tilt angle.

2. Calculating Particle Velocity and Position in (x,y) direction using drag force, Rep, Cd and Verlet Algorithm.											
x	y	Vx	Vy	Droplet Diameter	Re_p	Cd	Drag Force x (N)	Drag Force y (N)	Particle Mass (	Acceleration x	acceleration, y
0.01	2.00	10.000	-0.005	6.49993E-05	2.10E-02	1155.443656	0.00E+00	5.53E-11	1.44E-10	0	-9.425088951
0.02	2.00	10.000	-0.010	6.49986E-05	1.52E+00	19.08445915	-4.78E-09	3.44E-12	1.44E-10	-3.32E+01	-9.786077676
0.03	2.00	9.983	-0.015	6.49978E-05	4.186436805	8.085608598	-1.54E-08	3.27E-12	1.44E-10	-106.8162026	-9.787281572
0.04	2.00	9.930	-0.019	6.49967E-05	7.443508646	5.166404572	-3.10E-08	3.70E-12	1.44E-10	-215.7946194	-9.784270337
0.05	2.00	9.822	-0.024	6.49955E-05	10.74932399	3.950902087	-4.95E-08	4.42E-12	1.44E-10	-344.1848614	-9.77923935
0.06	2.00	9.650	-0.029	6.49943E-05	13.70885666	3.335104292	-6.79E-08	5.39E-12	1.44E-10	-472.5794994	-9.772479277
0.07	2.00	9.414	-0.034	6.49929E-05	16.1090807	2.991294782	-8.41E-08	6.62E-12	1.44E-10	-585.3169188	-9.763963923
0.08	2.00	9.121	-0.039	6.49915E-05	17.88685503	2.791730723	-9.68E-08	8.11E-12	1.44E-10	-673.53136	-9.753575109
0.09	2.00	8.784	-0.044	6.49901E-05	19.07491467	2.677409586	-1.06E-07	9.89E-12	1.44E-10	-734.6509189	-9.741155336
0.10	2.00	8.417	-0.049	6.49886E-05	19.75396167	2.617706876	-1.11E-07	1.20E-11	1.44E-10	-770.3597483	-9.726523338
0.10	2.00	8.032	-0.054	6.49871E-05	20.02004021	2.595317249	-1.13E-07	1.44E-11	1.44E-10	-784.5230627	-9.709479621

Figure S5: Second step of calculating particle velocity and position using Verlet Algorithm [39].

3. Calculating the evaporation rate of the droplet by using Sherwood # and the resulting change in diameters.	
Sherwood #	drp/dt (m/s)
1.04E+00	-3.45E-07
1.34E+00	-4.46E-07
1.57E+00	-5.21E-07
1.76E+00	-5.84E-07
1.92E+00	-6.35E-07
2.03E+00	-6.74E-07
2.12E+00	-7.03E-07
2.18E+00	-7.23E-07
2.22E+00	-7.36E-07
2.24E+00	-7.43E-07

Figure S6: Third and final step of calculating evaporation rate.

Appendix B: (Supplementary material for Chapter 3)

Table S1: Sound measurement inside and outside the aerosol hood with blower setting change.

Speed	Speed	Location	Min (dBA)	Max (dBA)	Average (dBA)
	Blower Off	Inside Center	51.3	54.9	53.1
	Blower Off	Outside (right)	57.1	62.8	59.95
	Blower Off	Outside (left)	56.5	61.7	59.1
Blower Off	Blower Off	Outside(back)	56.9	63.2	60.05
	Half Power	Inside Center	71.0	73.7	72.4
	Half Power	Outside (right)	59.3	62.2	60.75
	Half Power	Outside (left)	67.9	68.6	68.25
Half Power	Half Power	Outside(back)	60.9	62.2	61.55
	Full Power	Inside Center	90.5	94.7	92.6
	Full Power	Outside (right)	69.4	77.3	73.35
	Full Power	Outside (left)	82.1	88.6	85.35
Full Power	Full Power	Outside(back)	76.3	78.8	77.55

dBA	Examples	DECIBEL LEVELS MEANING	Decibel Effect
0	Healthy hearing threshold	0-30 dB, Very Faint.	Barely audible
10	A pin dropping		
20	Rustling leaves	31-50 dB, Faint	One-sixteenth as loud as 70 dB. Very Quiet
30	Whisper, Soft music		
40	A babbling brook, Computer		One-eighth as loud as 70 dB.
50	Light traffic, Refrigerator		One-fourth as loud as 70 dB.
60	Conversational speech, Air conditioner	46-70 dB, Average.	Half as loud as 70 dB. Fairly quiet
70	Shower, Dishwasher		The arbitrary base of comparison. The Upper 70s are annoyingly loud to some people.
75	Toilet flushing, Vacuum cleaner		
80	Alarm clock, Garbage disposal	70-85 dB, Moderate.	2 times as loud as 70 dB. Possible damage in 8 h exposure.
85	Passing diesel truck, Snowblower.	91-100 dB, Very Loud.	4 times as loud as 70 dB. Likely damage 8 hr exp
90	Squeeze toy, Lawnmower, Arc welder.		
95	Inside subway car, Food processor,		8 times as loud as 70 dB. Serious

Figure S1: Level of Noise (Source: Levels Of Noise In Decibels (dB) Level Comparison Chart - Sound Proofing Guide)

Table S2: Log Tchebycheff fractions of duct inner diameter measurement for flow meter.

Depths	Fraction of Inner Diameter	Actual Depth
Depth # 1	0.0	0.2
Depth # 2	0.1	0.8
Depth # 3	0.3	1.9
Depth # 4	0.7	4.1
Depth # 5	0.9	5.2
Depth # 6	1.0	5.8
Duct Diameter	6 inches	
Area (ft^2)	0.196	

Table S3: Flow rate measurement using Log Tchebycheff fraction of duct inner diameters from Table S2.

Location		Average Velocity [ft/min] over an interval of 10 seconds		Flow Rate [cfm]	
Position	**Depth**	**1/2 Power**	**Full Power**	**1/2 Power**	**Full Power**
Hole 1	Depth # 1	414.0	959.0	81.3	188.3
Hole 1	Depth # 2	518.0	1074.0	101.7	210.8
Hole 1	Depth # 3	511.0	1012.0	100.3	198.7
Hole 1	Depth # 4	365.0	704.0	71.7	138.2
Hole 1	Depth # 5	307.0	621.0	60.3	121.9
Hole 1	Depth # 6	287.0	583.0	56.4	114.5
Hole 2	Depth # 1	316.0	705.0	62.0	138.4
Hole 2	Depth # 2	337.0	669.0	66.2	131.4
Hole 2	Depth # 3	401.0	733.0	78.7	143.9
Hole 2	Depth # 4	496.0	972.0	97.4	190.9
Hole 2	Depth # 5	461.0	908.0	90.5	178.3
Hole 2	Depth # 6	448.0	909.0	87.9	178.5
Hole 3	Depth # 1	438.0	724.0	86.0	142.2
Hole 3	Depth # 2	420.0	866.0	82.5	170.0
Hole 3	Depth # 3	458.0	874.0	89.9	171.6
Hole 3	Depth # 4	369.0	791.0	72.5	155.3
Hole 3	Depth # 5	336.0	699.0	65.9	137.3
Hole 3	Depth # 6	329.0	707.0	64.6	138.8
Average		400.6	806.1	78.7	158.3
			STD of DEV	14.3	28.2
		Coeffiecient of Variation		0.182	0.178

Table S4: Flow rate profile of the aerosol hood front panel opening.

Location	Width (ft)	Height (ft)	Flow Rate (cfm) When No Blower Power	Flow Rate (cfm) When Half Blower Power	Flow Rate (cfm) When Full Blower Power
Top Left	0	1.42	9	77	162
Top Center	1	1.42	6	102	122
Top Right	2	1.42	43	79	210
Middle Left	0	0.71	0	40	102
Center	1	0.71	3	82	153
Middle Right	2	0.71	40	68	122
Bottom Left	0	0	9	23	128
Bottom Center	1	0	28	57	85
Bottom Right	2	0	11	34	113
Average			16	62	133

Table S5: Flow rate profile of the HEPA filter of the aerosol hood on top panel.

Setting 4		**Setting 8**	
Velocity [ft/min]	Flow Rate [cfm]	Velocity [ft/min]	Flow Rate [cfm]
27	76.41	57	161.31
36	101.88	43	121.69
28	79.24	74	209.42
14	39.62	36	101.88
29	82.07	54	152.82
24	67.92	43	121.69
8	22.64	45	127.35
20	56.6	30	84.9
12	33.96	40	113.2
Avg	62.26	Avg	132.6955556
STD DEV	25.97594705	STD DEV	37.07312002
Coefficient of Variation	0.4172172671	Coefficient of Variation	0.2793847907

Table S6: Air changes/hour (ACH) and time required for airborne-contaminant removal by efficiency [28]

The number of air changes per hour and time and efficiency.		
ACH § ¶	**Time (mins.) required for removal 99% efficiency**	**Time (mins.) required for removal 99.9% efficiency**
2	138	207
4	69	104
6+	46	69
8	35	52
10+	28	41
12+	23	35
15+	18	28
20	14	21
50	6	8

+ Denotes frequently cited ACH for patient-care areas.

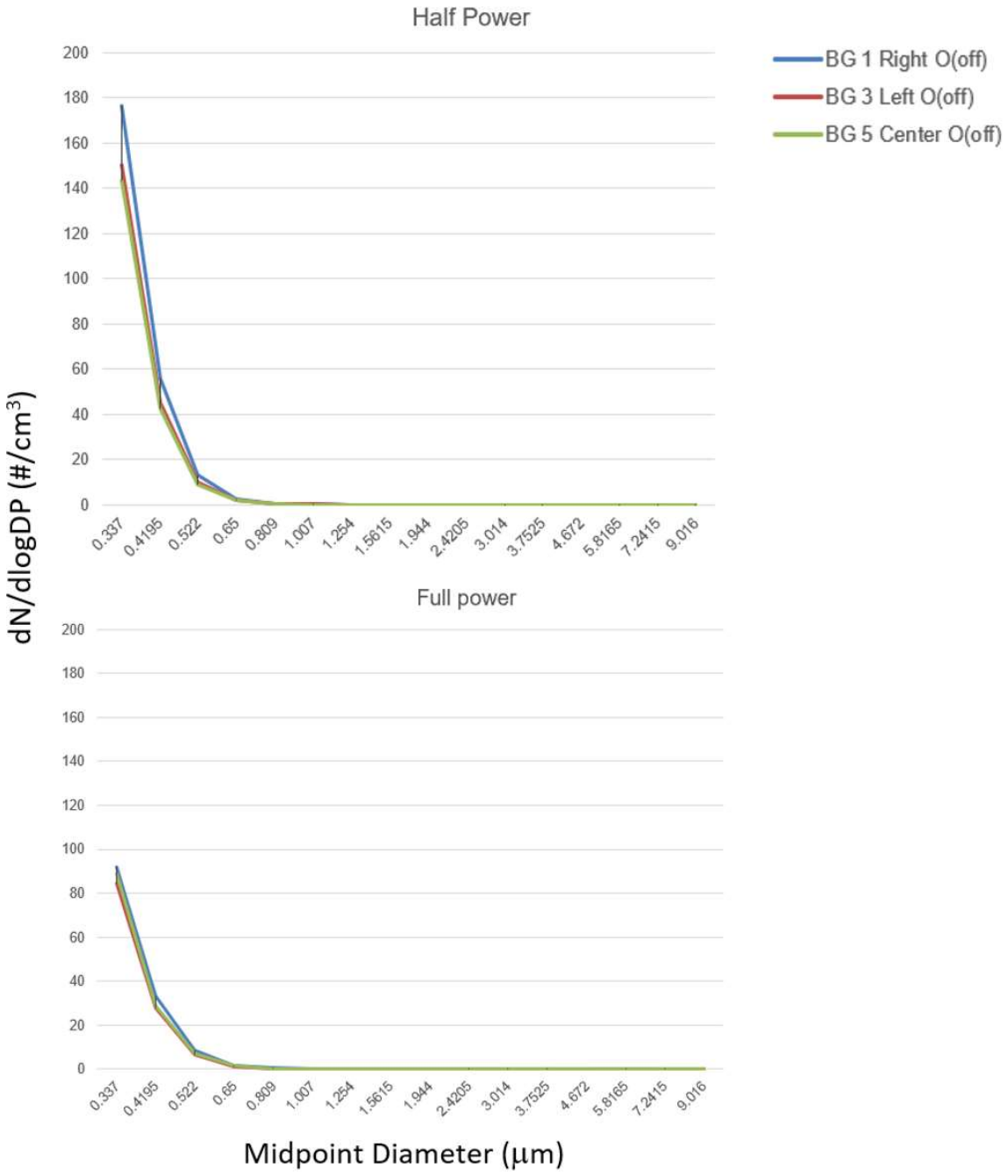

Figure S2: Background particle concentration measurement with the blower on and aerosol generation off.

Appendix C: (Supplementary material for Chapter 4)

Protocol for Participant Tasks - *Aerosol Hood Study*

START SCENARIO

1. **REVIEW EQUIPMENT**
    - BVM, Mask, Laryngoscope, Mac Blade, Miller Blade, ETT, Syringe, and Tape will all be provided to you to use.
2. **PREOXYGENATE**
    - Apply mask for 1 minute. (You will be notified when 1 minute has elapsed.
3. **MEDICATIONS ARE VERBALLY GIVEN TO INDUCE SEDATION & PARALYSIS**
    - It is not necessary for the participant to give medications. Participants will be notified that "The patient is now under sedation & Paralyzed, they have adequate SPO2 saturation. Intubation can now be attempted."
4. **APPLY EYE TAPE**
    - Participants should apply eye tape to protect patients' eyes from injury.
5. **INTUBATE**
    - Place Endotracheal Tube. (Participants may notice an orange haze coming from the dye being pumped through the manikin's airway. For this reason, all first intubation attempts will be considered successful)
6. **SECURE ETT WITH TAPE**
    - Participant should apply tape around tube to secure ETT.
7. **VERBALIZE PATIENT ON MECHANICAL VENTILATOR**
    - Participant should announce that they have started the patient on a mechanical ventilator and are monitoring any changes.

END OF SCENARIO

*(*Stepwise process has been altered from UMN Anesthesia Department - Medical Student General Intubation outline)*

Figure S1: Standardized intubation procedure steps for participants to use during the clinical study.

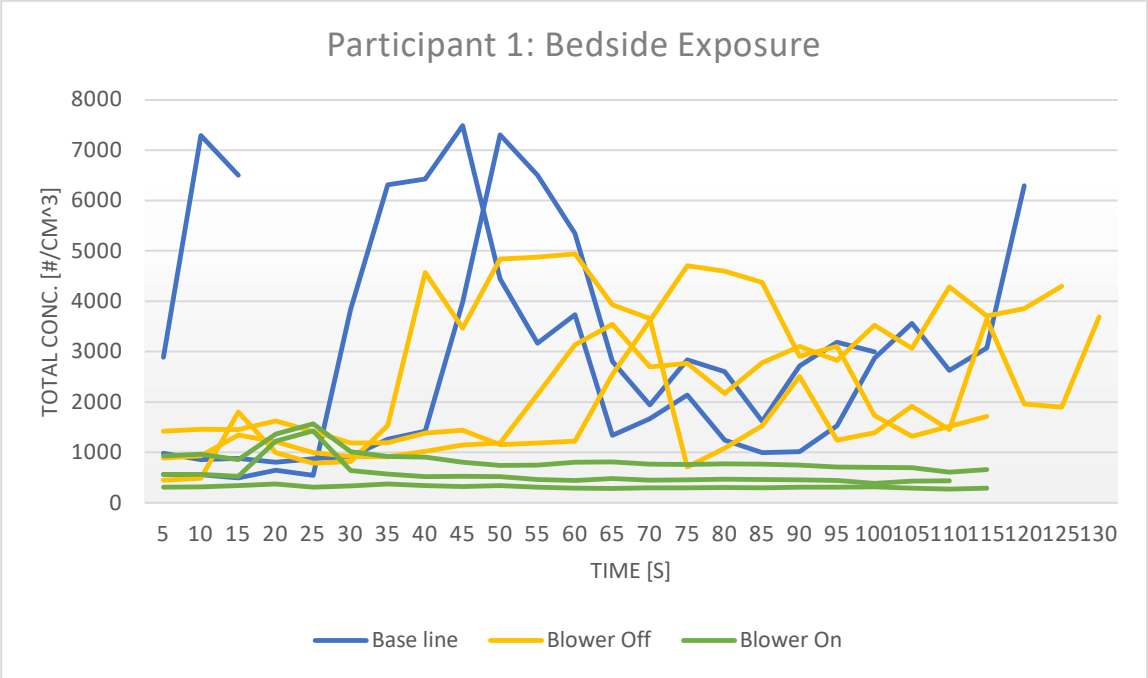

Figure S2: Replicates of participant 1 bedside exposure total particle concentration.

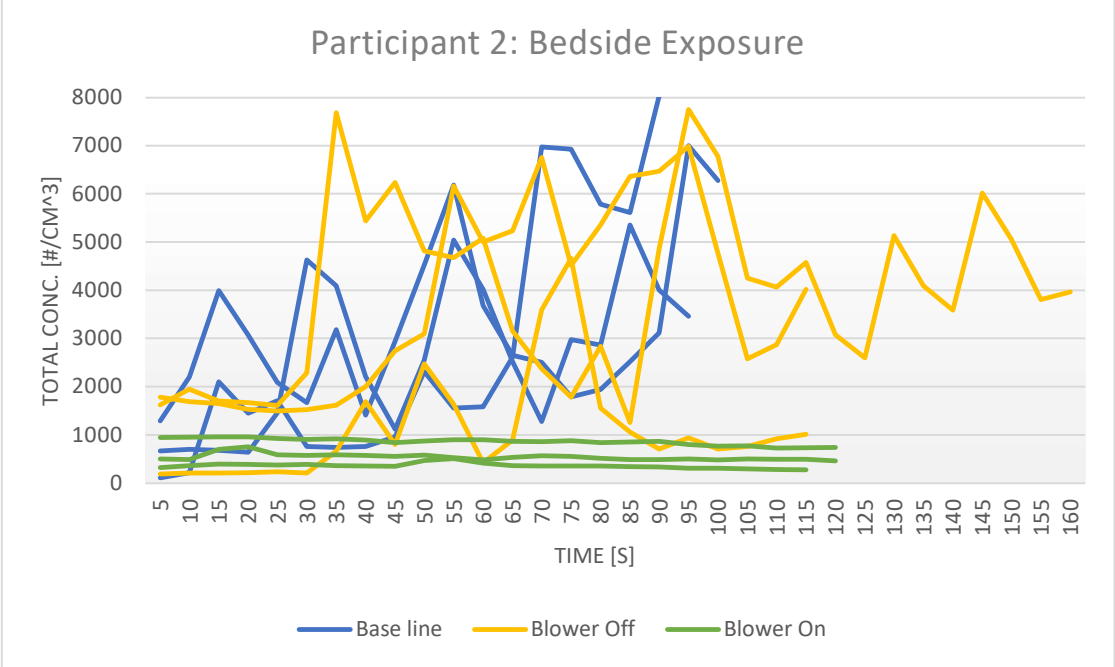

Figure S3: Replicates of participant 2 bedside exposure total particle concentration.

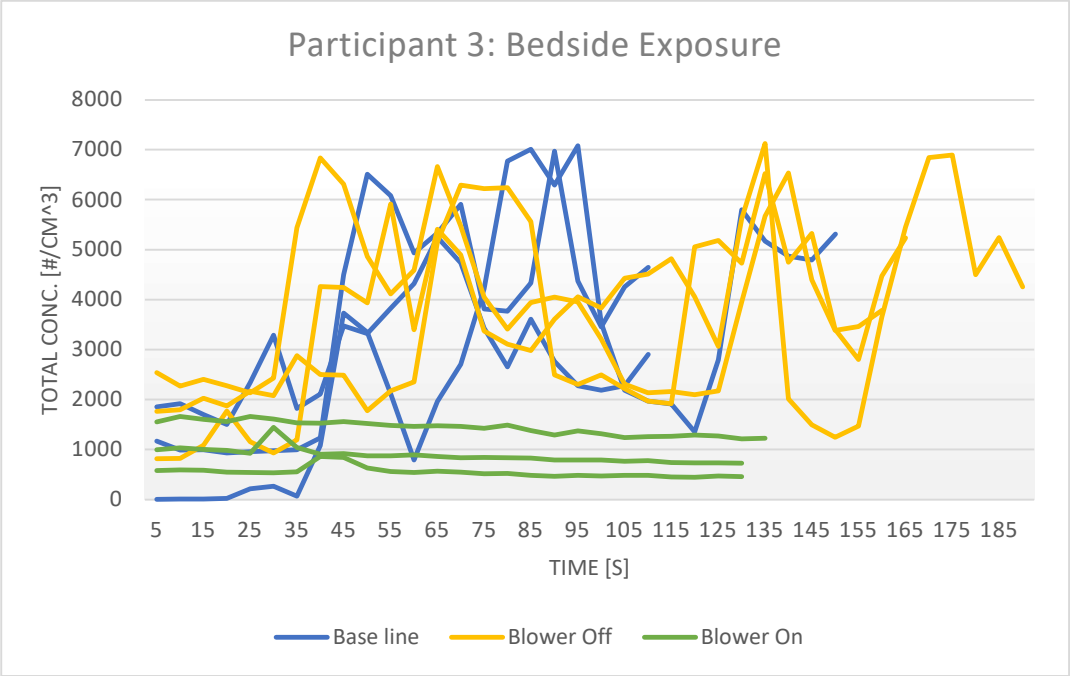

Figure S4: Replicates of participant 3 bedside exposure total particle concentration.

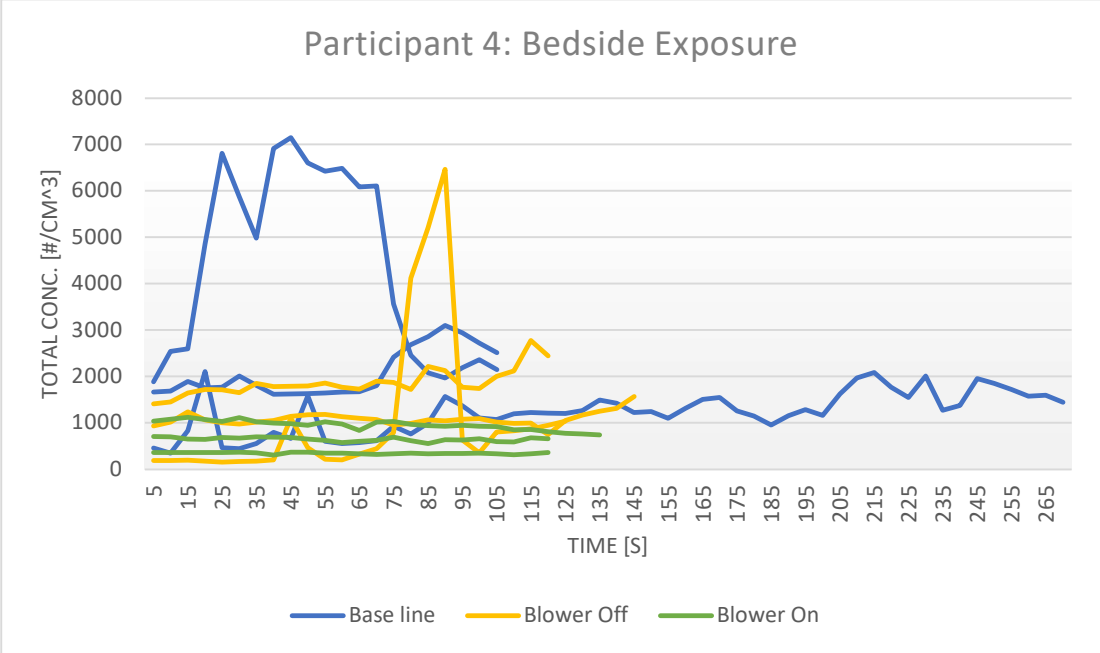

Figure S5: Replicates of participant 4 bedside exposure total particle concentration.

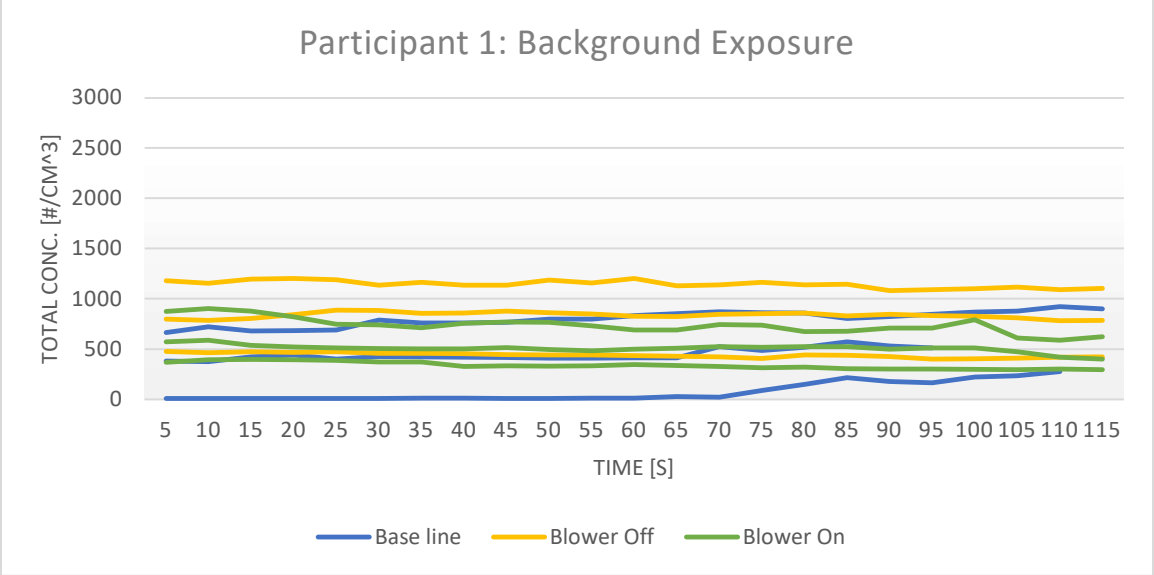

Figure S6: Replicates of participant 1 background exposure total particle concentration.

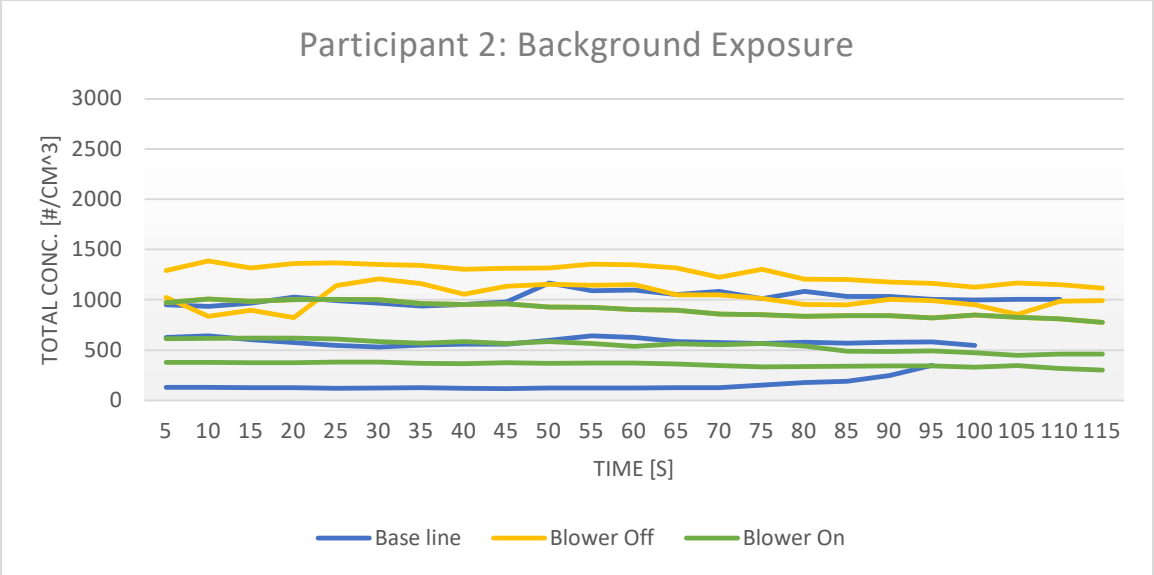

Figure S7: Replicates of participant 2 background exposure total particle concentration.

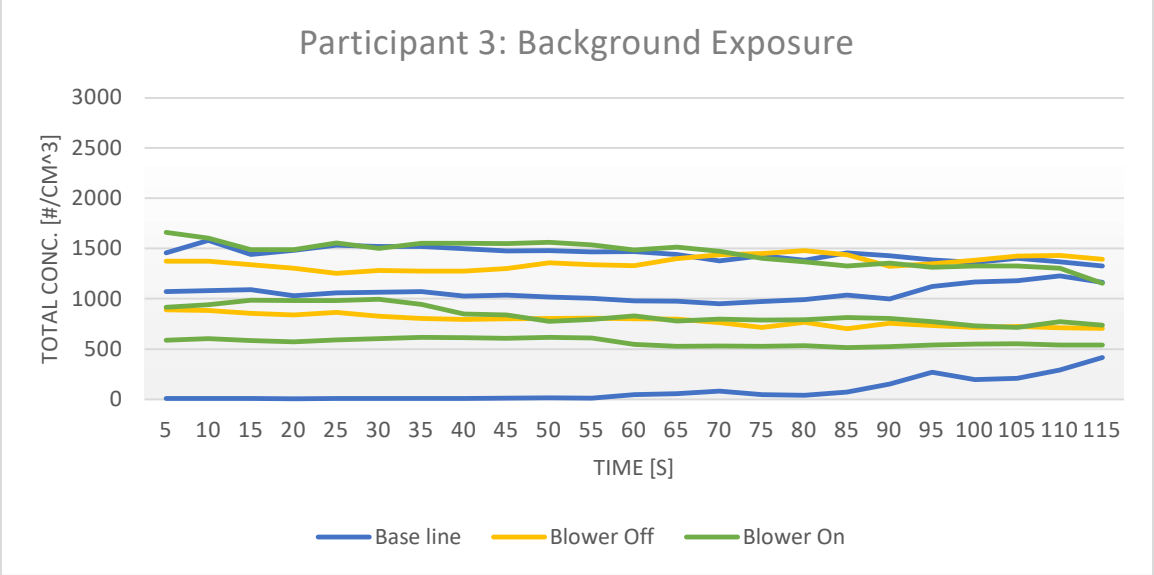

Figure S8: Replicates of participant 3 background exposure total particle concentration.

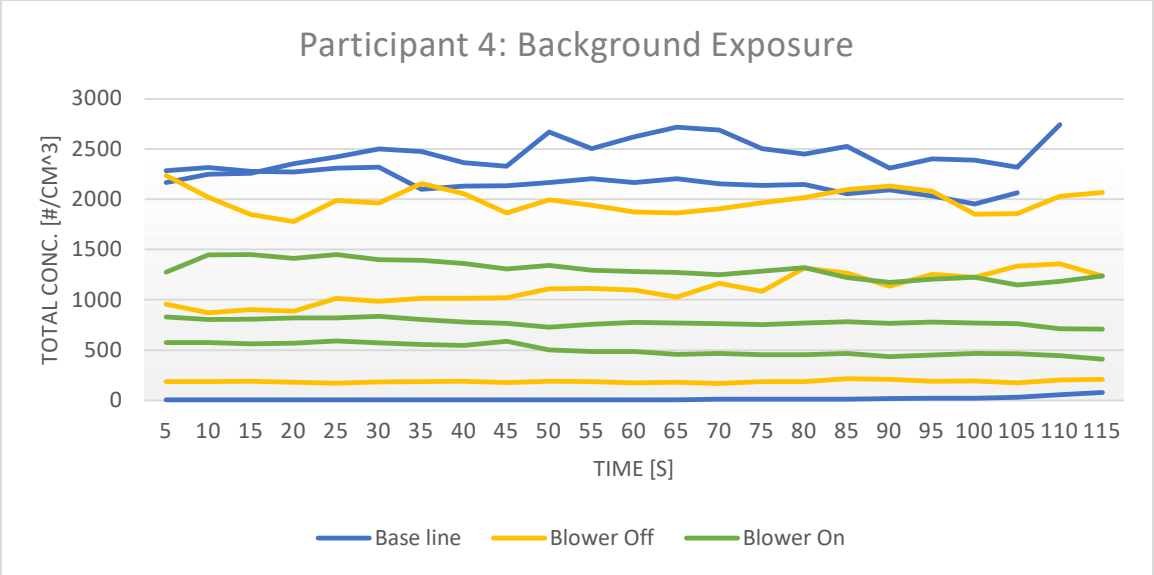

Figure S9: Replicates of participant 4 background exposure total particle concentration.

Participant 1: Interview Response Debrief

Experience with intubation:

- Approximately 10,000 times (40 years of experience)
- 100% comfort level given the patient anatomy (appropriate upper airway anatomy, decent range of motion, no receding chin, long neck etc.)

Feedback:

Negatives:

- Actual airway management scenario felt "pretty artificial" due to the mannequin
- Constraining trying to work with arms and hands inside the box; in a real intubation scenario, "we are used to having a great deal of freedom of motion"
- To be used clinically, it would require a fair amount of conscious preparation on the part of the user – e.g., placing tools in a specific manner before the intubation starts
- Would be difficult to perform intubations for people with severe respiratory illness as they do not lie still

Positives:

- Was eventually able to adapt to it and made accommodations to adjust to the box
- Practical and feasible for anesthesiologists – yes, however in a setting where they are doing fast intubations on multiple people, this would not be feasible to use this device
- Felt successful following the protocol, practice runs were helpful

Other key points:

- Most other providers would prefer using other PPE to the box
- "Chronic nursing tool for general protection" - would be helpful for COVID patients or patients with severe respiratory illness not during intubation but generally as it would be safer for the nurses and other hospital staff
- The whole process was well thought out and smooth

Figure S10: Participant 1 feedback on the aerosol hood

Participant 2: Interview Response Debrief

Experience with intubation:

- 5 years of experience excluding residency and fellowships, 9 years of experience performing intubation procedures – intubated 1000s of times
- Comfort level - "very comfortable"

Feedback:

Negatives:

- Was harder due to less range of motion, compact space
- Mannequins do not reflect the human anatomy very accurately
- Is not very accurate to how intubation would be in real life because every patient is different and with the mannequin, the intubation becomes a little mechanical
- The study does not take into account "surprising physiological situations" like difficult airway - secretions, aspirations, vomiting events, agitated patient, tooth injuries, oral bleeding, precipitous desaturations
- Would be a scary for children, claustrophobic patients and mentally impaired adults if a box is being placed on top of them in the operating room, can also have an injury risk if they try to get up

Positives:

- Felt comfortable performing the intubation procedure today, no significant trouble intubating the mannequins
- Over the course of the intubation trials, it got easier as he got used to the anatomy of the mannequin
- The first 1-2 run throughs helped with understanding how to place arms, and strategize tool placement etc.

Other key points:

- Would be good to use in a clinical setting given that the practitioners have had time to train on the box and understand a few times
- Does not think it would be helpful for healthy patients and in fact would be a little dangerous as it would impair access to the patient, but is worth the additional impairment for COVID or other respiratory diseases that are aerosolized
- Would be helpful for patients with communicable diseases who are in the wards (but would need a bigger box for that)

Figure S11: Participant 2 feedback on the aerosol hood

Participant 3: Interview Response Debrief

Experience with intubation:

- Anesthesia resident, 2 years of experience in the US and has done residency in India as well - 9 years of experience with anesthesiology
- At least one intubation a day for the past 9 years
- "Pretty 'comfortable

Feedback:

Negatives:

- Harder to intubate a mannequin compared to a human being
- Would be okay for most patients once the muscle memory kicks in but would be challenging for difficult airways in unexpected situations like poor laryngeal view on direct laryngoscopy and in these cases a C-MAC is used immediately as the patient is desaturating. This would be harder to manage with the hood since 2 sets of hands are preferred
- In certain situations, physicians would like to get closer to the patient which is not possible with the box
- Sometimes patients can throw up during intubation and physicians keep handy suction equipment for those situations, but fast movement during that time can be tricky due to the box
- Had to get used to looking through the glass
- For bigger patients, the head needs to be positioned strategically by possibly placing blankets under the head and doing that with the box might not be ideal
- Would also be more difficult for pediatric patients for the same reasons

Positives:

- Felt successful doing the intubation after getting used to the mannequin since the anatomy is different
- Having all the equipment in the hood made it easier to intubate
- Was able to strategize and calibrate eventually
- Easy to use as long as the all the equipment is in the hood

Other key points:

- Would be useful for patients with tuberculosis or any other aerosolizing infections

Figure S12: Participant 3 feedback on the aerosol hood

Participant 4: Interview Response Debrief

Experience with intubation:

- Practicing since 1995 – performs intubation as part of his practice
- 4 intubations per year because most go to the fellows first, did more intubations early in the career
- Comfort level – very comfortable

Feedback:

Negatives:

- Different than usual clinical experience because there is usually another set of hands helping with suction etc.
- Could not see the oropharynx, could not visualize the cord, anatomy was difficult the first time
- Only one field of view
- Low ease of intubation

Positives:

- Made adjustments which helped with the intubation eventually
- Can see the anatomy better when the ventilator was on and the smoke was not near the patient
- Did not have to change the mechanics but simply ventilation allowed for better visualization

Other key points:

- Would have someone else use the side ports for the extra set of hands in a clinical setting
- More applicable for viruses like COVID-19 than Ebola virus
- A dome like shape would be better than a box
- 2 handed intubation is not common, so the box might not be a popular choice
- Trying out the experiment with a pediatric mannequin would be important

Figure S13: Participant 4 feedback on the aerosol hood